

The Lucas Orchard

Ian Martin*

27 November, 2007

Abstract

I solve for asset prices, expected returns and the term structure of interest rates in a continuous-time endowment economy in which a representative agent with power utility consumes the dividends of multiple assets. The assets are Lucas trees; a collection of Lucas trees is a Lucas orchard. The dividend growth of each asset is i.i.d. over time, though there may be correlations between the dividends of different assets. This framework allows for jumps in dividends. The model replicates various features of the data. There is significant comovement even between assets whose dividend streams are independent. Assets with high price-dividend ratios have low risk premia. Small assets exhibit momentum. There is excess volatility in the aggregate market. High yield spreads forecast high excess returns on long term bonds and on the market. When dividends are subject to jumps, the model generates contagion and flight to quality. The quantities of interest—price-dividend ratios, expected returns and interest rates—are expressed in terms of integrals that can easily be evaluated numerically. In the two-asset case, closed-form solutions are available if dividends follow geometric Brownian motions or, for general dividend processes, in the limit as an asset becomes small relative to the market. Conditions are provided under which a vanishingly small asset with idiosyncratic fundamentals covaries with the market and earns a positive risk premium.

*iwmartin@fas.harvard.edu; <http://www.people.fas.harvard.edu/~iwmartin/>. First draft: 9 October 2006. I thank Tobias Adrian, Malcolm Baker, Thomas Baranga, Robert Barro, John Cochrane, George Constantinides, Josh Coval, Emmanuel Farhi, Xavier Freixas, Jakub Jurek, David Laibson, Greg Mankiw, Emi Nakamura, Martin Oehmke, Roberto Rigobon, David Skeie, Jon Steinsson, Aleh Tsyvinski, Pietro Veronesi, Luis Viceira and James Vickery for their comments. In particular, I am very grateful to John Campbell and Chris Rogers for their advice.

This paper investigates the properties of asset prices, risk premia, and the term structure of interest rates in a continuous-time economy in which a representative agent with power utility consumes the sum of the dividends of N assets. The assets can be thought of as Lucas trees, so I call the collection of assets a Lucas orchard.

Each of the assets is assumed to have i.i.d. dividend growth over time, though there may be correlation between the growth rates of different assets. Formally, the vector of log dividends follows a Lévy process. This framework allows for the case in which dividends follow geometric Brownian motions, but also allows for a rich structure of jumps in dividends. Standard lognormal models make poor predictions for key asset-pricing quantities such as the equity premium and riskless rate (Mehra and Prescott (1985)), and recently there has been increased interest in models which allow for the possibility of disasters (Rietz (1988), Barro (2006)). By allowing for jumps in dividends, I avoid these puzzles without relying on implausible levels of risk aversion or dividend growth volatility.

If $N = 1$, the model reduces to the familiar power-utility-i.i.d. consumption-based model in which the riskless rate and the risk premium and price-dividend ratio of the single asset—the consumption claim—are each constant over time.

This paper addresses the case in which there are $N \geq 2$ assets. For simplicity, the majority of the paper (and the discussion in this introduction) focusses on the case $N = 2$. Depending on context, the assets may be thought of as industries, countries or asset classes. The model generates several phenomena that have been documented in the empirical literature and emphasizes, as Brainard and Tobin (1968) put it, “the importance of explicit recognition of the essential interdependences of markets in theoretical and empirical specifications of financial models.”

A central feature of the paper is that assets whose dividends make up a large proportion of consumption are riskier, all else equal, than assets that make up a small proportion of consumption. Large assets have low price-dividend ratios; small assets have high price-dividend ratios. (For simplicity, I temporarily assume that assets are independent and have fundamentally the same prospects—the same mean dividend growth rate, dividend volatility, susceptibility to disasters, and so on.)

Various properties of the model spring from this fact. Since dividend growth is i.i.d., it is not forecastable. High price-dividend ratios therefore *cannot* forecast high dividend growth, and are instead associated with low expected returns. In calibrations, I also show that assets with high price-dividend ratios also have low expected *excess* returns: the value-growth effect of Fama and French (1993). Moreover, the expected excess return on a value-minus-growth strategy is time-varying and moves with the value spread (the difference in dividend yields between value and growth assets), as has been found in the data by Cohen, Polk and Vuolteenaho (2003).

The model generates price comovement even between assets whose dividends are independent. To see why this happens, suppose that one asset’s price increases as a result of a positive shock to dividends. The other asset now contributes a smaller proportion of overall consumption, and (typically) has, therefore, a lower risk premium and hence a higher price. Such comovement is a feature of the data. Shiller (1989) demonstrates, using data from 1919 to 1987, that stock prices in the US and UK move together more closely than do fundamentals; Forbes and Rigobon (2002) allow for heteroskedasticity in returns and find consistently high levels of interdependence between markets.

At the aggregate level, too, high market price-dividend ratios forecast low market expected returns. It follows that the market displays “excess” volatility, as in Shiller (1981), in the sense that its returns are more volatile than its dividends.

The riskless rate varies over time, so the term structure of interest rates is not flat. The term structure can be upward-sloping, downward-sloping or hump-shaped (with medium-term bonds earning higher yields than short- and long-term bonds). When the term structure slopes up—the more usual case in the scenarios I consider—long-term bonds earn positive risk premia. High yield spreads forecast high excess returns on the market and high excess returns on long-term bonds, replicating a finding of the empirical literature (for example, Fama and French (1989)).

I decompose realized returns into dividend-driven returns and valuation-driven returns. The latter are returns due to changes in price-dividend ratios—for example, when one asset comoves with another that has received good news, it earns a positive valuation-driven return. Most of the variance in asset returns, particularly for large assets, is due to cashflow news. For small assets, however, valuation-driven returns are more important. Small assets also exhibit momentum, in the sense that their dividend-driven returns and valuation-driven returns are negatively correlated.

I present two calibrations, each intended to highlight different features of the model. In the first, dividends follow geometric Brownian motions with 10% dividend volatility. The features described above are present.

In the second calibration, dividend volatility is 2% and occasional disasters afflict the two assets. This calibration, like that of Barro (2007), avoids the equity premium and riskless rate puzzles. The phenomena described above are present, and there are now some new features. First, jumps are transmitted across assets. When a large asset experiences a disaster, the price of the other (small) asset also jumps downwards. This corresponds to the “typical” case of comovement described above. When, on the other hand, a very small asset suffers a disaster, the other (large) asset’s price jumps *up* due to a sudden drop in interest rates. I label these phenomena “contagion” and “flight-to-quality”.

Contagion effects provide a new channel through which disasters can contribute to high

risk premia, even in assets which are not themselves subject to disasters. For example, suppose that asset 1 has perfectly stable dividends, but that asset 2 is subject to occasional disastrous declines in dividends. Contagion leads to declines in the price of asset 1 at times when asset 2 experiences a disaster. These occasional price drops may induce a substantial risk premium in asset 1, an ostensibly perfectly safe asset.

One contribution of this paper is methodological: I solve for asset prices, expected returns and the term structure of interest rates using techniques from complex analysis. Prices, returns and interest rates are expressed in terms of integral formulas that can, effectively instantly, be evaluated numerically in *Mathematica* or *Maple*. These integral formulas are valid for arbitrary i.i.d. dividend growth processes, subject to conditions that ensure finiteness of the representative agent's expected utility (and hence of asset prices). When dividends follow geometric Brownian motions, the integral formulas simplify to closed-form expressions.

I next consider the limit in which one of the two assets is negligibly small by comparison with the other. This case is of special interest because it represents the most extreme departure from simple models in which price-dividend ratios are constant. Closed-form solutions are available without any restrictions on the dividend growth process, and an unexpected phenomenon emerges.

To illustrate this, suppose that the two assets have independent dividend streams. Intuition suggests that a small idiosyncratic asset earns no risk premium, that its expected return is therefore equal to the riskless rate and that it can be valued using a Gordon growth formula; in other words, its dividend yield should equal the riskless rate minus expected dividend growth. I show that this intuition is correct whenever the result of the calculation is meaningful, which is to say positive. What happens if the riskless rate (determined by the characteristics of the large asset) is less than the mean dividend growth of the small asset? I show that the negligibly small asset then has a well-defined price-consumption ratio that, as one would hope, tends to zero in the limit. It has, however, an extremely high valuation in the sense that its price-dividend ratio is infinite in the limit. This valuation effect is reminiscent of, and complementary to, that present in the papers of Pástor and Veronesi (2003, 2006). Despite its independent fundamentals and negligible size, such an asset also has a positive market beta and earns a risk premium. In the general case, I provide a precise characterization of when the Gordon growth model does and does not work, and solve for limiting expected returns and price-dividend ratios in closed form.

The tractability of the model in the general i.i.d. (as opposed to lognormal) case is heavily dependent on the use of cumulant-generating functions (CGFs). Martin (2007) expresses the riskless rate, risk premium and consumption-wealth ratio in terms of the CGF in the standard one-asset case, and the expressions found there are echoed in the more complicated

scenario considered here. In effect, working with CGFs makes the mathematics no harder than when working with lognormal models; the advantage of doing so is that one then “gets jumps for free”. In fact, the use of CGFs may even make things *simpler* because one can follow the CGF’s progress through the algebra: the mathematical equivalent of a barium meal! Furthermore, CGFs have general properties that I use in various proofs. In particular, the conditions for finiteness of asset prices, and hence expected utility, can be considerably simplified using properties of CGFs.

Various authors have investigated related models. Cole and Obstfeld (1991) consider a similar framework, but focus on the welfare gains from international risk sharing rather than the implications for asset prices, and they do not present any analytical results in the case considered here, in which the dividends of the two assets are perfect substitutes.¹ Brainard and Tobin (1992, section 8) investigate a framework that is almost identical to the one presented here, differing only in that the dividends of the two assets are very good, rather than perfect, substitutes, and in that per-period endowments are specified by a Markov chain with a small number of states. They present limited numerical results, and—after noting that their “model is simple and abstract; nevertheless it is not easy to analyze”—no analytical results. Menzly, Santos and Veronesi (2004) and Santos and Veronesi (2006) present models in which the dividend shares of assets are assumed to follow mean-reverting processes. By picking convenient functional forms for these processes, closed-form pricing formulas are available. Pavlova and Rigobon (2007) investigate the consequences of demand shocks in an international asset pricing model, but impose log-linear preferences, so price-dividend ratios are constant.

The most closely related paper is that of Cochrane, Longstaff and Santa-Clara (2007), who solve a model in which a representative investor with log utility consumes the dividends of two assets whose dividend processes follow geometric Brownian motions. My solution technique is entirely different, and permits me to allow for power utility, for jumps in dividends and for $N \geq 2$ assets. I also solve for bond yields, and hence expand the set of predictions made by the model.

Section 1 sets up the model in the two-asset case. Section 2 explains why it is hard to solve and introduces a suggestive special case which is easily solved. Section 3 presents integral formulas for prices, expected returns and real interest rates. Section 4 shows how these formulas lead to closed-form solutions in the Brownian motion case. Section 5 illustrates the results by exploring various calibrations. Section 6 investigates the asymptotic limit in which one asset has a vanishingly small dividend share. Section 7 provides integral formulas in the N -asset case. Section 8 concludes. Proofs are collected in the appendices.

¹The approach of this paper can also be used, essentially unchanged, to solve the model with imperfect substitution; this is work in progress.

1 Setup

I work with a representative investor model. Time is continuous, and runs from 0 (the present) to infinity. For the time being, I restrict to the two-asset case for clarity. General results in the N -asset case are presented in Section 7.

Setting the model up amounts to making *technological* assumptions about dividend processes; making assumptions about *preferences* which, together with consumption, pin down the stochastic discount factor; and closing the model by specifying that the representative investor's consumption is equal to the sum of the two assets' dividend processes.

1.1 The stochastic discount factor

The two assets, indexed $i = 1, 2$, throw off random dividend streams D_{it} . The representative agent's consumption process, C_t , is equal to the sum of the two dividend streams: $C_t = D_{1t} + D_{2t}$. The representative agent has power utility with coefficient of relative risk aversion γ and time preference rate ρ , so maximizes

$$\mathbb{E} \int_{t=0}^{\infty} e^{-\rho t} \frac{C_t^{1-\gamma}}{1-\gamma} dt \quad \text{if } \gamma \neq 1, \quad \text{or} \quad \mathbb{E} \int_{t=0}^{\infty} e^{-\rho t} \log C_t dt \quad \text{if } \gamma = 1. \quad (1)$$

The Euler equation, derived by Lucas (1978) and applied in the two-country context by Lucas (1982), states that the price of an asset which pays dividend stream $\{X_t\}$ is

$$P_X = \mathbb{E} \int_0^{\infty} e^{-\rho t} \left(\frac{C_t}{C_0} \right)^{-\gamma} \cdot X_t dt. \quad (2)$$

1.2 Dividend processes

Dividends are positive, which makes it natural to work with log dividends, $y_{it} \equiv \log D_{it}$. At time 0, the dividends (y_{10}, y_{20}) of the two assets are arbitrary. The vector $\tilde{\mathbf{y}}_t \equiv \mathbf{y}_t - \mathbf{y}_0 \equiv (y_{1t} - y_{10}, y_{2t} - y_{20})$ is assumed to follow a Lévy process.²

²A stochastic process $(L_t)_{t \geq 0}$ taking values in \mathbb{R}^d is a *Lévy process* if

- (i) $L_0 = 0$
- (ii) With probability one, L_t is right continuous on $[0, \infty)$, with left limits on $(0, \infty)$.
- (iii) For any $n \in \mathbb{N}$ and $0 \leq t_0 < t_1 < \dots < t_n$, the random variables $L_{t_0}, L_{t_1} - L_{t_0}, L_{t_2} - L_{t_1}, \dots, L_{t_n} - L_{t_{n-1}}$ are independent.
- (iv) The probability distribution of $L_{t+h} - L_t$ does not depend on t .
- (v) For all $t \geq 0$ and $\varepsilon > 0$, $\lim_{s \rightarrow t} \mathbb{P}(|X_s - X_t| > \varepsilon) = 0$.

This is the continuous-time analogue of the familiar discrete-time assumption that dividend growth is i.i.d. It is helpful to keep in mind the special case in which $\tilde{\mathbf{y}}$ is a jump-diffusion, in which case we can write

$$\mathbf{y}_t = \mathbf{y}_0 + \boldsymbol{\mu}t + \mathbf{A}\mathbf{Z}_t + \sum_{k=1}^{N(t)} \mathbf{J}^k . \quad (3)$$

Here $\boldsymbol{\mu}$ is a two-dimensional vector of “drifts”, \mathbf{A} a 2×2 matrix of factor loadings, \mathbf{Z}_t a 2-dimensional Brownian motion, $N(t)$ a Poisson process with arrival rate ω that represents the number of jumps that have taken place by time t , and \mathbf{J}^k are two-dimensional random variables which are distributed like the random variable \mathbf{J} , and which are assumed to be i.i.d. across time. The covariance matrix of the diffusion components of the two dividend processes is $\boldsymbol{\Sigma} \equiv \mathbf{A}\mathbf{A}'$, whose elements I write as σ_{ij} .

The following definition introduces an object which turns out to capture all relevant information about the stochastic processes driving dividend growth.

Definition 1. *The cumulant-generating function $\mathbf{c}(\boldsymbol{\theta})$ of the Lévy process $\tilde{\mathbf{y}}_t$ is defined by*

$$\mathbf{c}(\boldsymbol{\theta}) \equiv \log \mathbb{E} \exp \boldsymbol{\theta}'(\tilde{\mathbf{y}}_{t+1} - \tilde{\mathbf{y}}_t) . \quad (4)$$

By properties (i) and (iv) of the definition of a Lévy process, given in footnote 2, I could equivalently have defined $\mathbf{c}(\boldsymbol{\theta}) = \log \mathbb{E} \exp \boldsymbol{\theta}'\tilde{\mathbf{y}}_1$, but the expression (4) emphasizes the fact that the cumulant-generating function (CGF) summarizes information about dividend *growth*. Specifically, the CGF summarizes information about the higher moments of $\tilde{\mathbf{y}}$; Martin (2007) has more discussion of the role of CGFs in the standard consumption-based framework with one asset.

Some conditions on the Lévy process $\tilde{\mathbf{y}}$ are required to ensure that asset prices are finite; these are discussed further below. In particular, they will ensure that the CGF exists in an appropriate open set containing the origin.

If log dividends follow Brownian motions, the CGF takes the simple form

$$\mathbf{c}(\boldsymbol{\theta}) = \boldsymbol{\theta}'\boldsymbol{\mu} + \frac{1}{2}\boldsymbol{\theta}'\boldsymbol{\Sigma}\boldsymbol{\theta} .$$

If log dividends follow a jump-diffusion as in (3), then

$$\mathbf{c}(\boldsymbol{\theta}) = \boldsymbol{\theta}'\boldsymbol{\mu} + \frac{1}{2}\boldsymbol{\theta}'\boldsymbol{\Sigma}\boldsymbol{\theta} + \omega \left(\mathbb{E} e^{\boldsymbol{\theta}'\mathbf{J}} - 1 \right) .$$

If the jumps in log dividends are driven by Normally distributed shocks, so $\mathbf{J} \sim N(\boldsymbol{\mu}_J, \boldsymbol{\Sigma}_J)$, then the CGF becomes

$$\mathbf{c}(\boldsymbol{\theta}) = \boldsymbol{\theta}'\boldsymbol{\mu} + \frac{1}{2}\boldsymbol{\theta}'\boldsymbol{\Sigma}\boldsymbol{\theta} + \omega \left(\exp \left\{ \boldsymbol{\theta}'\boldsymbol{\mu}_J + \frac{1}{2}\boldsymbol{\theta}'\boldsymbol{\Sigma}_J\boldsymbol{\theta} \right\} - 1 \right) .$$

2 A simple example

Consider the problem of pricing the claim to asset 1's output in the simplest case $\gamma = 1$: log utility. We have

$$\begin{aligned}
 P(D_1) &= \mathbb{E} \int_0^\infty e^{-\rho t} \left(\frac{C_t}{C_0} \right)^{-1} \cdot D_{1t} dt \\
 &= \mathbb{E} \int_0^\infty e^{-\rho t} \frac{D_{10} + D_{20}}{D_{1t} + D_{2t}} \cdot D_{1t} dt \\
 &= (D_{10} + D_{20}) \int_0^\infty e^{-\rho t} \mathbb{E} \left(\frac{1}{1 + D_{2t}/D_{1t}} \right) dt;
 \end{aligned}$$

and, unfortunately, the expectation is not easily calculated. If, say, the D_{it} are geometric Brownian motions, then we have to compute the expected value of the reciprocal of one plus a lognormal random variable. This, essentially, is the major analytical challenge confronted by Cochrane, Longstaff and Santa-Clara (2007).

Here, though, is an instructive case in which the expectation simplifies considerably. Suppose that $D_{2t} < D_{1t}$ at all times t . Perhaps, for example, D_{1t} is constant and initially larger than D_{2t} , which is subject to downward jumps at random times.³ (The jumps may be random in size, but they must always be downwards.) Then $D_{2t}/D_{1t} < 1$ and so we can expand the expectation as a geometric sum. To make things simple, set $D_{1t} \equiv 1$: then,

$$\begin{aligned}
 \mathbb{E} \left(\frac{1}{1 + D_{2t}} \right) &= \mathbb{E} [1 - D_{2t} + D_{2t}^2 - \dots] \\
 &= \sum_{n=0}^{\infty} (-1)^n D_{20}^n \mathbb{E} [(D_{2t}/D_{20})^n] \\
 &= \sum_{n=0}^{\infty} (-1)^n D_{20}^n e^{c(0,n)t}.
 \end{aligned}$$

Substituting back, we find that

$$\begin{aligned}
 P(D_1) &= (1 + D_{20}) \int_{t=0}^{\infty} e^{-\rho t} \sum_{n=0}^{\infty} (-1)^n D_{20}^n e^{c(0,n)t} dt \\
 &= (1 + D_{20}) \sum_{n=0}^{\infty} (-1)^n D_{20}^n \int_{t=0}^{\infty} e^{-[\rho - c(0,n)]t} dt \\
 &= (1 + D_{20}) \sum_{n=0}^{\infty} \frac{(-1)^n D_{20}^n}{\rho - c(0,n)}
 \end{aligned}$$

If we define $s \equiv D_{10}/(D_{10} + D_{20})$ to be the share of asset 1 in global output—a definition which is maintained throughout—we can rewrite this in a form that is more directly

³This approach fails in the Brownian motion case, since if either D_{1t} or D_{2t} has a Brownian component we cannot say that $D_{2t} < D_{1t}$ with probability one.

comparable with subsequent results:

$$P/D_1 = \frac{1}{\sqrt{s(1-s)}} \sum_{n=0}^{\infty} \frac{(-1)^n \left(\frac{1-s}{s}\right)^{n+1/2}}{\rho - \mathbf{c}(0, n)} \quad (5)$$

P/D_1 is the price-dividend ratio of asset 1 at time 0. When time subscripts are dropped, here and elsewhere, it should be understood that the relevant time is time 0.

The expression (5) is not in closed form, but it is easy to evaluate numerically, once the process driving the dividends of asset 2—and hence $\mathbf{c}(0, n)$ —is specified. For example, if asset 2’s log dividend is subject to downward jumps of constant size $-b$ which occur at intervals dictated by a Poisson process with arrival rate ω , then $\mathbf{c}(0, n) = \omega(e^{-bn} - 1)$, so $\rho - \mathbf{c}(0, n) \rightarrow \rho + \omega$ as $n \rightarrow \infty$. Meanwhile, $(1-s)/s < 1$ so the terms in the numerator of the summand decline at geometric rate. A numerical summation will therefore converge fast.

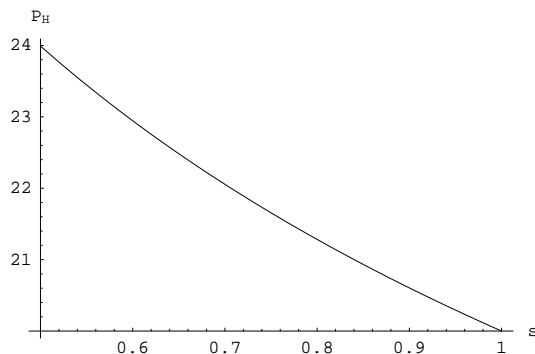


Figure 1: The price of asset 1, P_H , against its dividend share, s .

Figure 1 shows the price of asset 1 plotted against its dividend share s . Despite the fact that asset 1 has perfectly stable fundamentals— $D_{1t} \equiv 1$ —the asset’s price changes over time. Whenever asset 2 experiences a disaster, asset 1’s dividend share, s , increases and (looking at the graph) the price of asset 1 jumps down. Even in this simple example, then, there is “contagion”. Moreover, since asset 1 has stable fundamentals, we see what looks like excess volatility.

Although the simple approach taken here only works in very special cases, it turns out to be possible, using more sophisticated techniques, to solve for asset prices (and hence returns) in the general case, and to find expressions that are reminiscent of (5). When dividend processes are continuous, it is in fact possible—even with $\gamma > 1$ —to move beyond the analogue of (5) and to give closed form solutions.

2.1 Two Trees

In the simple symmetric case in which the log dividend processes follow independent drifting Brownian motions with volatility σ , Cochrane, Longstaff and Santa-Clara (2007) show that the price-dividend ratio of asset 1 is given, in my notation, by

$$P/D_1 = \frac{1}{2(\rho + \sigma\sqrt{\rho})(1-s)} F\left(1, 1 + \frac{\sqrt{\rho}}{\sigma}; 2 + \frac{\sqrt{\rho}}{\sigma}; \frac{s}{s-1}\right) + \frac{1}{2\rho s} F\left(1, \frac{\sqrt{\rho}}{\sigma}; 1 + \frac{\sqrt{\rho}}{\sigma}; \frac{s-1}{s}\right). \quad (6)$$

$F(a, b; c; z)$ is a member of the family of hypergeometric functions. It is defined in the region $|z| < 1$ by the power series

$$F(a, b; c; z) = 1 + \frac{a \cdot b}{1! \cdot c} z + \frac{a(a+1) \cdot b(b+1)}{2! \cdot c(c+1)} z^2 + \frac{a(a+1)(a+2) \cdot b(b+1)(b+2)}{3! \cdot c(c+1)(c+2)} z^3 + \dots \quad (7)$$

There is a difficulty here: whenever $s < 1/2$, we have $|(s-1)/s| > 1$, and whenever $s > 1/2$, we have $|s/(s-1)| > 1$, so the power series interpretation of (6) is invalid. Fortunately, there is an integral representation which extends the hypergeometric function to allow for $|z| \geq 1$ and complex-valued a, b, c and z :⁴

$$F(a, b; c; z) = \frac{\Gamma(c)}{\Gamma(b)\Gamma(c-b)} \int_0^1 w^{b-1} (1-w)^{c-b-1} (1-wz)^{-a} dw \quad \text{if } \operatorname{Re}(c) > \operatorname{Re}(b) > 0.$$

Now $\Gamma(z)$ is yet another integral, defined for complex numbers z with positive real part⁵ by

$$\Gamma(z) = \int_0^\infty t^{z-1} e^{-t} dt. \quad (8)$$

In short, the solution for the general Brownian case is somewhat complicated. Intriguingly, Cochrane, Longstaff and Santa-Clara also present a solution for the special case in which the log dividend processes follow independent and symmetric Brownian motions, and the time discount rate of the marginal investor, ρ , happens to equal σ^2 . In this case,

$$P/D_1 = \frac{1}{2\rho s} \left[1 + \left(\frac{1-s}{s} \right) \log(1-s) - \left(\frac{s}{1-s} \right) \log s \right]. \quad (9)$$

I show in Appendix D.1 how (and why) relatively simple expressions such as (9) can be found in the Brownian motion case when parameters are chosen judiciously.

⁴These objects boast an unimpeachable pedigree: Gauss considered the hypergeometric series in a famous paper presented to the Royal Society of Sciences at Göttingen in 1812, and Euler discovered the integral representation.

⁵See Appendix A for a summary of various concepts in complex analysis.

3 Prices, returns and real interest rates

The model is solved using techniques from complex analysis. Appendix A contains a summary of the relevant results.

It is convenient to work with a generic asset with dividend stream $D_{\alpha,t} \equiv D_{1t}^{\alpha_1} D_{2t}^{\alpha_2}$. The cases $\alpha \equiv (\alpha_1, \alpha_2) \in \{(1, 0), (0, 1), (0, 0)\}$ are of particular interest, the three alternatives representing asset 1, asset 2 and a perpetuity respectively.

3.1 Prices

The price of the asset is P_{α} , defined by

$$P_{\alpha} \equiv \mathbb{E} \int_{t=0}^{\infty} e^{-\rho t} \left(\frac{C_t}{C_0} \right)^{-\gamma} D_{\alpha,t} dt. \quad (10)$$

Asset prices turn out to depend on the value of a single state variable, the dividend share, defined by

$$s = \frac{D_{10}}{D_{10} + D_{20}}$$

As asset 1 becomes negligibly small by comparison with asset 2, s tends to zero; as asset 1 becomes large, s tends to one.

The following Proposition puts the right-hand side of (10) in a form which is perfectly suited for numerical implementation but also permits further analytical results to be derived.

Proposition 1 (The general pricing formula). *The price-dividend ratio on a generic asset which pays dividend stream $D_{\alpha,t} \equiv D_{1t}^{\alpha_1} D_{2t}^{\alpha_2}$ is given by the expression⁶*

$$\frac{P_{\alpha}}{D_{\alpha}}(s) = \frac{1}{\sqrt{s^{\gamma}(1-s)^{\gamma}}} \int_{-\infty}^{\infty} \frac{\mathcal{F}_{\gamma}(v) \left(\frac{1-s}{s} \right)^{iv}}{\rho - \mathbf{c}(\alpha_1 - \gamma/2 - iv, \alpha_2 - \gamma/2 + iv)} dv, \quad (11)$$

where $\mathcal{F}_{\gamma}(v)$ is defined by

$$\mathcal{F}_{\gamma}(v) \equiv \frac{1}{2\pi} \cdot \frac{\Gamma(\gamma/2 + iv)\Gamma(\gamma/2 - iv)}{\Gamma(\gamma)}. \quad (12)$$

Proof. See Appendix B. □

The gamma function $\Gamma(\cdot)$ was defined in (8). For real v and integer $\gamma > 0$, $\mathcal{F}_{\gamma}(v)$ is a strictly positive function which is symmetric about $v = 0$, where it attains its maximum, and decays exponentially fast towards zero as v tends to plus or minus infinity.

⁶Wherever it appears, i is the complex number $\sqrt{-1}$. Complex quantities drop out in the course of evaluating the integral, so price-dividend ratios are real, as one would hope.

In its present form, the pricing formula (11) appears rather complicated, but it is worth emphasizing that it allows for different assets (α) and for the stochastic process governing log outputs to be *any* Lévy process that leads to finite asset prices—a class which includes, for example, constant deterministic growth, drifting Brownian motion, compound Poisson processes, variance gamma processes, Normal inverse Gaussian processes and a host of others, including linear combinations of the processes mentioned.

We do, however, require that expected utility and asset prices are finite. I show in Appendix B.2.1 that finiteness of the prices of the two assets, which implies that expected utility (1) is finite, is assured by the *finiteness condition* that

$$\rho - \mathbf{c}(1 - \gamma/2, -\gamma/2) > 0 \quad \text{and} \quad \rho - \mathbf{c}(-\gamma/2, 1 - \gamma/2) > 0. \quad (13)$$

Given that perpetuities in zero net supply plausibly also have finite prices, we may also want to impose a requirement that ensures that this is the case,

$$\rho - \mathbf{c}(-\gamma/2, -\gamma/2) > 0.$$

This restriction is not necessary from a mathematical point of view; I impose it because it seems empirically plausible that real perpetuities in zero net supply have finite prices. (If either of the assets in positive net supply *is* a perpetuity, then this restriction is implied by (13).)

These assumptions ensure that aggregate wealth is finite for all $s \in (0, 1)$. I impose one final restriction, that aggregate wealth is finite at the one-tree limit points, $s = 0$ and $s = 1$. Asset 1's price-dividend ratio is finite as $s \rightarrow 1$ if and only if $\rho - \mathbf{c}(1 - \gamma, 0) > 0$; asset 2's price-dividend ratio is finite as $s \rightarrow 0$ if and only if $\rho - \mathbf{c}(0, 1 - \gamma) > 0$. These assumptions are summarized in Table 1.

Restriction	Reason
$\rho - \mathbf{c}(1 - \gamma/2, -\gamma/2) > 0$	finite price of asset 1
$\rho - \mathbf{c}(-\gamma/2, 1 - \gamma/2) > 0$	finite price of asset 2
$\rho - \mathbf{c}(-\gamma/2, -\gamma/2) > 0$	finite perpetuity price
$\rho - \mathbf{c}(1 - \gamma, 0) > 0$	finite aggregate wealth in limit $s \rightarrow 1$
$\rho - \mathbf{c}(0, 1 - \gamma) > 0$	finite aggregate wealth in limit $s \rightarrow 0$

Table 1: The restrictions imposed on the model.

For many practical purposes this is, in a sense, the end of the story, since the integral formula is very well behaved and can be calculated effectively instantly in *Mathematica* or *Maple*. After providing similar integral formulas for expected returns, the riskless rate and bond yields, I take this simple and direct route in section 5. Nonetheless, it is possible to push the pen-and-paper approach further and I do so, in two directions.

First, the price-dividend ratio, expected returns and the riskless rate can be found in closed form in the case in which log dividends follow drifting Brownian motions. See section 4. Second, analytic solutions can be found for the case in which the asset of interest is negligibly small relative to the aggregate market. In this case, closed forms can be obtained for general dividend processes. Moreover, an interesting phenomenon emerges: a negligibly small idiosyncratic asset can earn positive excess returns. See section 6.

For analytic purposes such as these, it is more convenient to work with the state variable u , a monotonic transformation of s which is defined by

$$u = \log\left(\frac{1-s}{s}\right) = y_{20} - y_{10}$$

While s ranges between 0 and 1, u takes values between $-\infty$ and $+\infty$. As asset 1 becomes small, u tends to infinity; as asset 1 becomes large, u tends to minus infinity.

Proposition 2 (The general pricing formula, alternative version). *In terms of the state variable u , the price-dividend ratio on a generic asset which pays dividend stream $D_{\alpha,t} \equiv D_{1t}^{\alpha_1} D_{2t}^{\alpha_2}$ is given by the expression*

$$\frac{P_{\alpha}}{D_{\alpha}}(u) = [2 \cosh(u/2)]^{\gamma} \cdot \int_{-\infty}^{\infty} \frac{e^{iuv} \mathcal{F}_{\gamma}(v)}{\rho - \mathbf{c}(\alpha_1 - \gamma/2 - iv, \alpha_2 - \gamma/2 + iv)} dv \quad (14)$$

or equivalently by

$$\frac{P_{\alpha}}{D_{\alpha}}(u) = \frac{\int_{-\infty}^{\infty} \frac{e^{iuv} \mathcal{F}_{\gamma}(v)}{\rho - \mathbf{c}(\alpha_1 - \gamma/2 - iv, \alpha_2 - \gamma/2 + iv)} dv}{\int_{-\infty}^{\infty} e^{iuv} \mathcal{F}_{\gamma}(v) dv} \quad (15)$$

Proof. See Appendix B. □

Equation (15) will be used, in Section 6, for thinking about limiting price-dividend ratios as an asset becomes small: that is, for considering the limit $u \rightarrow \infty$. Both the numerator and denominator of (15) tend to zero in this limit, while their ratio may tend to a finite positive quantity or to infinity.

3.2 Returns

An expression for the expected return on a general asset paying dividend stream $D_{\alpha,t}$ can be found in terms of integrals very similar to those that appear in the general price-dividend formula. The instantaneous expected return on the α -asset is defined by

$$R_{\alpha} dt \equiv \underbrace{\frac{\mathbb{E}dP_{\alpha}}{P_{\alpha}}}_{\text{capital gains}} + \underbrace{\frac{D_{\alpha}}{P_{\alpha}} dt}_{\text{dividend yield}} \quad (16)$$

Proposition 3 (Expected returns). R_{α} , the instantaneous expected return on an asset which pays dividend stream $D_{1t}^{\alpha_1} D_{2t}^{\alpha_2}$, is given as a function of the state variable u by

$$R_{\alpha}(u) = \frac{\sum_{m=0}^{\gamma} \binom{\gamma}{m} e^{-mu} \int_{-\infty}^{\infty} h(v) e^{iuv} \cdot \mathbf{c}(\mathbf{w}_m(v)) dv}{\sum_{m=0}^{\gamma} \binom{\gamma}{m} e^{-mu} \int_{-\infty}^{\infty} h(v) e^{iuv} dv} + \frac{D_{\alpha}}{P_{\alpha}}(u). \quad (17)$$

where

$$h(v) \equiv \frac{\mathcal{F}_{\gamma}(v)}{\rho - \mathbf{c}(\alpha_1 - \gamma/2 - iv, \alpha_2 - \gamma/2 + iv)}, \quad (18)$$

and

$$\mathbf{w}_m(v) \equiv (\alpha_1 - \gamma/2 + m - iv, \alpha_2 + \gamma/2 - m + iv)'$$

An analogous formula written in terms of the state variable s can be obtained by substituting $(1-s)/s$ for e^u throughout (17).

Proof. Appendix B contains the details of the capital gains calculation. The dividend yield component is given by the reciprocal of (14). \square

3.3 Interest rates

The calculations of sections 3.1 and 3.2 deal with assets which pay a constant stream of dividends. This section calculates zero coupon bond prices and yields.

First, some notation. I write B_T for the time-0 price of a zero-coupon bond which pays one unit of the consumption good at time T . The (zero-coupon) yield to time $T > 0$, $\mathcal{Y}(T)$, is defined by

$$B_T = e^{-\mathcal{Y}(T) \cdot T}.$$

Interest rates are not constant in this economy unless the two assets have identical, perfectly correlated, output processes. For example, the prices of perpetuities and zero coupon bonds fluctuate over time. Define, therefore, the instantaneous riskless rate, r , by

$$r \equiv \lim_{T \downarrow 0} \mathcal{Y}(T).$$

The following Proposition summarizes the behavior of real interest rates, in terms of the state variable u .

Proposition 4 (Real interest rates). *The yield to time T is*

$$\mathcal{Y}(T) = \rho - \frac{1}{T} \log \left\{ [2 \cosh(u/2)]^{\gamma} \int_{-\infty}^{\infty} \mathcal{F}_{\gamma}(v) e^{iuv} \cdot e^{\mathbf{c}(-\gamma/2 - iv, -\gamma/2 + iv)T} dv \right\}. \quad (19)$$

The instantaneous riskless rate is

$$r = [2 \cosh(u/2)]^\gamma \int_{-\infty}^{\infty} \mathcal{F}_\gamma(v) e^{iuv} \cdot [\rho - \mathbf{c}(-\gamma/2 - iv, -\gamma/2 + iv)] dv. \quad (20)$$

As always, we can substitute $(1 - s)/s$ for e^u , wherever it occurs, to express yields and the riskless rate in terms of the output share s .

Proof. See Appendix B. □

Equation (19) describes the term structure of interest rates in terms of the state variable u . Depending on the particular stochastic process driving dividends, the model can generate upward- or downward-sloping curves and humped curves with a local maximum.

4 The Brownian motion case

When dividends follow geometric Brownian motions,⁷ closed-form solutions can be obtained.

The resulting expressions are rather complicated and not obviously more informative than the more general (14), which applies equally well to non-Brownian dividend processes, and for this reason I do not supply formulas for expected returns and the riskless rate, although these can be calculated after some algebra. Nonetheless, the solution technique suggests a way to pick parameters carefully—say, to choose ρ carefully—in order to obtain far simpler closed-form expressions. I discuss this possibility in Appendix D.1.

Suppose, then, that log dividend processes are driven by a pair of Brownian motions,

$$dy_i = \mu_i dt + \sqrt{\sigma_{ii}} dz_i, \quad (21)$$

where dz_1 and dz_2 may be correlated: $dz_1 dz_2 = \sigma_{12} dt$.

We have the following result.

Proposition 5 (The Brownian motion case). *When log dividends are determined by equation (21), the price-dividend ratio of asset 1 is given by*

$$P/D_1(s) = \frac{1}{B(\lambda_1 - \lambda_2)} \left[\frac{1}{(\gamma/2 + \lambda_1) s^\gamma} F\left(\gamma, \gamma/2 + \lambda_1; 1 + \gamma/2 + \lambda_1; \frac{s-1}{s}\right) + \frac{1}{(\gamma/2 - \lambda_2) (1-s)^\gamma} F\left(\gamma, \gamma/2 - \lambda_2; 1 + \gamma/2 - \lambda_2; \frac{s}{s-1}\right) \right] \quad (22)$$

As before, $F(a, b; c; z)$ is Gauss's hypergeometric function.

⁷Under the Lévy process assumption, this is the unique case in which dividends are not subject to jumps. See Rogers and Williams (2000, pp. 76–77) for a proof.

The variables λ_1, λ_2 and B are given by

$$B \equiv \frac{1}{2}X^2 \quad (23)$$

$$\lambda_1 \equiv \frac{\sqrt{Y^2 + X^2 Z^2} - Y}{X^2} \quad (24)$$

$$\lambda_2 \equiv -\frac{\sqrt{Y^2 + X^2 Z^2} + Y}{X^2}, \quad (25)$$

where

$$X^2 \equiv \sigma_{11} - 2\sigma_{12} + \sigma_{22} \quad (26)$$

$$Y \equiv \mu_1 - \mu_2 + \sigma_{11} - \sigma_{12} - \frac{\gamma}{2}(\sigma_{11} - \sigma_{22}) \quad (27)$$

$$Z^2 \equiv 2(\rho - \mu_1 - \sigma_{11}/2) + \gamma(\mu_1 + \mu_2 + \sigma_{11} + \sigma_{12}) - \frac{\gamma^2}{4}(\sigma_{11} + 2\sigma_{12} + \sigma_{22}); \quad (28)$$

as the notation suggests, X^2 and Z^2 are strictly positive.

Proof. See Appendix D. □

This result generalizes the result of Cochrane, Longstaff and Santa-Clara (2007) (equation (50) in their paper) to allow for γ higher than one. It can be modified to supply the price-dividend ratio on asset 2 in the obvious manner: switch subscripts 1 and 2 throughout the definitions (26)–(28) and map $s \mapsto 1 - s$ in (22).

5 Two calibrations

I now present two simple calibrations. In each, the representative agent has time discount rate $\rho = 0.03$ and relative risk aversion $\gamma = 4$.

5.1 Dividends follow geometric Brownian motions

To explore the distinctive features of the model in a setting that is as simple as possible, consider a calibration in which the two assets are independent and have dividends which follow geometric Brownian motions. Each has mean log dividend growth of 2% and dividend volatility of 10%. In the notation of equation (3), $\mu_1 = \mu_2 = 0.02$, $\sigma_{11} = \sigma_{22} = 0.1^2$ and $\sigma_{12} = 0$.

Although the dividend processes for the individual assets are i.i.d., consumption is *not* i.i.d., as documented in Figure 2. In this calibration, both assets have the same mean dividend growth, so mean consumption growth does not vary with s . But the standard deviation of consumption growth does vary: it is lower “in the middle”, where there is most diversification. At the edges, where s is close to 0 or to 1, one of the two assets dominates

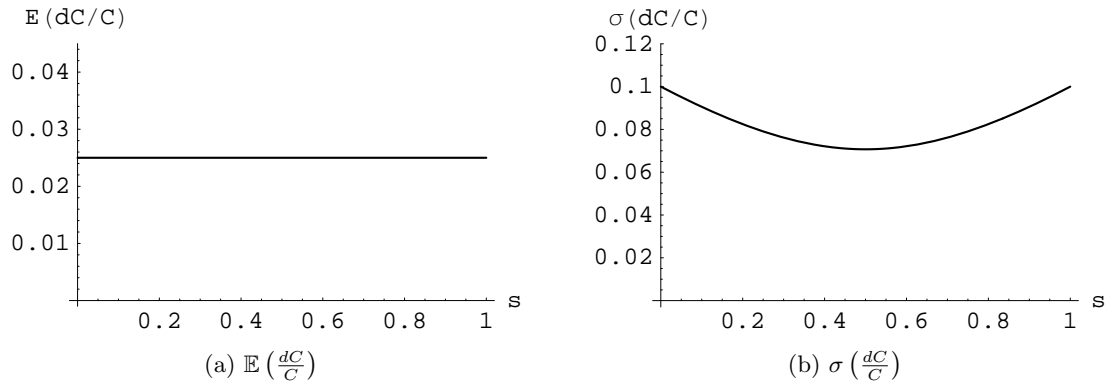


Figure 2: Left: Mean consumption growth, $\mathbb{E}(dC/C)$, against asset 1's dividend share, s . Right: The standard deviation of consumption growth, $\sigma(dC/C)$, against s .

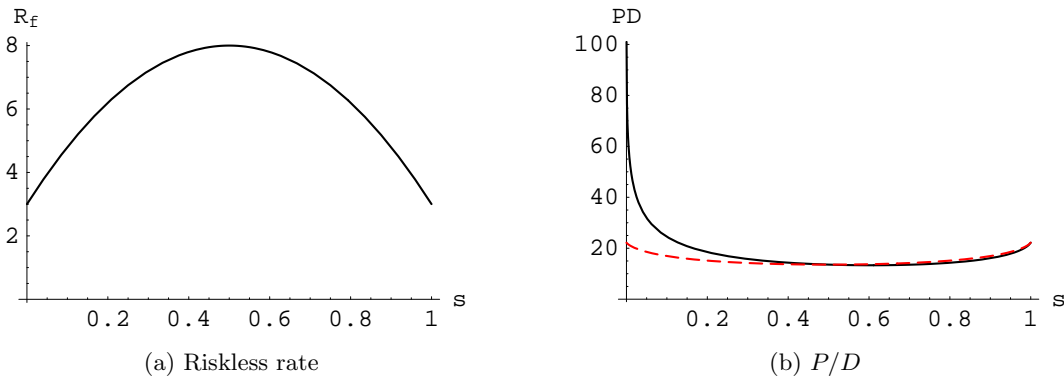


Figure 3: Left: The riskless rate against s . Right: The price-dividend ratio of asset 1 (solid) and of the market (dashed) against s .

the economy, and consumption growth is more volatile: the representative agent's eggs are all in one basket.

Time-varying consumption growth volatility leads to a time-varying riskless rate. Figure 3a plots the riskless rate against asset 1's share of output s . Riskless rates are high for intermediate values of s because consumption volatility is low, which diminishes the motive for precautionary saving.

The right-hand graph, Figure 3b, shows the price-dividend ratio of asset 1 (solid) and of the market (dashed).⁸ When asset 1 is a small part of the market, it has very high valuations— P/D shoots up to the left of the figure—because it has very little systematic

⁸The market price-dividend ratio is calculated by observing that

$$\frac{P_1 + P_2}{D_1 + D_2} = s \cdot \frac{P_1}{D_1} + (1 - s) \cdot \frac{P_2}{D_2}.$$

risk. As asset 1's share increases from $s = 0$, its discount rate increases both because the riskless rate increases and because its risk premium increases, as discussed further below.

Another notable feature of figure 3b is that the model predicts the existence of extreme growth assets (at the left of the figure) but not of extreme value assets. This extreme growth case is of particular interest because it represents the most radical departure from a constant discount rate framework in which price-dividend ratios are constant; I explore it in detail in section 6.

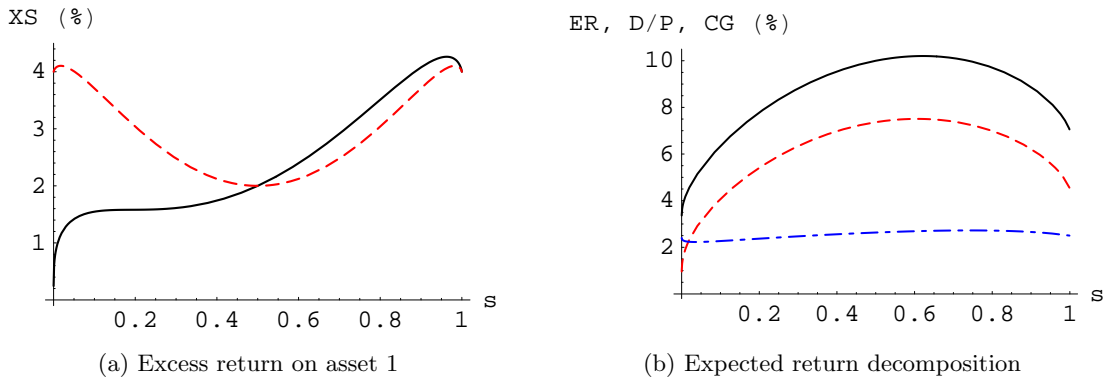


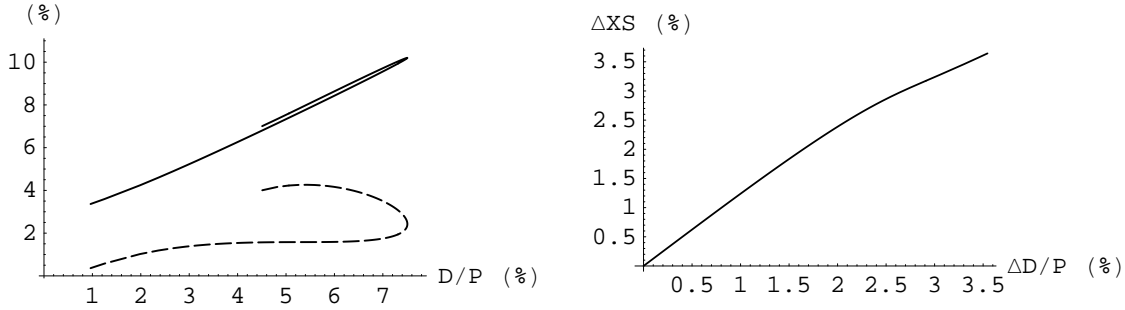
Figure 4: Left: The excess return on asset 1 (solid) and on the market (dashed), against s . Right: Decomposition of expected returns (solid) into dividend yield (dashed) and expected capital gains (dot-dashed).

Figure 4a shows how the risk premium on asset 1 and on the market depends on the state variable s . Due to the diversification effect discussed above, the market risk premium is smallest when the two assets are of equal size. The risk premium on asset 1 increases as asset 1's dividend share increases. In the limit as s tends to zero, the risk premium on asset 1 tends to zero. The figure shows, however, that in this calibration even very small assets earn economically significant risk premia. In other calibrations, asset can earn strictly positive risk premia even in the limit in which they become negligible; see Section 6.

A comparison of figures 3b and 4a reveals that there is a value-growth effect: assets with high valuations earn low excess returns.

Figure 4b decomposes expected returns into a dividend yield component and an expected capital gains component. In this calibration, almost all cross-sectional variation in expected returns can be attributed to cross-sectional differences in dividend yield.

Figure 5a makes this point in a different way, by plotting expected returns and risk premia against dividend yield. Figure 5b demonstrates that the excess return on a zero-cost investment in a value-minus-growth portfolio is increasing in the value spread (that is, the difference in dividend yield between the value and the growth asset). This echoes the empirical finding of Cohen, Polk and Vuolteenaho (2003) that “the expected return

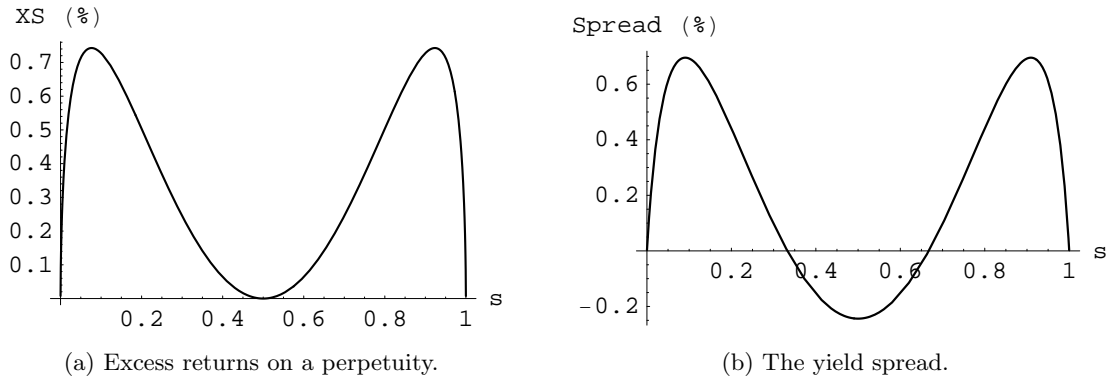


(a) Expected returns and expected excess returns on asset 1 against D/P .

(b) Expected excess returns on the value-minus-growth strategy, plotted against the value spread.

Figure 5: Left: Expected returns (solid) and expected excess returns (dashed) on asset 1 against asset 1's dividend yield. Right: Expected excess return on the value-minus-growth strategy against the value spread.

on value-minus-growth strategies is atypically high at times when their spread in book-to-market ratios is wide.”



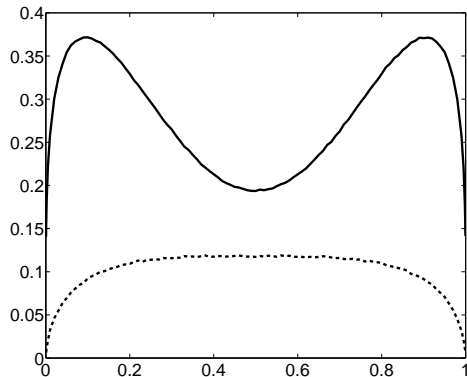
(a) Excess returns on a perpetuity.

(b) The yield spread.

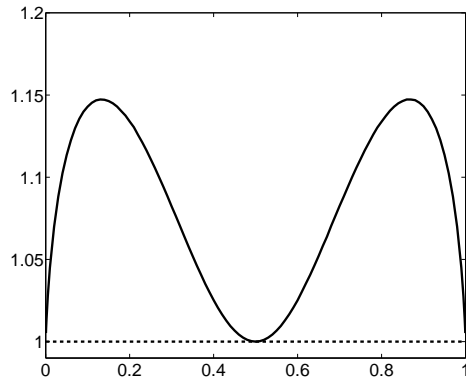
Figure 6: A high yield spread, $\mathcal{Y}(30) - \mathcal{Y}(0)$, signals high expected excess returns on a perpetuity.

It is also of interest to consider the behavior of assets in zero net supply, such as perpetuities and zero coupon bonds. Figure 6a plots the risk premium on a real perpetuity which pays one unit of consumption good per unit time. Figure 6b shows how the spread in yields between a 30-year zero-coupon bond and the instantaneous riskless rate varies with s . A high yield spread forecasts high excess returns on long-term bonds. Looking back at figure 4a, we see that a high yield spread also forecasts high excess returns on the market.

Figure 7a demonstrates that the model generates significant comovement between the



(a) Correlation between asset returns.



(b) Excess volatility on the market.

Figure 7: Left: The correlation between the returns of asset 1 and asset 2 against s . Right: The ratio of market return volatility to dividend volatility against s . Solid lines, $\gamma = 4$; dashed lines, $\gamma = 1$.

returns of the two assets, even though the two assets have independent fundamentals.⁹ There is considerably more comovement when $\gamma = 4$ than in the log utility case. Figure 7b shows that the model generates excess volatility in the aggregate market when $\gamma > 1$. (When $\gamma = 1$ —the log utility case, indicated with a dashed line—there is no excess volatility because the price-dividend ratio of the aggregate market is constant. For the same reason, there is no excess volatility in the $\gamma = 4$ case when $s = 1/2$: the market price-dividend ratio is locally flat, as a function of s , at this point.)

What drives asset 1’s returns? In the two-asset case, two types of shock move an asset’s price: a shock to its dividends, or a shock to the other asset’s dividends, which changes the asset’s price by changing its price-dividend ratio. In the terminology of Campbell (1991), the first type of shock corresponds to the arrival of “cashflow news” and the second to the arrival of “discount-rate news”. Figure 8a plots the percentage price response of asset 1 (solid) and asset 2 (dashed) to a 1% increase in asset 1’s dividends. When asset 1 is small, it

⁹These figures, unlike the preceding ones, are calculated by Monte Carlo methods, as follows. For each of 109 different starting values of $s \in [0, 1]$, I generate 4000 sample paths of log dividends. (The 109 different values are the points 0.01, 0.02, ..., 0.99, five points between 0 and 0.01 and five points between 0.99 and 1.) Each sample path simulates a drifting Brownian motion over a very short time horizon: 3×10^{-5} years, slightly less than 16 minutes. Over this time horizon, each drifting Brownian motion is simulated by dividing the interval into 600 time steps; Normal random variables determine the evolution of log dividends between these time steps. Given a particular sample path for dividends, prices can be calculated, given the price-dividend functions; and hence also total returns, and the covariance matrix of realized returns on the two assets. Finally, I estimate variances and covariance between the two assets, at each value of s , by averaging over the covariance matrices estimated for each of the 4000 sample paths.

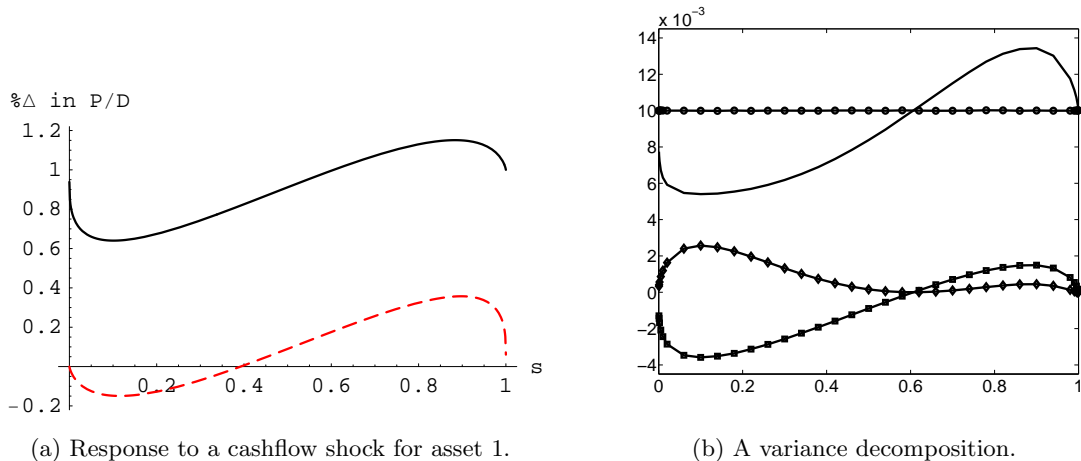


Figure 8: Left: The response of asset 1 (solid) and asset 2 (dashed) to a +1% increase in the dividend of asset 1. Right: Decomposition of the variance of returns (solid) into three parts: the variance of dividend-driven returns (circles), the variance of valuation-driven returns (diamonds) and the covariance between the two types of returns (squares).

underreacts to good news about its own cashflow shock: the price response is considerably less than 1%. At the same time, asset 2 moves in the opposite direction. When asset 1 is large, it overreacts to good news about its own cashflow shock, and asset 2 moves in the same direction. Note also that asset 2’s price moves considerably more, in response to dividend news for asset 1, when asset 1 is large than when asset 1 is small.

A better understanding of these effects can be gained by exploiting a simple identity that breaks realized returns on any asset into two pieces:

$$\begin{aligned}
 R_{t+1} &= \frac{P_{t+1} + D_{t+1}}{P_t} \\
 &= \underbrace{\frac{D_{t+1}}{D_t} \left(1 + \frac{D_t}{P_t}\right)}_{\text{dividend-driven}} + \underbrace{\frac{D_{t+1}}{D_t} \frac{D_t}{P_t} \left(\frac{P_{t+1}}{D_{t+1}} - \frac{P_t}{D_t}\right)}_{\text{valuation-driven}} \\
 &\equiv R_{D,t+1} + R_{V,t+1}. \tag{29}
 \end{aligned}$$

The last line defines the *dividend-driven return* $R_{D,t+1}$ and the *valuation-driven return* $R_{V,t+1}$. In an economy in which price-dividend ratios are constant—for example, one with a single Lucas tree with i.i.d. dividend growth and a representative agent with power utility or Epstein-Zin preferences—the valuation-driven component disappears, and returns are exclusively dividend-driven. The above identity holds exactly, with no log-linearizations needed. It is similar to the decomposition of Campbell (1991), but changes in price-dividend

ratio appear on the right-hand side of (29), as opposed to the changes in future returns that appear in Campbell's decomposition.¹⁰

Using the decomposition in (29), we have

$$\text{var}_t R_{t+1} = \text{var}_t R_{D,t+1} + \text{var}_t R_{V,t+1} + 2 \text{cov}_t(R_{D,t+1}, R_{V,t+1}), \quad (30)$$

an equation that provides another way to think about the sources of variation in expected returns.

In the continuous-time case relevant for the purposes of this paper, the above equations are modified slightly: we have

$$R_{t+dt} = \frac{D_{t+dt}}{D_t} \left(1 + \frac{D_t}{P_t} dt \right) + \frac{D_{t+dt}}{D_t} \frac{D_t}{P_t} \left(\frac{P_{t+dt}}{D_{t+dt}} - \frac{P_t}{D_t} \right),$$

and again the first term on the right-hand side can be thought of as the dividend-driven return $R_{D,t+dt}$ and the second as the valuation-driven return $R_{V,t+dt}$.

I estimate the three components, $\text{var}_t R_{D,t+dt}$, $\text{var}_t R_{V,t+dt}$, and $\text{cov}_t(R_{D,t+dt}, R_{V,t+dt})$ by simulating the underlying Brownian processes as described in Footnote 9. The results are shown in figure 8b. The figure shows that (i) most of the variance in asset returns is driven by cash-flow news, (ii) dividend-driven returns and valuation-driven returns are negatively correlated for small assets and positively correlated for large assets,¹¹ (iii) for large assets, a far higher proportion of variation in expected returns is due to cashflow news than to discount rate news, while (iv) for small assets, valuation-driven returns are much more important: the variance of dividend-driven returns is only about four times higher than the variance of valuation-driven returns.

Appendix G contains some supplementary figures. Figure 17 plots the probability that the dividend share at time t , s_t , remains in the region $[0.2, 0.8]$ for t between 0 and 200 years, and for starting shares $s_0 = 0.1, 0.3, 0.5$. (The cases $s_0 = 0.7, 0.9$ can also be read off the graph, because the world is symmetric.) It also plots the value weight of asset 1 in the aggregate market against s .

5.2 Dividends are subject to occasional disasters

The second calibration is intended to highlight the effect of disasters. Again, the two assets are symmetric. In the notation of equation (3), the drifts are $\mu_1 = \mu_2 = 0.02$. The two Brownian motions driving dividends are independent and each has volatility of 2%, so $\sigma_{11} = \sigma_{22} = 0.02^2$ and $\sigma_{12} = 0$.

¹⁰It also has the advantage that the two components can be estimated directly from historical data.

¹¹In the language of Campbell (1991), cashflow news and discount-rate news are *positively* correlated for small assets and negatively correlated for large assets.

There are also jumps in dividends, caused by the arrival of disasters, of which there are three types. One type affects only asset 1: it arrives at times dictated by a Poisson process with rate $0.017/2$. When the disaster strikes, it shocks log dividends by a Normal random variable with mean -0.38 and standard deviation 0.25 . The second is exactly the same, except that it affects only asset 2. The third type arrives at rate $0.017/2$ and shocks the log dividends of *both* assets by the same amount,¹² which is, again, a random variable with mean -0.38 and standard deviation of 0.25 . If the two assets are thought of as claims to a country's output, then the first two types are examples of local disasters while the third is a global disaster.

From the perspective of either asset, then, disasters occur at rate $0.017/2 + 0.017/2 = 0.017$: on average, about once every 60 years. There is a 50-50 chance that any given disaster is local or global. These disaster arrival rates—and the mean and standard deviation of the disaster sizes—are chosen to match exactly the empirical disaster frequency estimated by Barro (2006), and to match approximately the disaster size distribution documented in the same paper.

Taking everything into account, these parameter values imply an unconditional mean dividend growth rate (in levels, not logs) of 1.6%. Conditional on disasters not occurring, the mean dividend growth rate is 2.0%.

Figure 9 exhibits the central features of asset prices and returns in this calibration. In broad outline, the pictures are very similar to those presented previously—and for the same reasons—but some new features stand out. The riskless rate is lower across the range of values of s . Also, despite considerably lower Brownian volatility, the presence of jumps induces a higher risk premium, both at the individual asset level and at the market level. As in Rietz (1988) and Barro (2007), incorporating rare disasters makes it easier to match the observed riskless rate and equity premium. A more unusual feature is that disasters can propagate to apparently safe assets: since the state variable can jump, interest rates can jump, and hence bond prices can jump. Consequently, at times when the current riskless rate is low (for $s \approx 0$ or $s \approx 1$), the risk premium on a perpetuity is significantly higher than previously, despite the fact that disasters do not affect its cashflows. A perpetuity earns a negative risk premium near $s = 1/2$, since in this state long-dated bonds act as a hedge against disasters: when a disaster strikes one of the assets, s jumps either up or down, riskless rates drop sharply and the price of a long-dated bond jumps up.¹³

¹²These disasters are therefore simultaneous and of perfectly correlated—in fact, identical—sizes; the framework also easily handles the case in which disasters are simultaneous but uncorrelated or imperfectly correlated.

¹³Various other figures are in Appendix G: the expected return decomposition, the plot of expected returns and risk premia against dividend yield, a figure showing price responses to a 1% dividend shock to asset 1, and the yield spread. The qualitative features are substantially the same as in the previous calibration in

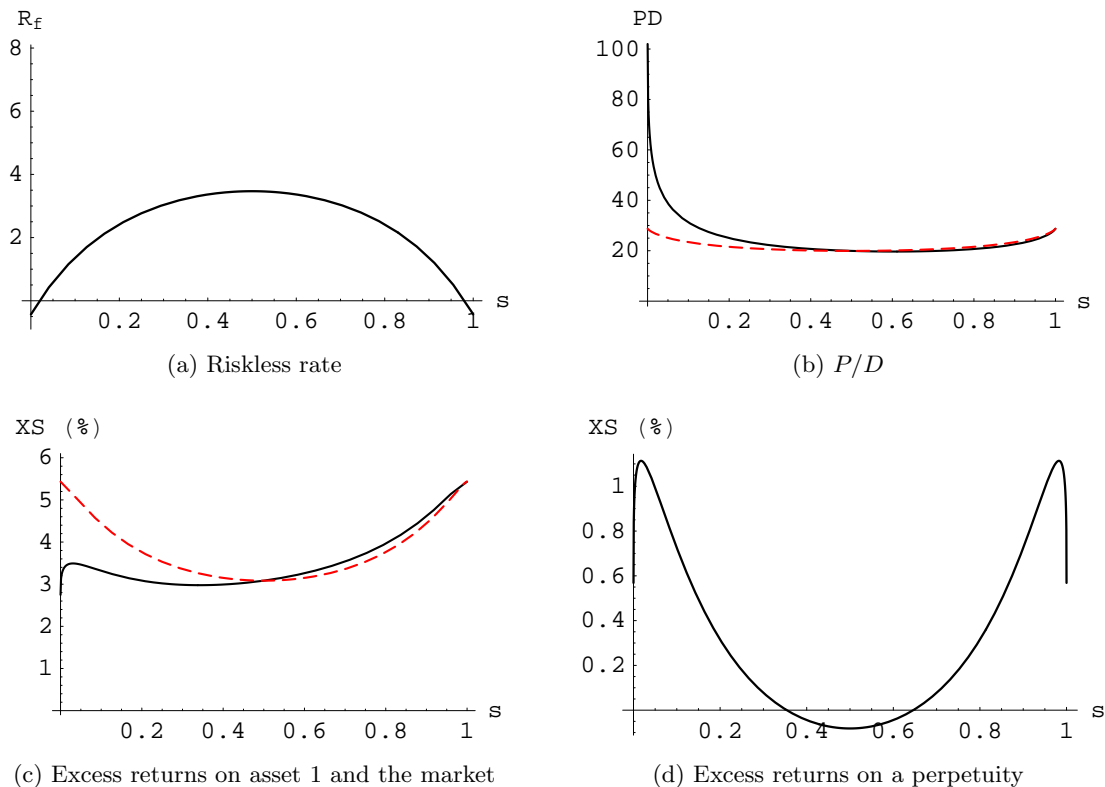


Figure 9: The riskless rate; price-dividend ratio on asset 1 (solid) and on the market (dashed); excess returns on asset 1 (solid) and on the market (dashed); and excess returns on a perpetuity.

In the presence of jumps, the cross-asset effects present in the previous calibration become more pronounced. Notably, disasters propagate across assets.

This is shown graphically in Figure 10, which plots a single sample time series. Time, along the x -axis, runs from 0 to 60 years. The sequence of figures should be read clockwise, starting from the top left. Asset 1 (in red) is the small asset—with an initial dividend share of 10%. Asset 2 is shown in black. From exogenous dividend processes we calculate the state variable, the dividend share of asset 1, and hence price-dividend ratios. Finally, from dividends and price-dividend ratios, we calculate prices.

In the particular realization shown here, each asset suffers one negative shock to fundamentals; there is no “global” shock. When the large asset suffers its disaster, after about 26 years, its dividend drops by 25% and its price drops by 28%. Two forces act on the small asset. A disaster to the large asset makes the economy more balanced, so riskless rates jump up; at the same time, the risk premium on the small asset jumps up because it

each case. In the case of price responses to a cashflow shock, the graph is quantitatively very similar too.

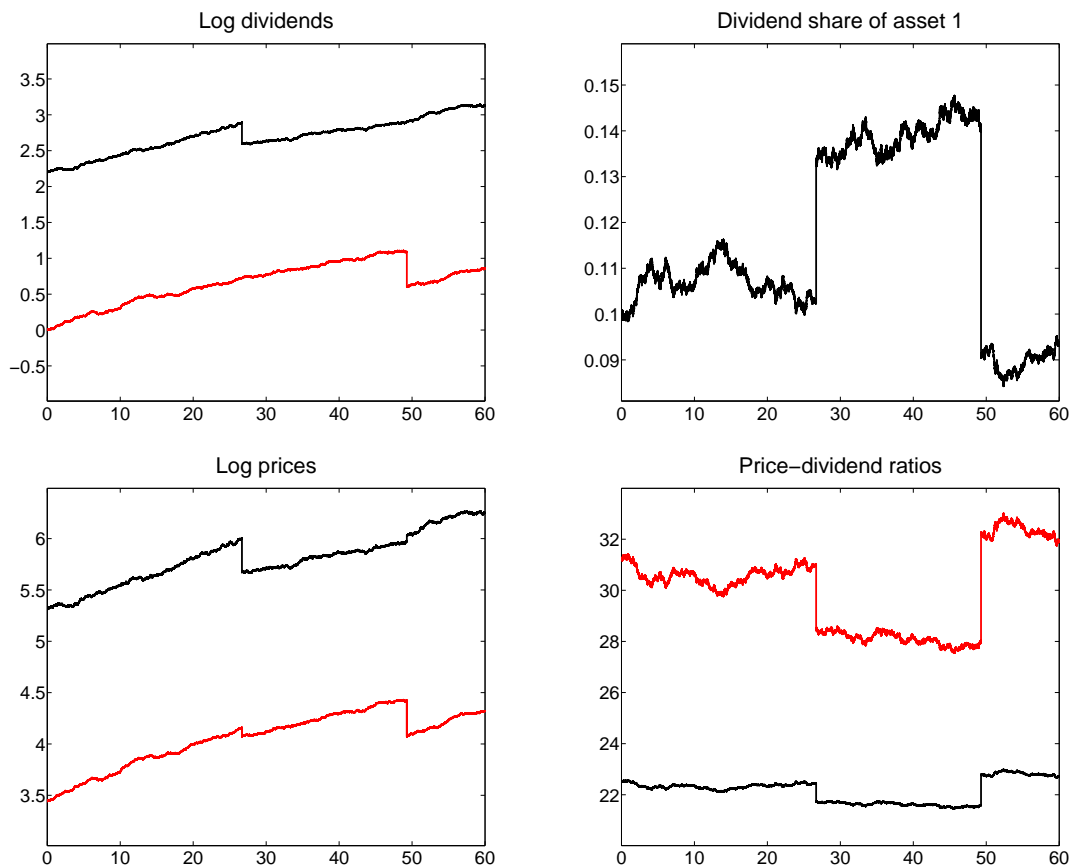


Figure 10: Dividends, the dividend share, prices and price-dividend ratios in a time series featuring contagion and flight-to-quality. The figures should be read in clockwise order from the top left. Asset 1, the small asset, is shown in red. Asset 2 is in black.

is a larger part of the economy. These effects act in the same direction, and the small asset experiences a downward price jump of 8.2%: contagion.

When the small asset suffers its disaster, after about 49 years, its dividend drops by 39% and its price drops by 30%. Now, two *opposing* forces act on the large asset. On one hand, its risk premium rises as it is a larger share of the market. On the other, the riskless rate declines in response to the increasingly unbalanced world. The riskless rate effect dominates, and the large asset experiences an upward price jump of 5.7%: flight-to-quality.

We can also calculate rolling 1-year realized return correlations along this sample path, as shown in Figure 11. During normal times, the correlation hovers around 0.3, despite the fact that, conditional on no jumps, the two assets have independent dividend streams. When the first disaster (“contagion”) takes place, the measured correlation spikes up almost as far as +1 due to the spectacular outlying return. When the second disaster (“flight-to-

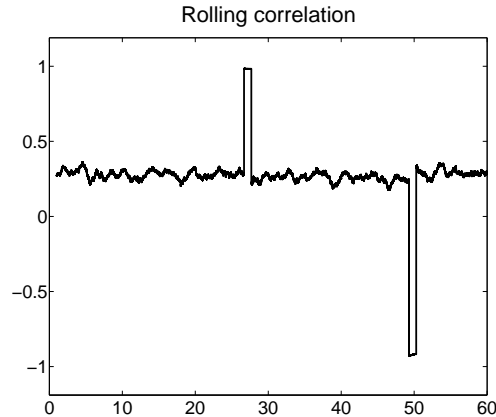


Figure 11: The one-year rolling correlation between assets 1 and 2, calculated along the sample path of Figure 10.

quality”) takes place, the measured correlation spikes down almost as far as -1 . Despite the fact that naively calculated correlations display occasional spikes, the correlation between the two assets, conditional on some given s , is constant over time—and is economically significant even if one conditions on jumps not taking place. These results are therefore reminiscent of the findings of Forbes and Rigobon (2002), who demonstrate that although naively calculated correlations spike at times of crisis, once one corrects for the heteroskedasticity induced by high market volatility at times of crisis, it can be seen that markets have a high level of “interdependence” in all states of the world.

In Appendix G, I show that *both* high risk aversion (γ at least about 4) and rare disasters are needed to get reasonable numbers out of this model, assuming we restrict to Brownian volatility parameters (here, $\sigma_{11} = \sigma_{22} = 0.02^2$) which are standard in the consumption-based asset pricing literature.

The results of these two, rather different, calibrations give some reassurance that the magnitude and broad qualitative outline of the results obtained do not depend on carefully tuned parameter values.

6 Extreme growth assets

A distinctive qualitative prediction of the model is that there should exist extreme growth assets, but not extreme value assets. (Look back at the left-hand side of Figure 3b.) The extreme growth case also represents the starkest departure from simple models in which price-dividend ratios are constant (as, for example, in a one-tree model with power utility and i.i.d. dividend growth). Furthermore, it is important to understand whether the com-

plicated dynamics exhibited above are relevant for small assets.¹⁴ These considerations lead me to investigate the price behavior of asset 1 in the limit $s \rightarrow 0$ in which it becomes tiny relative to the rest of the market (that is, asset 2).

To preview the results, consider the problem of pricing a negligibly small asset, whose fundamentals are independent of all other assets, in an environment in which the (real) riskless rate is 6%. If the small asset has mean dividend growth rate of 4%, the following logic seems plausible. Since the asset is negligibly small, it need not earn a risk premium, so the appropriate discount rate is the riskless rate. Next, since dividends are supposed throughout to be i.i.d., it seems sensible to apply the Gordon growth model to conclude that for this small asset,

$$\begin{aligned} \text{dividend yield} &= \text{riskless rate} - \text{mean dividend growth} \\ &= 6\% - 4\% \\ &= 2\%. \end{aligned}$$

It turns out that this argument can be made formal; I do so below.

Now, consider the (more realistic) situation in which the riskless real rate is 2%. If the asset does not earn a risk premium, Gordon growth logic seems to suggest that the dividend yield should be $2\% - 4\% = -2\%$, an obviously nonsensical result. I show below how to value assets in situations such as these, in which the Gordon growth model breaks down. In the limit, such an asset has a price-consumption ratio of zero, as one would expect. More surprisingly, though, it has an infinite price-dividend ratio—reminiscent of Pástor and Veronesi (2003, 2006)—and a strictly positive risk premium. Moreover, since the dividend yield is zero, expected returns on the asset are entirely attributable to expected capital gains.

I now return to the general setup in which the assets may have correlated dividend growth and make a pair of definitions.

Definition 2. *If the inequality*

$$\rho - \mathbf{c}(1, -\gamma) > 0 \tag{31}$$

holds then we are in the subcritical case.

If the reverse inequality

$$\rho - \mathbf{c}(1, -\gamma) < 0 \tag{32}$$

*holds then we are in the supercritical case.*¹⁵

¹⁴This is analogous to the “small-country case” in international finance.

¹⁵There is also a third case, the *critical* case in which $\rho - \mathbf{c}(1, -\gamma) = 0$; I omit it for the sake of brevity. Briefly, price-dividend ratios are asymptotically infinite and excess returns asymptotically zero, assuming independent dividend growth. The simple example presented in Section 1 of Cochrane, Longstaff and Santa-Clara (2007) is precisely critical. This is no coincidence: the condition that implies criticality also ensures that the expression for the price-dividend ratio is relatively simple. See Appendix D.1.

In the supercritical case, define θ^* to be the unique $\theta \in (0, 1)$ which satisfies

$$\rho - \mathbf{c}(1 - \theta, \theta - \gamma) = 0. \quad (33)$$

In the supercritical case we have $\theta^* \in (0, 1)$ because equation (33) is negative at $\theta = 0$ by (32) and positive at $\theta = 1$ by the finiteness assumptions in Table 1. In the Brownian motion case, (33) is simply a quadratic equation in θ . More generally, the fact that the solution is unique follows from the fact, proved in Appendix E, that $\rho - \mathbf{c}(1 - \theta, \theta - \gamma)$ is a concave function of θ .

The next two Propositions supply various asymptotics, which depend on θ^* in the supercritical case. To highlight the link with the traditional Gordon growth formula, I write $G_1 \equiv \mathbf{c}(1, 0) = \log \mathbb{E}D_{11}/D_{10}$ and $G_2 \equiv \mathbf{c}(0, 1) = \log \mathbb{E}D_{21}/D_{20}$ for (log) mean dividend growth, and R_1 and R_2 for the expected instantaneous returns on assets 1 and 2.

Proposition 6. *In the subcritical case, in the limit as $s \downarrow 0$, we have*

$$R_f = \rho - \mathbf{c}(0, -\gamma) \quad (34)$$

$$R_1 = \rho - \mathbf{c}(1, -\gamma) + \mathbf{c}(1, 0) \quad (35)$$

$$D/P_1 = R_1 - G_1 \quad (36)$$

If the two assets are independent, then in this limit

$$R_f = R_1 < R_2. \quad (37)$$

Proof. See Appendix E. □

The results of Proposition 6, correspond to the first example above. A small idiosyncratic asset with i.i.d. dividend growth can be valued with the Gordon growth model (36). Moreover, (37) shows that the expected return that is plugged into the Gordon growth model is the riskless rate: the asset earns no risk premium. The next result shows that this is not the whole story, however. More intriguing behavior may emerge.

Proposition 7. *In the supercritical case, in the limit as $s \downarrow 0$, we have*

$$R_f = \rho - \mathbf{c}(0, -\gamma) \quad (38)$$

$$R_1 = \mathbf{c}(1 - \theta^*, \theta^*) \quad (39)$$

$$D/P_1 = 0 \quad (40)$$

If the two assets are independent, then in this limit

$$R_f < R_1 < R_2. \quad (41)$$

If $G_1 \geq G_2$, we have the additional bound $R_1 < G_1$.

Proof. See Appendix E. □

These results are much more surprising. To understand what is going on, consider the case in which dividend growth is independent across assets so that, as in the second example above, the risk in question is both small and idiosyncratic. Proposition 7 demonstrates that in the supercritical regime, such an asset has an enormous valuation ratio and earns a strictly positive risk premium.

A naive attempt to apply the Gordon growth model breaks down in the supercritical case because (32) holds and so the riskless rate minus dividend growth is *negative*. Nonetheless, the asymptotically small asset still has a well-defined dividend-price ratio and expected return, as demonstrated in Proposition 7. What happens to the price in the asymptotic limit?

The first point is that this is not quite the right question. Suppose that we are in the supercritical scenario, and imagine holding the dividend of asset 1 fixed while allowing the dividend of asset 2 (and hence total consumption) to increase without limit. Since s then tends to zero, this is one way asset 1 can become “small”. Because D_1 is held constant, the price of asset 1—measured, as always, in units of consumption—is unbounded in this limit. A more informative question is to ask for the asymptotic behavior of the price-consumption ratio.

Alternatively, imagine holding the dividend of asset 2 fixed while the dividend of asset 1, and hence s , tends to zero. The price-dividend ratio goes to infinity, but the dividend goes to zero: what happens to the price? The answer is that since consumption remains finite in this example, the price is zero, finite or infinite in the limit depending on whether the price-consumption ratio is zero, finite or infinite in the limit.

In short, it is useful to focus on the price-consumption ratio, $P/C = s \cdot P/D$. Appendix E shows that the fact that the price-consumption ratio is zero in the limit follows from the fact that $\theta^* < 1$.

Examination of the subcritical condition (31) and supercritical condition (32) reveals that the supercritical regime occurs whenever ρ is sufficiently small. More generally, the supercritical regime is relevant in environments in which the riskless rate is low.

I now exhibit these phenomena in the simple Brownian motion example considered earlier in the paper. This will make it clear that, first, the supercritical case is neither pathological nor dependent on extreme parameter values and, second, the size of the strictly positive excess return earned on the small asset in the supercritical case is economically meaningful. To recap, the world is symmetric, and the two assets are independent with 2% mean dividend growth and 10% dividend volatility.

As usual, $\gamma = 4$. If the time discount rate $\rho = 0.05$, then we are in the subcritical case.¹⁶

¹⁶In the calibration presented earlier, I set $\rho = 0.03$. This case is also subcritical. I have chosen to use

If on the other hand $\rho = 0.01$, we are in the supercritical case.

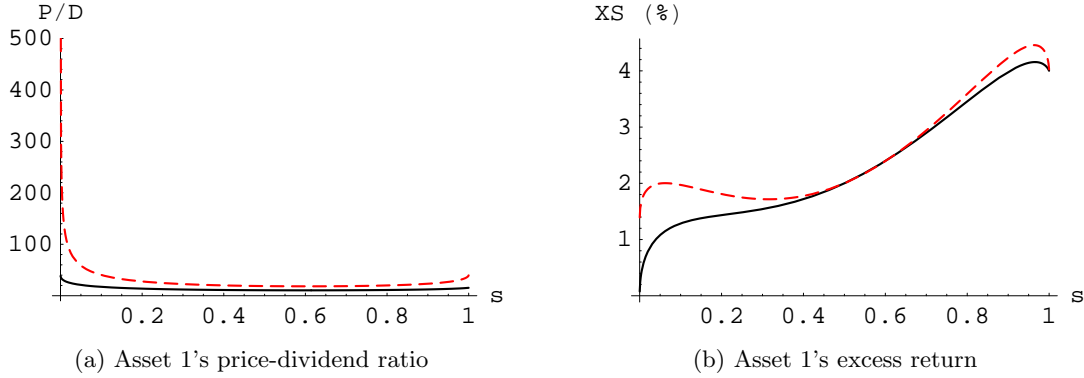


Figure 12: Left: Price-dividend ratio of asset 1 against s . Right: Excess return of asset 1 against s . Supercritical case is dashed, subcritical case is solid.

Figure 12 shows the price-dividend ratio and excess return of asset 1 against s . The asymptotic limits are to the left of the graph, as $s \downarrow 0$. In the subcritical case, the price-dividend ratio remains below 40 for all s and the excess return tends to zero. In the supercritical case, the price-dividend ratio explodes and the excess return tends to roughly 1.3 per cent. (Notice also that for intermediate values of the state variable, the risk premium on asset 1 is not sensitive to the value of ρ , as would be the case in a standard one-tree model.) Asymptotically, the dividend yield is zero, so all of the expected return of the small asset can be attributed to expected capital gains.

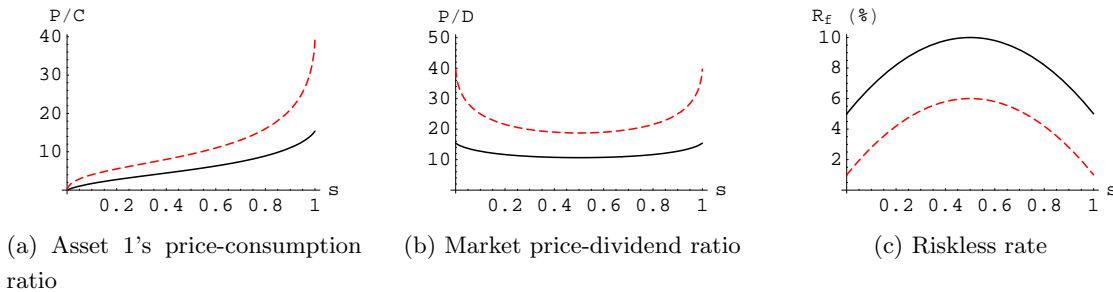


Figure 13: The price-consumption ratio of asset 1, market price-dividend ratio and riskless rate plotted against asset 1's share of output, s . Supercritical case is dashed, subcritical case is solid.

Finally, to allay suspicions that something strange is going on in the background, Figure 13 demonstrates that asset 1's price-consumption ratio, the market price-dividend ratio and the riskless rate are all well-behaved in the limit.

$\rho = 0.05$ here in order to make the distinction between the two cases clearer in the figures.

7 N assets

The general results presented in Section 3 can be generalized to the case in which the representative agent's consumption stream is provided by the output of N assets,

$$C_t = D_{1t} + D_{2t} + \cdots + D_{Nt}.$$

With this modification, equations (1)–(4) are unchanged, except that boldface vectors are now understood to have N entries, as opposed to just two. The fundamental ideas underlying the calculation are also the same. The main technical difficulty lies in calculating $\mathcal{F}_\gamma^N(\mathbf{v}) \equiv \mathcal{F}_\gamma^N(v_1, \dots, v_{N-1})$, the generalization of $\mathcal{F}_\gamma(v)$ to the N -tree case. It turns out that we have

$$\mathcal{F}_\gamma^N(\mathbf{v}) = \frac{\Gamma(\gamma/N + iv_1 + iv_2 + \cdots + iv_{N-1})}{(2\pi)^{N-1}\Gamma(\gamma)} \cdot \prod_{k=1}^{N-1} \Gamma(\gamma/N - iv_k). \quad (42)$$

Before stating the main result, it will be useful to recall some old, and to define some new, notation. Let \mathbf{e}_j be an N -vector with a one at the j th entry and zeros elsewhere, and define the N -vectors $\mathbf{y}_0 \equiv (y_{10}, \dots, y_{N0})'$ and $\boldsymbol{\gamma} \equiv (\gamma, \dots, \gamma)'$, and the $(N-1) \times N$ matrix \mathbf{U} and the $(N-1)$ -vector \mathbf{u} by

$$\mathbf{U} \equiv \begin{pmatrix} -1 & 1 & 0 & \cdots & 0 \\ -1 & 0 & 1 & \ddots & \vdots \\ \vdots & \vdots & \ddots & \ddots & 0 \\ -1 & 0 & \cdots & 0 & 1 \end{pmatrix} \quad \text{and} \quad \mathbf{u} \equiv \begin{pmatrix} u_2 \\ u_3 \\ \vdots \\ u_N \end{pmatrix} \equiv \mathbf{U}\mathbf{y}_0. \quad (43)$$

In the two-asset case, there was one state variable. We worked with s , the dividend share of asset one, or with $u = \log(1-s)/s = y_{20} - y_{10}$. With N assets, there are $N-1$ state variables. One natural set of state variables is $\{s_i\}$, $i = 1, \dots, N-1$, where

$$s_i = \frac{D_{i0}}{D_{10} + \cdots + D_{N0}}$$

is the dividend share of asset i ; in fact, though, it turns out to be more convenient to work with the $(N-1)$ -dimensional state vector \mathbf{u} . The first entry of \mathbf{u} is $u_2 = y_{20} - y_{10}$, which corresponds to the state variable u of previous sections. More generally, $u_k = y_{k0} - y_{10}$ is a measure of the size of asset k relative to asset 1. Consistent with this notation, I will also write $u_1 \equiv y_{10} - y_{10} = 0$ and define the N -vector $\mathbf{u}_+ \equiv (u_1, u_2, \dots, u_N)' = (0, u_2, \dots, u_N)'$ to make subsequent formulas easier to read.

The following Proposition generalizes earlier integral formulas to the N -asset case. All integrals are over \mathbb{R}^{N-1} : \mathbf{v} is an $(N-1)$ -vector. Again, they can be evaluated on the computer.

Proposition 8 (Integral formulas in the N -tree case). *The price-dividend ratio on asset j is*

$$P/D = e^{-\gamma' \mathbf{u}_+/N} (e^{u_1} + \dots + e^{u_N})^\gamma \int \frac{\mathcal{F}_\gamma^N(\mathbf{v}) e^{i\mathbf{u}'\mathbf{v}}}{\rho - \mathbf{c}(\mathbf{e}_j - \gamma/N + i\mathbf{U}'\mathbf{v})} d\mathbf{v}. \quad (44)$$

Defining the expected return by $ER dt \equiv \mathbb{E}(dP + D dt)/P$, we have

$$ER = \frac{\Phi}{P/D} + D/P, \quad (45)$$

where

$$\Phi = \sum_{\mathbf{m}} \binom{\gamma}{\mathbf{m}} e^{(\mathbf{m} - \gamma/N)' \mathbf{u}_+} \int \frac{\mathcal{F}_\gamma^N(\mathbf{v}) e^{i\mathbf{u}'\mathbf{v}} \mathbf{c}(\mathbf{e}_j + \mathbf{m} - \gamma/N + i\mathbf{U}'\mathbf{v})}{\rho - \mathbf{c}(\mathbf{e}_j - \gamma/N + i\mathbf{U}'\mathbf{v})} d\mathbf{v}.$$

The summation is over all vectors $\mathbf{m} = (m_1, \dots, m_N)'$ whose entries are non-negative and add up to γ . I have made use of the multinomial coefficient

$$\binom{\gamma}{\mathbf{m}} = \frac{\gamma!}{m_1! \dots m_N!}.$$

The zero-coupon yield to time T is

$$\mathcal{Y}(T) = \rho - \frac{1}{T} \log \left[e^{-\gamma' \mathbf{u}_+/N} (e^{u_1} + \dots + e^{u_N})^\gamma \int \mathcal{F}_\gamma^N(\mathbf{v}) e^{i\mathbf{u}'\mathbf{v}} e^{\mathbf{c}(-\gamma/N + i\mathbf{U}'\mathbf{v})T} d\mathbf{v} \right]. \quad (46)$$

The riskless rate is

$$r = e^{-\gamma' \mathbf{u}_+/N} (e^{u_1} + \dots + e^{u_N})^\gamma \int \mathcal{F}_\gamma^N(\mathbf{v}) e^{i\mathbf{u}'\mathbf{v}} [\rho - \mathbf{c}(-\gamma/N + i\mathbf{U}'\mathbf{v})] d\mathbf{v}. \quad (47)$$

These formulas can be expressed in terms of the dividend shares $\{s_i\}$ by making the substitution $u_k = \log(s_k/s_1)$.

Proof. See Appendix F. □

The integral formula (44), for example, is a generalization of (14). As an illustration of these results, Figure 14 extends the second calibration presented above to the three-asset case, and shows how price-dividend ratios depend on the two state variables s_1 and s_2 .

7.1 The robustness of contagion and flight-to-quality

Above, I presented a two-asset calibration in which a small asset experiences a negative shock (“contagion”) if a large asset has bad dividend news. On the other hand, a sufficiently large asset experiences a *positive* shock when a sufficiently small asset has bad dividend news; this was labelled “flight-to-quality”. This flight-to-quality effect was dependent on a decrease in the riskless rate outweighing the effect of an increase in the risk premium on the large asset.

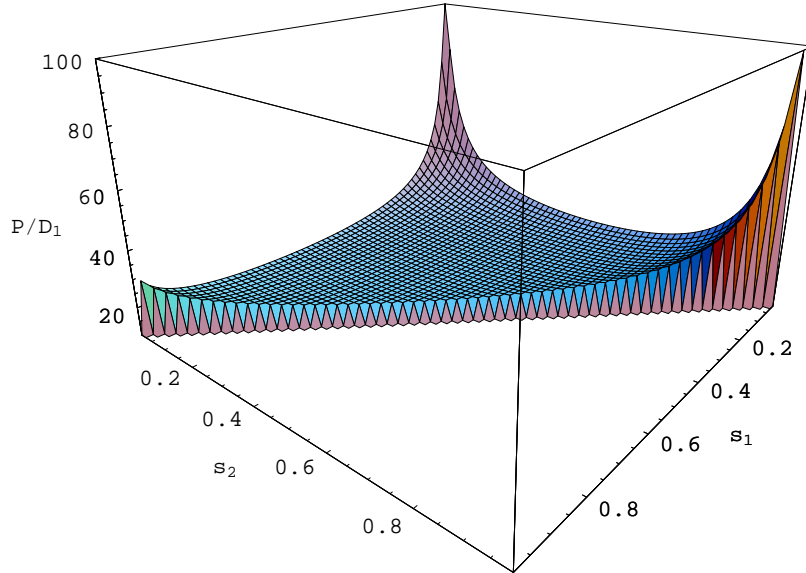


Figure 14: An illustration of the three-asset case. Graph shows P/D for asset one on the z -axis and s_1 and s_2 on the x and y axes. The three assets are identical but independent of one another.

How robust is this effect? Intuition suggests that when more assets are introduced, the riskless rate effect will be muted, while the risk premium effect will continue to matter for individual assets. This section evaluates that intuition.

In the two-asset case, an asset is subject to contagion when its price-dividend ratio is decreasing in its dividend share, and to flight-to-quality when its price-dividend ratio is increasing in its dividend share. In the calibration of Section 5.1, the share, s^* , at which the transition takes place occurs at the minimum point of the price-dividend curve shown in Figure 3b: that is, at $s^* \approx 0.61$.

In the N -asset case, whether an asset experiences contagion or flight-to-quality depends on the $(N - 1)$ -dimensional state vector and also on which other asset is assumed to experience a shock. To simplify the analysis by reducing the dimensionality, suppose that there are $N - 1$ equally sized small assets, and an N th large asset. As in the two-asset case, I calculate the critical dividend share, s^* , above which the N th asset exhibits flight-to-quality, and below which the N th asset exhibits contagion, following a negative dividend shock to (any) one of the $N - 1$ small assets.

All assets are assumed to have independent and identically distributed dividend processes, following geometric Brownian motions with $\mu = 0.02$ and $\sigma = 0.1$, as in the calibration presented in Section 5.1.

N	Critical share, s^*	Relative share
2	0.61	1.56
3	0.48	1.83
4	0.41	2.11
5	0.37	2.38
6	0.35	2.66

Table 2: Above the critical share the large asset experiences flight-to-quality; below, it experiences contagion. Relative share is the implied ratio of the large asset’s dividend to one of the small asset’s dividends, at this critical share.

Table 2 demonstrates that s^* is decreasing in N . An alternative measure of the large asset’s size, which captures the extent to which the economy is unbalanced, is the ratio of the large asset’s dividends to the dividends of any one of the $N - 1$ small assets. This quantity is reported as “Relative share” in Table 2. The relative share is increasing in N : when $N = 6$, an asset that has dividends two and a half times as large as any other asset will still experience contagion rather than flight-to-quality, whereas such an asset experiences flight-to-quality if $N \leq 5$.

This evidence is dependent on a particular calibration; nonetheless, it suggests that when there are several assets of broadly similar size, contagion, not flight-to-quality, is the norm.

8 Conclusion

It seems worthwhile to summarize the solution method for readers who are not inclined to look through the appendices. Broadly speaking, there are two steps, which I now outline for the price-dividend ratio in the two-asset case:

- (i) I use a change of measure followed by a Fourier transform to convert the Lucas asset-pricing equation (2) into the integral formula (11) which can be solved numerically.
- (ii) In certain special cases, the integral formula can be simplified further by using techniques from complex analysis to express it as an infinite sum of residues.
 - (a) In the Brownian motion case, the sum of residues can be evaluated in closed form, giving the expression (22).
 - (b) In the limit as the asset in question becomes negligibly small, only one of the residues is relevant, which leads to the tractable expressions (36) and (40) which are valid for general dividend processes.

Complicated, interesting, and empirically relevant phenomena emerge from simple assumptions. In various regions of the parameter space, the model exhibits momentum, mean-reversion, contagion, flight to quality, the value-growth effect and excess volatility. Closed-form expressions are available when dividends are driven by Brownian motions. In the small asset limit, the quantities of interest can be calculated in closed-form when log dividends follow *any* Lévy process which is consistent with the consumption-based asset pricing framework. Vanishingly small idiosyncratic assets can earn positive and economically meaningful risk premia. The expected returns on such assets are entirely attributable to expected capital gains, since dividend yields are zero in the limit.

The solution method is novel and is robust to some generalizations of the model. In work currently in progress, I allow for non-infinite elasticity of substitution between the dividends of two assets—now interpreted as countries—so that the consumption index $C = D_1 + D_2$ of this paper is replaced by the more complicated

$$C = \left(D_1^{(\eta-1)/\eta} + D_2^{(\eta-1)/\eta} \right)^{\eta/(\eta-1)},$$

where η lies between 1 (the Cobb-Douglas case, in which price-dividend ratios are constant) and infinity (the case considered in this paper). With this modification, real exchange rates come into the picture.

9 Bibliography

Andrews, G. E., Askey, R., and R. Roy (1999), *Special Functions*, 1st edition, Cambridge University Press, UK.

Barro, R. J. (2006), “Rare Disasters and Asset Markets in the Twentieth Century,” *Quarterly Journal of Economics*, 121:3:823–866.

Billingsley, P. (1995), *Probability and Measure*, 3rd edition, John Wiley & Sons, New York, NY.

Brainard, W. C. and J. Tobin (1968), “Pitfalls in Financial Model Building,” *American Economic Review*, 58:2:99–122.

Brainard, W. C. and J. Tobin (1992), “On the Internationalization of Portfolios,” *Oxford Economic Papers*, 44:533–565.

Campbell, J. Y. (1991), “A Variance Decomposition for Stock Returns,” *Economic Journal*, 101:157–179.

Cochrane, J. H., Longstaff, F. A., and P. Santa-Clara (2007), “Two Trees,” *Review of Financial Studies*, forthcoming.

Cohen, R. B., Polk, C., and T. Vuolteenaho (2003), “The Value Spread,” *Journal of Finance*, 58:2:609–641.

- Cole, H. L. and M. Obstfeld (1991), “Commodity Trade and International Risk Sharing,” *Journal of Monetary Economics*, 28:3–24.
- Cont, R. and P. Tankov (2004), *Financial Modelling with Jump Processes*, Chapman & Hall/CRC, Boca Raton, FL.
- Dugué, D. (1951), “Analyticité et Convexité des Fonctions Caractéristiques,” *Annales de l’Institut Henri Poincaré*, 12:1:45–56.
- Edwards, J. (1922), *A Treatise on the Integral Calculus, Vol. II*, Macmillan and Co., London, UK.
- Fama, E. F. and K. R. French (1989), “Business Conditions and Expected Returns on Stocks and Bonds,” *Journal of Financial Economics*, 25:23–49.
- Fama, E. F. and K. R. French (1993), “Common Risk Factors in the Returns on Stocks and Bonds,” *Journal of Financial Economics*, 33:131–155.
- Forbes, K. J. and R. Rigobon (2002), “No Contagion, Only Interdependence: Measuring Stock Market Comovements,” *Journal of Finance*, 57:5:2223–2261.
- Körner, T. W. (1988), *Fourier Analysis*, Cambridge University Press, Cambridge, UK.
- Lucas, R. E. (1978), “Asset Prices in an Exchange Economy,” *Econometrica*, 46:6:1429–1445.
- Lucas, R. E. (1982), “Interest Rates and Currency Prices in a Two-Country World,” *Journal of Monetary Economics*, 10:335–359.
- Lukacs, E. (1970), *Characteristic Functions*, Charles Griffin & Co., London, UK.
- Martin, I. W. R. (2007), “Consumption-Based Asset Pricing with Higher Cumulants,” working paper.
- Mehra, R. and E. C. Prescott (1985), “The Equity Premium: A Puzzle,” *Journal of Monetary Economics*, 15:145–161.
- Menzly, L., Santos, T., and P. Veronesi (2004), “Understanding Predictability,” *Journal of Political Economy*, 112:1:1–47.
- Pástor, L. and P. Veronesi (2003), “Stock Valuation and Learning about Profitability,” *Journal of Finance*, 58:5:1749–1789.
- Pástor, L. and P. Veronesi (2006), “Was There a NASDAQ Bubble in the Late 1990s?” *Journal of Financial Economics*, 81:61–100.
- Pavlova, A. and R. Rigobon (2007), “Asset Prices and Exchange Rates,” *Review of Financial Studies*, 20:4:1139–1181.
- Priestley, H. A. (1995), *Introduction to Complex Analysis*, Oxford University Press, Oxford, UK.
- Rietz, T. A. (1988), “The Equity Premium: A Solution,” *Journal of Monetary Economics*, 22:117–131.
- Rogers, L. C. G., and D. Williams (2000), *Diffusions, Markov Processes, and Martin-*

gales, Volume 1, Cambridge University Press, Cambridge, UK.

Santos, T. and P. Veronesi (2006), “Labor Income and Predictable Stock Returns,” *Review of Financial Studies*, 19:1:1–44.

Shiller, R. J. (1981), “Do Stock Prices Move Too Much to be Justified by Subsequent Changes in Dividends?” *American Economic Review*, 71:421–436.

Shiller, R. J. (1989), “Comovements in Stock Prices and Comovements in Dividends,” *Journal of Finance*, 44:3:719–729.

Slater, L. J. (1966), *Generalized Hypergeometric Functions*, Cambridge University Press, Cambridge, UK.

A Some results from complex analysis

This section provides a brief summary of the definitions and results from complex analysis that are invoked in the body of the paper. Proofs of the results cited will be found in any introductory complex analysis textbook; I have drawn on Priestley (1995).

A complex number z is specified by a pair of real numbers x and y ; we can write $z = x + iy$, where i is a complex number which satisfies $i^2 = -1$. The complex number z can be identified with the point $(x, y) \in \mathbb{R}^2$. The real part of z is x ; the imaginary part of z is y . ($\operatorname{Re} z = x$; $\operatorname{Im} z = y$.) The modulus, or absolute value, of z is written $|z|$ and is equal to $\sqrt{x^2 + y^2}$. (This is just the length of the vector (x, y) .) Alternatively, we can think in polar coordinates and identify z with $(r \cos \theta, r \sin \theta) \in \mathbb{R}^2$. With this notation, $|z| = r$ and we can define the argument of z , $\operatorname{Arg} z$, to equal the angle $\theta \in [0, 2\pi)$. In rectangular coordinates, we think of $z = x + iy$; in polar coordinates, we think of $z = r \cos \theta + ir \sin \theta$. Since $e^{i\theta} = \cos \theta + i \sin \theta$, the polar notation can be written more neatly as $z = re^{i\theta}$. The set of complex numbers is written \mathbb{C} .

The real axis is $\{z : \operatorname{Im} z = 0\}$. The imaginary axis is $\{z : \operatorname{Re} z = 0\}$. The *upper half-plane* is $\{z : \operatorname{Im} z > 0\}$. We will need some more notation. Write $D(a; r)$ for the open disc with center a and radius $r > 0$:

$$D(a; r) \equiv \{z \in \mathbb{C} : |z - a| < r\}$$

Write $D'(a; r)$ for the punctured disc centered on a with radius $r > 0$:

$$D'(a; r) \equiv \{z \in \mathbb{C} : 0 < |z - a| < r\}$$

Throughout this section, let f be a complex-valued function. The function f is said to be *holomorphic* in G , which is some subset of the complex plane, if

$$\lim_{h \rightarrow 0} \frac{f(z + h) - f(z)}{h}$$

exists for every point z in some open set containing G . Note that the limit must be the same no matter what direction h approaches 0 from: for example, it may tend to zero along the imaginary axis or along the real axis. Polynomials, convergent power series, the exponential function, sine and cosine are holomorphic, as are compositions and finite sums and products of these functions. So, for example, the hyperbolic cosine, $\cosh z \equiv (e^z + e^{-z})/2$ is holomorphic.

Evidently, to be holomorphic is to be complex-differentiable. The reason for the flashy terminology is to emphasize that not every function which “looks” holomorphic is. For example, not every function which is differentiable when considered as a function from $\mathbb{R}^2 \rightarrow \mathbb{R}^2$ is differentiable when considered as a function from $\mathbb{C} \rightarrow \mathbb{C}$. Complex conjugation, which maps $x + iy \mapsto x - iy$, is not holomorphic, although the function from \mathbb{R}^2 to \mathbb{R}^2 which maps $(x, y) \mapsto (x, -y)$ is differentiable.¹⁷

Result 1 (Holomorphic iff analytic). *A function f is holomorphic in the open set $D(a; r)$ if and only if it is analytic—that is, representable, in $D(a; r)$, by a power series:*

$$f(z) = \sum_{n=0}^{\infty} c_n(z - a)^n \quad z \in D(a; r)$$

Proof. See Priestley (1995), pp. 20–21 and 69. □

Complex integrals appear throughout the paper. Real integration takes place on subsets of the real line—for example,

$$\int_a^b f(x) dx$$

is an integral “along the path from a to b .” Complex integration takes place over paths in the complex plane. Since the complex plane is two-dimensional (as opposed to the one dimension of the real line), these paths can be more complicated. For example, an integral might be “around the unit circle defined by $|z| = 1$,” or “along the real line from $-R$ to R , then around a semicircular arc lying in the upper half-plane from R back to $-R$.”

The integrals which occur in this paper (for example, (15)) feature integrands which are holomorphic everywhere except for at certain *singularities* at which they explode to infinity. (These singularities do not, of course, occur on the path of integration.) It is an amazing—and powerful—fact that such integrals depend on the behavior of the integrands at singularities elsewhere in the complex plane. I now introduce the mathematical apparatus used in the paper that relates to this fact.

If f is holomorphic in some punctured disc $D'(a; r)$ but not at the point a , then a is an *isolated singularity*. (Keep in mind the example $f(z) = 1/z$, which is holomorphic

¹⁷The increased “rigidity” of holomorphic functions is responsible for much of the power of the results from complex analysis which are quoted here.

everywhere except for at an isolated singularity at the origin.) In this case, f can be expanded as a unique power series of the form

$$f(z) = \sum_{n=-\infty}^{\infty} c_n(z-a)^n \quad z \in D'(a; r). \quad (48)$$

If $c_n = 0$ for all $n < 0$, the point a is a *removable singularity*. (In other words, it is not “really” a singularity at all. Consider the example $f(z) = (\sin z)/z$, which has a removable singularity at $z = 0$. If the function f is redefined slightly by specifying that $f(0) = 1$, then the singularity has been removed.) If there is some positive m such that $c_{-m} \neq 0$ and $c_k = 0$ for all $k < -m$ then the point a is a *pole of order m* .¹⁸

These concepts are best illustrated with an example that will become relevant in Appendix D. Take the function

$$f(v) = \frac{v}{2 \sinh \pi v}.$$

Singularities occur whenever $\sinh \pi v = 0$, in other words at $v = 0, \pm i, \pm 2i, \dots$ ¹⁹ However, it is easy to check that the singularity at the origin is removable. (By L'Hôpital's rule, $f(v)$ tends to $1/2\pi$ as v tends to zero.) In fact, the only non-removable singularities are poles of order 1 at $\pm i, \pm 2i, \pm 3i, \dots$

A function f which is holomorphic throughout the complex plane, except at poles, is called *meromorphic*. If a meromorphic function f has a pole at a then the *residue* of f at a , written $\text{Res}\{f(z); a\}$, is defined to be the coefficient on the term $(z-a)^{-1}$ in a power series expansion of the form (48). With this final piece of notation, I now state the residue theorem.

Result 2 (The Residue Theorem). *Let Ω denote a closed path of integration which is to be integrated around in an anticlockwise direction. Suppose f is holomorphic inside and on Ω , except for at a finite number of poles at points a_1, \dots, a_m inside Ω . Then*

$$\int_{\Omega} f(z) dz = 2\pi i \sum_{j=1}^m \text{Res}\{f(z); a_j\}$$

Proof. See Priestley (1995), chapter 7. □

The poles that occur in the course of this paper are almost invariably poles of order 1. This fact makes the computation of residues particularly simple. If $f(z) = g(z)/h(z)$ has a pole at a and $g(a) \neq 0$, $h(a) = 0$ and $h'(a) \neq 0$, then

$$\text{Res}\{f(z); a\} = \frac{g(a)}{h'(a)}. \quad (49)$$

¹⁸If there are arbitrarily large m such that $c_{-m} \neq 0$ then the point a is an *isolated essential singularity*, but this case is not relevant to this paper.

¹⁹Remember that when z is real, we have $\sinh(iz) = i \sin z$ and $\cosh(iz) = \cos z$.

A.1 An illustration

To illustrate these techniques, I now show how to evaluate the integral

$$\frac{1}{2\pi} \int_{-\infty}^{\infty} \frac{e^{-iuv}}{2 \cosh(u/2)} du \equiv \frac{K}{2\pi},$$

which is the case $\gamma = 1$ in (58).

The integrand has poles when $\cosh(u/2) = 0$. These occur when $u = \pi i, 3\pi i, 5\pi i, \dots$. We can solve the integral by integrating around a judiciously chosen path which encloses the first pole πi . Let N be a large positive real number, and let \square be the rectangle with corners at $-R, R, R + 2\pi i$ and $-R + 2\pi i$. We integrate around \square in the anticlockwise direction.

By the residue theorem,

$$\begin{aligned} \int_{\square} \frac{e^{-iuv}}{2 \cosh(u/2)} du &= 2\pi i \cdot \text{Res} \left\{ \frac{e^{-iuv}}{2 \cosh(u/2)}; \pi i \right\} \\ &= 2\pi i \cdot \frac{e^{\pi v}}{[2 \cosh(u/2)]' \big|_{u=\pi i}} \\ &= 2\pi i \cdot \frac{e^{\pi v}}{\sinh(\pi i/2)} \\ &= 2\pi e^{\pi v}. \end{aligned} \tag{50}$$

We can decompose the integral on the left-hand side of (50) into four parts, one for each side of the rectangle. Doing so gives

$$K_1 + K_2 + K_3 + K_4 = 2\pi e^{\pi v}, \tag{51}$$

where

$$\begin{aligned} K_1 &= \int_{-N}^N \frac{e^{-iuv}}{2 \cosh(u/2)} du \\ K_2 &= \int_0^{2\pi} \frac{e^{-iv(N+iu)}}{2 \cosh((N+iu)/2)} i du \\ K_3 &= \int_N^{-N} \frac{e^{-iv(u+2\pi i)}}{2 \cosh(u/2 + \pi i)} du \\ K_4 &= \int_0^{2\pi} \frac{e^{-iv(-N+iu)}}{2 \cosh((-N+iu)/2)} i du. \end{aligned}$$

Now consider the limit as N tends to infinity—in other words, the limit as the rectangle around which we are integrating becomes extremely wide. Equation (51) continues to hold in this limit because πi remains the only pole inside the contour. In this limit, K_1 tends to

K , the integral of interest, and K_3 tends to $e^{2\pi v} \cdot K$. On the other hand, both K_2 and K_4 tend to zero. To see this, consider K_2 . We have

$$\begin{aligned} |K_2| &\leq \int_0^{2\pi} \left| \frac{e^{-iv(N+iu)}}{2 \cosh((N+iu)/2)} i \right| du \\ &= \int_0^{2\pi} \frac{e^{uv}}{2 |\cosh((N+iu)/2)|} du. \end{aligned}$$

Since $\cosh((N+iu)/2)$ tends to 0 uniformly in u as N tends to infinity, we have $|K_2| \rightarrow 0$ and hence $K_2 \rightarrow 0$. The case of K_4 is very similar.

In conclusion, allowing N to tend to infinity in equation (51), we have $K + e^{2\pi v} K = 2\pi e^{\pi v}$, from which it follows that $K = \pi \operatorname{sech}(\pi v)$. Finally, we have

$$\frac{1}{2\pi} \int_{-\infty}^{\infty} \frac{e^{-iuv}}{2 \cosh(u/2)} du = \frac{K}{2\pi} = \frac{1}{2} \operatorname{sech}(\pi v).$$

B Prices, returns and interest rates

B.1 Preliminary mathematical results

B.1.1 An expectation

This section contains a calculation which is used below. It may be helpful to glance ahead to equation (64) for motivation. The goal is to evaluate

$$E \equiv \mathbb{E} \left(\frac{e^{\alpha_1 \tilde{y}_{1t} + \alpha_2 \tilde{y}_{2t}}}{[e^{y_{10} + \tilde{y}_{1t}} + e^{y_{20} + \tilde{y}_{2t}}]^\gamma} \right)$$

for general $\alpha_1, \alpha_2, \gamma > 0$. First, I rewrite the expectation, noting that

$$\begin{aligned} \mathbb{E} \left(\frac{e^{\alpha_1 \tilde{y}_{1t} + \alpha_2 \tilde{y}_{2t}}}{[e^{y_{10} + \tilde{y}_{1t}} + e^{y_{20} + \tilde{y}_{2t}}]^\gamma} \right) &= e^{-\gamma/2(y_{10} + y_{20})} \times \\ &\mathbb{E} \left(\frac{e^{(\alpha_1 - \gamma/2)\tilde{y}_{1t} + (\alpha_2 - \gamma/2)\tilde{y}_{2t}}}{[2 \cosh((y_{20} - y_{10} + \tilde{y}_{2t} - \tilde{y}_{1t})/2)]^\gamma} \right) \end{aligned} \quad (52)$$

To take care of the exponential in the numerator inside the expectation, I transform the probability law, defining

$$\tilde{\mathbb{E}}[Y] \equiv e^{-t\mathbf{c}(\alpha_1 - \gamma/2, \alpha_2 - \gamma/2)} \cdot \mathbb{E} \left[e^{(\alpha_1 - \gamma/2)\tilde{y}_{1t} + (\alpha_2 - \gamma/2)\tilde{y}_{2t}} \cdot Y \right]. \quad (53)$$

This is an Esscher transform of the original law, and it has the property that

$$\tilde{\mathbf{c}}(v_1, v_2) \equiv \log \tilde{\mathbb{E}} \left[e^{v_1 \tilde{y}_{11} + v_2 \tilde{y}_{21}} \right] = \mathbf{c}(\alpha_1 - \gamma/2 + v_1, \alpha_2 - \gamma/2 + v_2) - \mathbf{c}(\alpha_1 - \gamma/2, \alpha_2 - \gamma/2). \quad (54)$$

In terms of this transformed law, the right hand side of (52) equals

$$e^{-\gamma(y_{10}+y_{20})/2+\mathbf{c}(\alpha_1-\gamma/2,\alpha_2-\gamma/2)t}\tilde{\mathbb{E}}\left(\frac{1}{[2\cosh((y_{20}-y_{10}+\tilde{y}_{2t}-\tilde{y}_{1t})/2)]^\gamma}\right) \quad (55)$$

To make further progress, we can now attack the expectation in (55) by exploiting the fact that $1/[2\cosh(u/2)]^\gamma$ has a Fourier transform which can be found in closed form for integer $\gamma > 0$. Define the Fourier transform $\mathcal{F}_\gamma(v)$ by

$$\frac{1}{[2\cosh(u/2)]^\gamma} = \int_{-\infty}^{\infty} e^{iuv} \mathcal{F}_\gamma(v) dv \quad (56)$$

We have, then,

$$\begin{aligned} E &= e^{-\gamma(y_{10}+y_{20})/2+\mathbf{c}(\alpha_1-\gamma/2,\alpha_2-\gamma/2)t} \tilde{\mathbb{E}}\left(\int_{-\infty}^{\infty} e^{iv(y_{20}-y_{10}+\tilde{y}_{2t}-\tilde{y}_{1t})} \mathcal{F}_\gamma(v) dv\right) \\ &= e^{-\gamma(y_{10}+y_{20})/2+\mathbf{c}(\alpha_1-\gamma/2,\alpha_2-\gamma/2)t} \left(\int_{-\infty}^{\infty} e^{\tilde{\mathbf{c}}(-iv,iv)t} \cdot e^{iv(y_{20}-y_{10})} \mathcal{F}_\gamma(v) dv\right) \\ &= e^{-\gamma(y_{10}+y_{20})/2} \int_{-\infty}^{\infty} e^{\mathbf{c}(\alpha_1-\gamma/2-iv,\alpha_2-\gamma/2+iv)t} \cdot e^{iv(y_{20}-y_{10})} \mathcal{F}_\gamma(v) dv. \end{aligned} \quad (57)$$

B.1.2 The Fourier transform $\mathcal{F}_\gamma(v)$

By the Fourier inversion theorem,²⁰ definition (56) implies that

$$\begin{aligned} \mathcal{F}_\gamma(v) &= \frac{1}{2\pi} \int_{-\infty}^{\infty} \frac{e^{-iuv}}{(2\cosh(u/2))^\gamma} du \\ &= \frac{1}{2\pi} \int_{-\infty}^{\infty} \frac{e^{-iuv}}{(e^{u/2} + e^{-u/2})^\gamma} du. \end{aligned} \quad (58)$$

Make the change of variable

$$u = \log \frac{t}{1-t}. \quad (59)$$

It follows that

$$du = \frac{dt}{t(1-t)}$$

so on making this substitution in (58), we have

$$\begin{aligned} \mathcal{F}_\gamma(v) &= \frac{1}{2\pi} \int_0^1 \frac{\left(\frac{t}{1-t}\right)^{-iv}}{\left(\sqrt{\frac{t}{1-t}} + \sqrt{\frac{1-t}{t}}\right)^\gamma} \frac{dt}{t(1-t)} \\ &= \frac{1}{2\pi} \int_0^1 t^{\gamma/2-iv} (1-t)^{\gamma/2+iv} \frac{dt}{t(1-t)}. \end{aligned} \quad (60)$$

²⁰See Körner (1988, pp. 296–7) for a proof.

This is a Dirichlet surface integral. As shown in Edwards (1922, pp. 166–7) or Andrews, Askey and Roy (1999, p. 34), it can be evaluated in terms of Γ -functions, giving

$$\mathcal{F}_\gamma(v) = \frac{1}{2\pi} \frac{\Gamma(\gamma/2 - iv)\Gamma(\gamma/2 + iv)}{\Gamma(\gamma)}. \quad (61)$$

For future reference, it is useful to note an equivalent representation of $\mathcal{F}_\gamma(v)$. It was shown in Appendix A.1 that $\mathcal{F}_1(v) = \frac{1}{2}\operatorname{sech}\pi v$; a similar calculation reveals that $\mathcal{F}_2(v) = \frac{1}{2}v \operatorname{cosech}\pi v$. From these two facts, expression (61), and the fact that $\Gamma(x) = (x-1)\Gamma(x-1)$, it follows that for positive integer γ , we have

$$\mathcal{F}_\gamma(v) = \begin{cases} \frac{v \operatorname{cosech}(\pi v)}{2(\gamma-1)!} \cdot \prod_{n=1}^{\gamma/2-1} (v^2 + n^2) & \text{for even } \gamma, \\ \frac{\operatorname{sech}(\pi v)}{2(\gamma-1)!} \cdot \prod_{n=1}^{(\gamma-1)/2} (v^2 + (n-1/2)^2) & \text{for odd } \gamma. \end{cases} \quad (62)$$

B.1.3 An Itô calculation

Given a jump-diffusion \mathbf{y} , with

$$d\mathbf{y} = \boldsymbol{\mu}dt + \mathbf{A}d\mathbf{Z} + \mathbf{J}dN,$$

this section seeks a simple formula for

$$\mathbb{E}d(e^{\mathbf{w}'\mathbf{y}})$$

where \mathbf{w} is a constant vector.

First, define $x \equiv \mathbf{w}'\mathbf{y}$; then

$$dx = \mathbf{w}'\boldsymbol{\mu}dt + \mathbf{w}'\mathbf{A}d\mathbf{Z} + \mathbf{w}'\mathbf{J}dN$$

We seek $\mathbb{E}d(e^x)$. By Itô's formula for jump-diffusions, we have

$$d(e^x) = e^x \left[\left(\mathbf{w}'\boldsymbol{\mu} + \frac{1}{2}\mathbf{w}'\boldsymbol{\Sigma}\mathbf{w} \right) dt + \mathbf{w}'\mathbf{A}d\mathbf{Z} + \left(e^{\mathbf{w}'\mathbf{J}} - 1 \right) dN \right]$$

where $\boldsymbol{\Sigma} \equiv \mathbf{A}\mathbf{A}'$; and so, after taking expectations,

$$\begin{aligned} \mathbb{E}d(e^{\mathbf{w}'\mathbf{y}}) &= e^{\mathbf{w}'\mathbf{y}} \cdot \left[\mathbf{w}'\boldsymbol{\mu} + \frac{1}{2}\mathbf{w}'\boldsymbol{\Sigma}\mathbf{w} + \omega \left(\mathbb{E}e^{\mathbf{w}'\mathbf{J}} - 1 \right) \right] dt \\ &= e^{\mathbf{w}'\mathbf{y}} \cdot \mathbf{c}(\mathbf{w})dt. \end{aligned} \quad (63)$$

In the case in which \mathbf{y} is a general Lévy process, (63) holds by Proposition 8.20 of Cont and Tankov (2004).

B.2 Prices

B.2.1 Proof of Proposition 1

The price of the α -asset is

$$\begin{aligned} P_\alpha &= \mathbb{E} \int_0^\infty e^{-\rho t} \left(\frac{C_t}{C_0} \right)^{-\gamma} D_{1t}^{\alpha_1} D_{2t}^{\alpha_2} dt \\ &= (C_0)^\gamma \int_0^\infty e^{-\rho t} \mathbb{E} \left(\frac{e^{\alpha_1(y_{10} + \tilde{y}_{1t}) + \alpha_2(y_{20} + \tilde{y}_{2t})}}{[e^{y_{10} + \tilde{y}_{1t}} + e^{y_{20} + \tilde{y}_{2t}}]^\gamma} \right) dt \end{aligned}$$

It follows that

$$\frac{P_\alpha}{D_\alpha} = (e^{y_{10}} + e^{y_{20}})^\gamma \int_{t=0}^\infty e^{-\rho t} \mathbb{E} \left(\frac{e^{\alpha_1 \tilde{y}_{1t} + \alpha_2 \tilde{y}_{2t}}}{[e^{y_{10} + \tilde{y}_{1t}} + e^{y_{20} + \tilde{y}_{2t}}]^\gamma} \right) dt \quad (64)$$

The expectation inside the integral was calculated above in Appendix B.1.1. Substituting (57) into (64), interchanging the order of integration,²¹ and writing u for $y_{20} - y_{10}$, we get

$$\begin{aligned} \frac{P_\alpha}{D_\alpha} &= [2 \cosh(u/2)]^\gamma \int_{v=-\infty}^\infty \int_{t=0}^\infty e^{-\rho t} e^{\mathbf{c}(\alpha_1 - \gamma/2 - iv, \alpha_2 - \gamma/2 + iv)t} \cdot e^{iuv} \mathcal{F}_\gamma(v) dt dv \\ &\stackrel{(a)}{=} [2 \cosh(u/2)]^\gamma \int_{v=-\infty}^\infty \frac{e^{iuv} \mathcal{F}_\gamma(v)}{\rho - \mathbf{c}(\alpha_1 - \gamma/2 - iv, \alpha_2 - \gamma/2 + iv)} dv \end{aligned} \quad (65)$$

For equality (a) to hold, I have assumed that

$$\rho - \text{Re}[\mathbf{c}(\alpha_1 - \gamma/2 - iv, \alpha_2 - \gamma/2 + iv)] > 0 \quad \text{for all } v \in \mathbb{R}.$$

I show in Appendix C that this follows from the apparently weaker assumption that the inequality holds at $v = 0$:

$$\rho - \mathbf{c}(\alpha_1 - \gamma/2, \alpha_2 - \gamma/2) > 0 \quad (66)$$

In particular, for the problem under consideration to be well-defined, we must impose a requirement that expected utility (1) is finite. Finiteness of expected utility is guaranteed by the finiteness of the prices of the two assets. Therefore I refer to the two inequalities generated by substituting $(\alpha_1, \alpha_2) = (1, 0)$ and $(0, 1)$ into (66) as the *finiteness condition*. Throughout the paper, it is assumed that this condition holds. (See equation (13) and Table 1.)

In terms of the state variable s , the price-dividend ratio is therefore

$$\frac{P_\alpha}{D_\alpha} = \frac{1}{\sqrt{s^\gamma(1-s)^\gamma}} \cdot \int_{-\infty}^\infty \frac{\left(\frac{1-s}{s}\right)^{iv} \mathcal{F}_\gamma(v)}{\rho - \mathbf{c}(\alpha_1 - \gamma/2 - iv, \alpha_2 - \gamma/2 + iv)} dv \quad (67)$$

where I have defined $s \equiv D_{10}/(D_{10} + D_{20})$.

²¹Since the integrand is absolutely integrable, this is a legitimate application of Fubini's theorem.

B.2.2 Proof of Proposition 2

Since $u = \log[(1-s)/s]$, we have

$$\frac{1-s}{s} = e^u$$

and

$$\frac{1}{\sqrt{s^\gamma(1-s)^\gamma}} = [2 \cosh(u/2)]^\gamma .$$

Furthermore, $\mathcal{F}_\gamma(v)$ was defined by

$$\frac{1}{[2 \cosh(u/2)]^\gamma} = \int_{-\infty}^{\infty} e^{iuv} \mathcal{F}_\gamma(v) dv .$$

Substituting these observations into the pricing formula (11), we find the expressions of Proposition 2.

B.3 Returns

Expected returns contain a dividend yield component and a capital gain component:

$$R_\alpha dt = \frac{D_\alpha}{P_\alpha} dt + \frac{\mathbb{E}dP_\alpha}{P_\alpha}$$

The first term is supplied by the pricing formula derived in the previous section. This section therefore focusses on calculating $\mathbb{E}dP_\alpha/P_\alpha$ in the case in which γ is an integer.

We have

$$P_\alpha = (D_{10} + D_{20})^\gamma e^{(\alpha_1 - \gamma/2)y_{10} + (\alpha_2 - \gamma/2)y_{20}} \int_{-\infty}^{\infty} \frac{e^{iv(y_{20} - y_{10})} \mathcal{F}_\gamma(v)}{\rho - \mathbf{c}(\alpha_1 - \gamma/2 - iv, \alpha_2 - \gamma/2 + iv)} dv \quad (68)$$

For convenience, I write

$$h(v) \equiv \frac{\mathcal{F}_\gamma(v)}{\rho - \mathbf{c}(\alpha_1 - \gamma/2 - iv, \alpha_2 - \gamma/2 + iv)} \quad \text{and} \quad \binom{n}{m} \equiv \frac{n!}{m!(n-m)!}$$

throughout this section.

Introducing this notation,

$$\begin{aligned} P_\alpha &= \int_{-\infty}^{\infty} h(v) \cdot (e^{y_{10}} + e^{y_{20}})^\gamma e^{(\alpha_1 - \gamma/2 - iv)y_{10} + (\alpha_2 - \gamma/2 + iv)y_{20}} dv \\ &= \int_{-\infty}^{\infty} h(v) \cdot \sum_{m=0}^{\gamma} \left[\binom{\gamma}{m} e^{my_{10}} \cdot e^{(\gamma-m)y_{20}} \right] e^{(\alpha_1 - \gamma/2 - iv)y_{10} + (\alpha_2 - \gamma/2 + iv)y_{20}} dv \\ &= \sum_{m=0}^{\gamma} \binom{\gamma}{m} \int_{-\infty}^{\infty} h(v) \cdot e^{(\alpha_1 - \gamma/2 + m - iv)y_{10} + (\alpha_2 + \gamma/2 - m + iv)y_{20}} dv \\ &\equiv \sum_{m=0}^{\gamma} \binom{\gamma}{m} \int_{-\infty}^{\infty} h(v) \cdot e^{\mathbf{w}_m(v) \cdot \mathbf{y}} dv, \end{aligned} \quad (69)$$

where

$$\mathbf{w}_m(v) \equiv (\alpha_1 - \gamma/2 + m - iv, \alpha_2 + \gamma/2 - m + iv)'$$

The calculation of Appendix B.1.3, above, can now be used in (69) to show that

$$\mathbb{E}(dP_\alpha) = \left\{ \sum_{m=0}^{\gamma} \binom{\gamma}{m} \int_{-\infty}^{\infty} h(v) \cdot e^{\mathbf{w}_m(v) \cdot \mathbf{y}} \mathbf{c}[\mathbf{w}_m(v)] dv \right\} \cdot dt \quad (70)$$

Dividing (70) by (69) and rearranging, the expected capital gain is given by the formula

$$\frac{\mathbb{E}dP_\alpha}{P_\alpha} = \frac{\sum_{m=0}^{\gamma} \binom{\gamma}{m} e^{-mu} \int_{-\infty}^{\infty} h(v) e^{iuv} \cdot \mathbf{c}(\mathbf{w}_m(v)) dv}{\sum_{m=0}^{\gamma} \binom{\gamma}{m} e^{-mu} \int_{-\infty}^{\infty} h(v) e^{iuv} dv} \cdot dt \quad (71)$$

B.4 Real interest rates

From the Euler equation, we have

$$\begin{aligned} B_T &= \mathbb{E} \left[e^{-\rho T} \left(\frac{C_T}{C_0} \right)^{-\gamma} \right] \\ &= e^{-\rho T} C_0^\gamma \mathbb{E} \left[\frac{1}{(D_{1T} + D_{2T})^\gamma} \right] \end{aligned}$$

Using the result of Appendix B.1.1, we find that

$$\begin{aligned} B_T &= e^{-\rho T} (e^{y_{10}} + e^{y_{20}})^\gamma e^{-\gamma(y_{10} + y_{20})/2} \int_{-\infty}^{\infty} e^{iv(y_{20} - y_{10})} \mathcal{F}_\gamma(v) e^{\mathbf{c}(-\gamma/2 - iv, -\gamma/2 + iv)T} dv \\ &= e^{-\rho T} [2 \cosh(u/2)]^\gamma \int_{-\infty}^{\infty} \mathcal{F}_\gamma(v) e^{iuv} \cdot e^{\mathbf{c}(-\gamma/2 - iv, -\gamma/2 + iv)T} dv, \end{aligned}$$

as claimed. The yield, $\mathcal{Y}(T)$, follows directly from this expression:

$$\mathcal{Y}(T) = \rho - \frac{1}{T} \log \left\{ [2 \cosh(u/2)]^\gamma \int_{-\infty}^{\infty} \mathcal{F}_\gamma(v) e^{iuv} \cdot e^{\mathbf{c}(-\gamma/2 - iv, -\gamma/2 + iv)T} dv \right\}. \quad (72)$$

The riskless rate is found by taking the limit as $T \downarrow 0$ in (72). To calculate this limit, first use the fact that

$$[2 \cosh(u/2)]^\gamma \int_{-\infty}^{\infty} \mathcal{F}_\gamma(v) e^{iuv} dv = 1$$

to rewrite equation (72) as

$$\mathcal{Y}(T) = \rho - \frac{1}{T} \log \left\{ 1 + [2 \cosh(u/2)]^\gamma \int_{-\infty}^{\infty} \mathcal{F}_\gamma(v) e^{iuv} \left[e^{\mathbf{c}(-\gamma/2 - iv, -\gamma/2 + iv)T} - 1 \right] dv \right\}.$$

It follows, after applying L'Hôpital's rule, that

$$\begin{aligned} r &= \rho - [2 \cosh(u/2)]^\gamma \int_{-\infty}^{\infty} \mathcal{F}_\gamma(v) e^{iuv} \mathbf{c}(-\gamma/2 - iv, -\gamma/2 + iv) dv \\ &= [2 \cosh(u/2)]^\gamma \int_{-\infty}^{\infty} \mathcal{F}_\gamma(v) e^{iuv} \cdot [\rho - \mathbf{c}(-\gamma/2 - iv, -\gamma/2 + iv)] dv \end{aligned}$$

as required.

C The ridge property

This section expands on two closely related issues. First, as mentioned in Appendix B.2.1, the required assumption that

$$\rho - \operatorname{Re}[\mathbf{c}(\alpha_1 - \gamma/2 - iv, \alpha_2 - \gamma/2 + iv)] > 0 \quad \text{for all } v \in \mathbb{R}$$

follows from the apparently weaker assumption that the inequality holds at $v = 0$:

$$\rho - \mathbf{c}(\alpha_1 - \gamma/2, \alpha_2 - \gamma/2) > 0.$$

Second, when considering the small-asset asymptotic (see Section 6 and Appendix E), it is of interest to find the zero of

$$\rho - \mathbf{c}(\alpha_1 - \gamma/2 - iv, \alpha_2 - \gamma/2 + iv)$$

in the upper half-plane which is closest to the real axis (the *minimal* zero, in the terminology of Appendix E).

In either case, we are led to explore the properties of $\mathbf{c}(\alpha_1 - \gamma/2 - iv, \alpha_2 - \gamma/2 + iv)$, considered as a function of v . Recalling the change of measure of Appendix B.1.1, we can exploit the fact that

$$\mathbf{c}(\alpha_1 - \gamma/2 - iv, \alpha_2 - \gamma/2 + iv) = \tilde{\mathbf{c}}(-iv, iv) + \mathbf{c}(\alpha_1 - \gamma/2, \alpha_2 - \gamma/2)$$

where $\tilde{\mathbf{c}}(v_1, v_2)$ is the cumulant-generating function under the changed measure. Next, note that

$$\tilde{\mathbf{c}}(-iv, iv) = \log \tilde{\mathbb{E}} e^{iv(\tilde{y}_{21} - \tilde{y}_{11})} \equiv \log \psi(v)$$

which defines $\psi(v)$ as the *characteristic function* of the random variable $\tilde{y}_{21} - \tilde{y}_{11}$.

I now state a theorem proved in Dugué (1951) and discussed further by Lukacs (1970, pp. 191–5):

Result 3. *Let $\psi(v)$ be an analytic characteristic function defined in the horizontal strip $\{v : x_{\min} < \operatorname{Im} v < x_{\max}\}$. Then the maximum of $|\psi(v)|$ along any horizontal line in this strip is to be found on the imaginary axis.*

Proof. Let a and b be real and let $\psi(x)$ be the characteristic function of some real-valued random variable X . Then

$$\psi(a + ib) = \mathbb{E} \left(e^{iaX} e^{-bX} \right)$$

so

$$|\psi(a + ib)| = \left| \mathbb{E} \left(e^{iaX} e^{-bX} \right) \right| \leq \mathbb{E} \left| e^{iaX} e^{-bX} \right| = \mathbb{E} e^{-bX} = \psi(ib) = |\psi(ib)|$$

which is the desired result. \square

In other words, analytic characteristic functions have the “ridge property”. If $|\psi(v)|$ is thought of as a 3D plot, with $|\psi(v)|$ represented by height above the complex plane, there is a ridge running along the imaginary axis.

Since the log dividend processes dealt with in this paper all have finite moments of all orders, their characteristic functions can be expanded in the neighborhood of the origin as a power series, and are therefore analytic in a horizontal strip containing the origin.

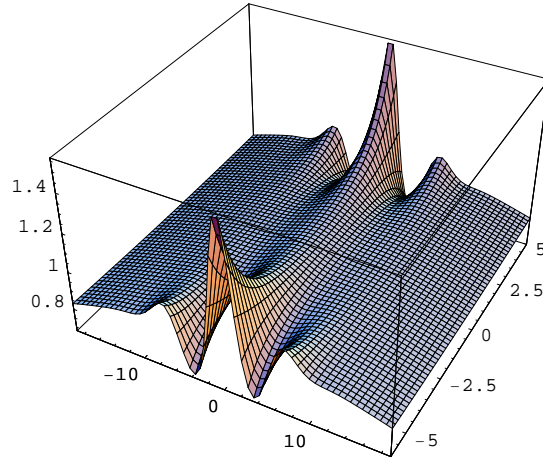


Figure 15: The ridge property. The figure plots $|\psi(v)|$ (on the z -axis) over a portion of the complex plane around the origin. A ridge runs up the imaginary axis.

Figure 15 illustrates the ridge property using the calibration of section 5.2.

Proposition 9. *The assumption that*

$$\rho - \text{Re}[\mathbf{c}(\alpha_1 - \gamma/2 - iv, \alpha_2 - \gamma/2 + iv)] > 0 \quad \text{for all } v \in \mathbb{R}.$$

follows from the apparently weaker assumption that the inequality holds at $v = 0$:

$$\rho - \mathbf{c}(\alpha_1 - \gamma/2, \alpha_2 - \gamma/2) > 0. \tag{73}$$

Proof. Suppose the apparently weaker inequality holds. In terms of the characteristic function ψ , we have

$$\rho - \mathbf{c}(\alpha_1 - \gamma/2 - iv, \alpha_2 - \gamma/2 + iv) = \rho - \mathbf{c}(\alpha_1 - \gamma/2, \alpha_2 - \gamma/2) - \log \psi(v); \quad (74)$$

note that the middle term on the right is real. So, for $v \in \mathbb{R}$, we have

$$\begin{aligned} \rho - \operatorname{Re}[\mathbf{c}(\alpha_1 - \gamma/2 - iv, \alpha_2 - \gamma/2 + iv)] &= \rho - \mathbf{c}(\alpha_1 - \gamma/2, \alpha_2 - \gamma/2) - \operatorname{Re} \log \psi(v) \\ &= \rho - \mathbf{c}(\alpha_1 - \gamma/2, \alpha_2 - \gamma/2) - \log |\psi(v)| \\ &\geq \rho - \mathbf{c}(\alpha_1 - \gamma/2, \alpha_2 - \gamma/2) - \log |\psi(0)| \\ &= \rho - \mathbf{c}(\alpha_1 - \gamma/2, \alpha_2 - \gamma/2) \\ &> 0 \quad \text{by assumption,} \end{aligned}$$

which establishes the claim. The first inequality in this chain follows by the ridge property, Result 3. \square

Under assumption (73) this proposition implies, for example, that there are no zeros of $\rho - \mathbf{c}(\alpha_1 - \gamma/2 - iv, \alpha_2 - \gamma/2 + iv)$ on the real axis. The following proposition documents an important property of the closest zero above the real axis.

Proposition 10. *Consider*

$$\rho - \mathbf{c}(\alpha_1 - \gamma/2 - iv, \alpha_2 - \gamma/2 + iv) \quad (75)$$

as a function of $v \in \mathbb{C}$, and suppose that the condition

$$\rho - \mathbf{c}(\alpha_1 - \gamma/2, \alpha_2 - \gamma/2) > 0 \quad (76)$$

holds. Then the zero of (75) in the upper half-plane which is closest to the real axis lies on the imaginary axis.

Proof. Using equation (74) above, any zero, z , satisfies

$$\rho - \mathbf{c}(\alpha_1 - \gamma/2, \alpha_2 - \gamma/2) = \log \psi(z).$$

Writing the left-hand side as $\widehat{\rho} \in \mathbb{R}$ for convenience, any zero z must satisfy $\psi(z) = \exp \widehat{\rho}$. The fact that $\widehat{\rho} > 0$ follows from (76).

Let z^* be the zero in the upper half-plane with smallest imaginary part, and suppose (for a contradiction) that $\operatorname{Re} z^* \neq 0$. Let $\tilde{z} = (\operatorname{Im} z^*)i$ be the projection of z^* onto the imaginary axis. By the ridge property, we have $\psi(\tilde{z}) > |\psi(z^*)| = \exp \widehat{\rho}$. So, $\psi(\tilde{z}) > \exp \widehat{\rho} > 1 = \psi(0)$. By continuity of ψ , there must be a purely imaginary \widehat{z} which lies between 0 and \tilde{z} and satisfies $\psi(\widehat{z}) = \exp \widehat{\rho}$ —but this contradicts the assumption that z^* had smallest imaginary part. Therefore the zero with smallest imaginary part must, in fact, lie on the imaginary axis. \square

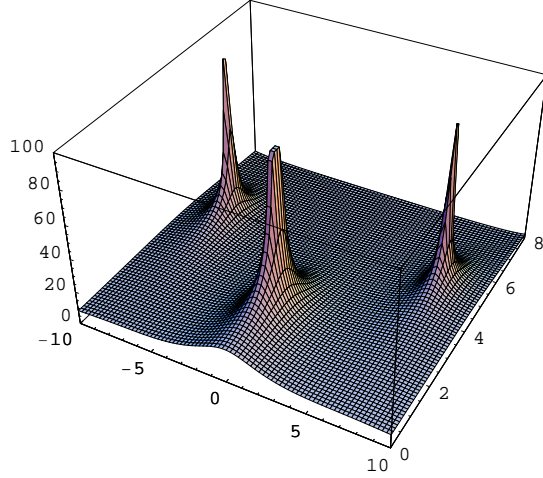


Figure 16: $1/|\rho - \mathbf{c}(1 - \gamma/2 - iv, -\gamma/2 + iv)|$ plotted for v in a region of the complex plane close to the origin. Zeros of $\rho - \mathbf{c}(1 - \gamma/2 - iv, -\gamma/2 + iv)$ occur at the spikes. The pole nearest the real axis lies on the imaginary axis, at roughly $3i$ in this example.

Condition (76) holds when $(\alpha_1, \alpha_2) = (1, 0)$ or $(0, 1)$ by the finiteness condition.

Figure 16 illustrates Proposition 10 (using the calibration of section 5.2) by plotting the real-valued function $1/|\rho - \mathbf{c}(1 - \gamma/2 - iv, -\gamma/2 + iv)|$ over a region of the complex plane close to the origin. When $\rho - \mathbf{c}(1 - \gamma/2 - iv, -\gamma/2 + iv)$ has a zero, this function explodes. Proposition 10 says that the spike which is closest to the real axis should lie on the imaginary axis—and of course it does.

D The Brownian motion case

The price-dividend ratio on asset 1 is determined by setting $(\alpha_1, \alpha_2) = (1, 0)$ in (14), in which case we have

$$P/D_1(u) = [2 \cosh(u/2)]^\gamma \cdot \int_{-\infty}^{\infty} \frac{e^{iuv} \mathcal{F}_\gamma(v)}{\rho - \mathbf{c}(1 - \gamma/2 - iv, -\gamma/2 + iv)} dv. \quad (77)$$

In this Brownian motion case, there are two solutions to the equation $\rho - \mathbf{c}(1 - \gamma/2 - iv, -\gamma/2 + iv)$, each of which lie on the imaginary axis. One—call it $\lambda_1 i$ —lies in the upper half-plane; the other—call it $\lambda_2 i$ —lies in the lower half-plane. We can then rewrite

$$\rho - \mathbf{c}(1 - \gamma/2 - iv, -\gamma/2 + iv) = B(v - \lambda_1 i)(v - \lambda_2 i)$$

for some $B > 0$.

The aim, then, is to evaluate

$$I \equiv \int_{-\infty}^{\infty} \frac{e^{iuv} \mathcal{F}_\gamma(v)}{B(v - \lambda_1 i)(v - \lambda_2 i)} dv, \quad (78)$$

in terms of which the price-dividend ratio is

$$P/D = [2 \cosh(u/2)]^\gamma \cdot I. \quad (79)$$

The proof of Proposition 5, which amounts to evaluating the integral (78), is somewhat involved, so I have divided it into several steps. Step 1 starts from the assumption that the state variable u is positive—an assumption that will later be relaxed—and demonstrates that the integral (77) can be calculated via the Residue Theorem (stated as Result 2 in Appendix A) by finding the residues at all poles of the integrand that occur in the upper half-plane. Steps 2 and 3 carry out the residue calculations and simplify. Step 4 demonstrates that the resulting expression is also valid for negative u . Step 5 calculates B, λ_1 and λ_2 in terms of fundamental parameters, which concludes the proof.

Step 1. Let $u > 0$. Consider the case in which γ is even. Let $R_n \equiv n + 1/2$, where n is an integer. Define the large semicircle Ω_n to be the semicircle whose base lies along the real axis from $-R_n$ to R_n and which has a semicircular arc (ω_n) passing through the upper half-plane from R_n through $R_n i$ and back to $-R_n$. I will first show that

$$I = \lim_{n \rightarrow \infty} \int_{\Omega_n} \frac{e^{iuv} \mathcal{F}_\gamma(v)}{B(v - \lambda_1 i)(v - \lambda_2 i)} dv. \quad (80)$$

Then, from the residue theorem, it will follow that

$$I = 2\pi i \cdot \sum \text{Res} \left\{ \frac{e^{iuv} \mathcal{F}_\gamma(v)}{B(v - \lambda_1 i)(v - \lambda_2 i)}; v_p \right\}, \quad (81)$$

where the sum is taken over all poles v_p in the upper half-plane.

The first step is to establish that (80) holds. The right-hand side is equal to

$$\lim_{n \rightarrow \infty} \underbrace{\int_{-R_n}^{R_n} \frac{e^{iuv} \mathcal{F}_\gamma(v)}{B(v - \lambda_1 i)(v - \lambda_2 i)} dv}_{I_n} + \underbrace{\int_{\omega_n} \frac{e^{iuv} \mathcal{F}_\gamma(v)}{B(v - \lambda_1 i)(v - \lambda_2 i)} dv}_{J_n}$$

The integral I_n tends to I as n tends to infinity. The aim, then, is to establish that the second term J_n tends to zero as n tends to infinity. Along the arc ω_n , we have $v = R_n e^{i\theta}$ where θ varies between 0 and π .

At this point of the argument it is convenient to work with the representation of $\mathcal{F}_\gamma(v)$ of equation (62). Substituting from (62), we have

$$J_n = \int_0^\pi \frac{e^{iuR_n \cos \theta - uR_n \sin \theta} P(R_n e^{i\theta})}{Q(R_n e^{i\theta}) (e^{\pi R_n (\cos \theta + i \sin \theta)} - e^{-\pi R_n (\cos \theta + i \sin \theta)})} \cdot R_n i e^{i\theta} d\theta$$

with $P(\cdot)$ and $Q(\cdot)$ polynomials.

To show that J_n tends to zero as n tends to infinity, I separate the range of integration $[0, \pi]$ into two parts: $[\pi/2 - \delta, \pi/2 + \delta]$ and its complement in $[0, \pi]$. Here δ will be chosen to be extremely small.

First, consider

$$\begin{aligned}
J_n^{(1)} &\equiv \left| \int_{\pi/2-\delta}^{\pi/2+\delta} \frac{P(R_n e^{i\theta}) e^{iuR_n \cos \theta - uR_n \sin \theta} R_n i e^{i\theta}}{Q(R_n e^{i\theta}) (e^{\pi R_n (\cos \theta + i \sin \theta)} - e^{-\pi R_n (\cos \theta + i \sin \theta)})} d\theta \right| \\
&\leq \int_{\pi/2-\delta}^{\pi/2+\delta} \left| \frac{P(R_n e^{i\theta})}{Q(R_n e^{i\theta})} \right| \frac{e^{-uR_n \sin \theta} R_n}{|e^{\pi R_n (\cos \theta + i \sin \theta)} - e^{-\pi R_n (\cos \theta + i \sin \theta)}|} d\theta \quad (82)
\end{aligned}$$

Pick δ sufficiently small that

$$\left| e^{\pi R_n (\cos \theta + i \sin \theta)} - e^{-\pi R_n (\cos \theta + i \sin \theta)} \right| \geq 2 - \varepsilon$$

for all $\theta \in [\pi/2 - \delta, \pi/2 + \delta]$; ε is some very small number close to but greater than zero. This is possible because the left-hand side is continuous and equal to 2 when $\theta = \pi/2$. Then,

$$J_n^{(1)} \leq \int_{\pi/2-\delta}^{\pi/2+\delta} \left| \frac{P(R_n e^{i\theta})}{Q(R_n e^{i\theta})} \right| \frac{e^{-uR_n \sin \theta} R_n}{2 - \varepsilon} d\theta \quad (83)$$

Since

- (i) we can also ensure that δ is small enough that $\sin \theta \geq \varepsilon$ for θ in the range of integration,
- (ii) $|P(R_n e^{i\theta})| \leq P_2(R_n)$, where P_2 is the polynomial obtained by taking absolute values of the coefficients in P ,
- (iii) $Q(R_n e^{i\theta})$ tends to infinity as R_n becomes large and
- (iv) decaying exponentials decay faster than polynomials grow, in the sense that for any positive k and λ , $x^k e^{-\lambda x} \rightarrow 0$ as $x \rightarrow \infty$, $x \in \mathbb{R}$,

we see, finally, that the right-hand side of (83), and hence $J_n^{(1)}$, tends to zero as n tends to infinity,

It remains to be shown that

$$J_n^{(2)} \equiv \left| \int_{[0, \pi/2-\delta] \cup [\pi/2+\delta, \pi]} \frac{P(R_n e^{i\theta}) e^{iuR_n \cos \theta - uR_n \sin \theta} R_n i e^{i\theta}}{Q(R_n e^{i\theta}) (e^{\pi R_n (\cos \theta + i \sin \theta)} - e^{-\pi R_n (\cos \theta + i \sin \theta)})} d\theta \right|$$

is zero in the limit. Since $\delta > 0$, for all θ in the range of integration we have that $|\cos \theta| \geq \zeta > 0$, for some small ζ . We have

$$J_n^{(2)} \leq \int_{[0, \pi/2-\delta] \cup [\pi/2+\delta, \pi]} \left| \frac{P(R_n e^{i\theta})}{Q(R_n e^{i\theta})} \right| \frac{e^{-uR_n \sin \theta} R_n}{|e^{\pi R_n (\cos \theta + i \sin \theta)} - e^{-\pi R_n (\cos \theta + i \sin \theta)}|} d\theta.$$

Now,

$$\begin{aligned}
&\left| e^{\pi R_n (\cos \theta + i \sin \theta)} - e^{-\pi R_n (\cos \theta + i \sin \theta)} \right| \\
&\geq \left| \left| e^{\pi R_n (\cos \theta + i \sin \theta)} \right| - \left| e^{-\pi R_n (\cos \theta + i \sin \theta)} \right| \right| \\
&= e^{\pi R_n |\cos \theta|} - e^{-\pi R_n |\cos \theta|} \\
&\geq e^{\pi R_n \zeta} - e^{-\pi R_n \zeta}
\end{aligned}$$

for all θ in the range of integration. So,

$$\begin{aligned} J_n^{(2)} &\leq \int_{[0, \pi/2 - \delta] \cup [\pi/2 + \delta, \pi]} \left| \frac{P(R_n e^{i\theta})}{Q(R_n e^{i\theta})} \right| \frac{e^{-u R_n \sin \theta} R_n}{e^{\pi R_n \zeta} - e^{-\pi R_n \zeta}} d\theta \\ &\leq \int_{[0, \pi/2 - \delta] \cup [\pi/2 + \delta, \pi]} \left| \frac{P(R_n e^{i\theta})}{Q(R_n e^{i\theta})} \right| \frac{R_n}{e^{\pi R_n \zeta} - e^{-\pi R_n \zeta}} d\theta \end{aligned}$$

which tends to zero as n tends to infinity.

The case of γ odd is almost identical. The only important difference is that we take $R_n = n$ (as opposed to $n + 1/2$) before allowing n to go to infinity. The reason for doing so is that we must take care to avoid the poles of $\mathcal{F}_\gamma(v)$ on the imaginary axis.

Step 2. From now on, I revert to the definition of $\mathcal{F}_\gamma(v)$ as

$$\mathcal{F}_\gamma(v) = \frac{1}{2\pi} \frac{\Gamma(\gamma/2 - iv)\Gamma(\gamma/2 + iv)}{\Gamma(\gamma)}.$$

The integrand is

$$\frac{e^{iuv}\Gamma(\gamma/2 - iv)\Gamma(\gamma/2 + iv)}{2\pi \cdot B \cdot \Gamma(\gamma) \cdot (v - \lambda_1 i)(v - \lambda_2 i)}, \quad (84)$$

which has poles in the upper half-plane at $\lambda_1 i$ and at points v such that $\gamma/2 + iv = -n$ for integers $n \geq 0$, since the Γ -function has poles at the negative integers and zero. In other words, the integrand has poles at $\lambda_1 i$ and at $(n + \gamma/2)i$ for $n \geq 0$.

By direct calculation using (49), the residue of (84) at $v = \lambda_1 i$ is

$$\frac{e^{-\lambda_1 u} \Gamma(\gamma/2 + \lambda_1) \Gamma(\gamma/2 - \lambda_1)}{2\pi i \cdot B \cdot \Gamma(\gamma) \cdot (\lambda_1 - \lambda_2)}. \quad (85)$$

$\Gamma(z)$ has residue $(-1)^n/n!$ at $z = -n$. (See, for example, Andrews, Askey and Roy (1999, p. 7).) Using this fact, it follows that the residue of (84) at $v = (n + \gamma/2)i$ for integers $n \geq 0$ is

$$\frac{-e^{-u(n+\gamma/2)} \cdot \Gamma(\gamma + n) \cdot \frac{(-1)^n}{n!}}{2\pi i \cdot B \cdot \Gamma(\gamma) \cdot (n + \gamma/2 - \lambda_1)(n + \gamma/2 - \lambda_2)} \quad (86)$$

Substituting (85) and (86) into (81), we find

$$I = \frac{e^{-\lambda_1 u} \Gamma(\gamma/2 + \lambda_1) \Gamma(\gamma/2 - \lambda_1)}{B \cdot \Gamma(\gamma) \cdot (\lambda_1 - \lambda_2)} - e^{-\gamma u/2} \sum_{n=0}^{\infty} \frac{(-e^{-u})^n \cdot \Gamma(\gamma + n) \cdot \frac{1}{n!}}{B \cdot \Gamma(\gamma) \cdot (n + \gamma/2 - \lambda_1)(n + \gamma/2 - \lambda_2)}$$

Since $|-e^{-u}| < 1$ under the assumption that $u > 0$, which for the time being is still maintained, we can use the series definition of Gauss's hypergeometric function given in equation (7), together with the fact that $\Gamma(\gamma + n)/\Gamma(\gamma) = \gamma(\gamma + 1) \cdots (\gamma + n - 1)$, to obtain

$$\begin{aligned} I &= \frac{e^{-\lambda_1 u}}{B(\lambda_1 - \lambda_2)} \frac{\Gamma(\gamma/2 - \lambda_1) \Gamma(\gamma/2 + \lambda_1)}{\Gamma(\gamma)} + \\ &+ \frac{e^{-\gamma u/2}}{B(\lambda_1 - \lambda_2)} \left[\frac{1}{\gamma/2 - \lambda_2} F(\gamma, \gamma/2 - \lambda_2; 1 + \gamma/2 - \lambda_2; -e^{-u}) - \right. \\ &\quad \left. - \frac{1}{\gamma/2 - \lambda_1} F(\gamma, \gamma/2 - \lambda_1; 1 + \gamma/2 - \lambda_1; -e^{-u}) \right] \quad (87) \end{aligned}$$

Step 3. A final simplification follows from the fact that

$$e^{-\lambda_1 u} \frac{\Gamma(\gamma/2 - \lambda_1) \Gamma(\gamma/2 + \lambda_1)}{\Gamma(\gamma)} = \frac{e^{\gamma u/2}}{\gamma/2 + \lambda_1} F(\gamma, \gamma/2 + \lambda_1; 1 + \gamma/2 + \lambda_1; -e^u) + \frac{e^{-\gamma u/2}}{\gamma/2 - \lambda_1} F(\gamma, \gamma/2 - \lambda_1; 1 + \gamma/2 - \lambda_1; -e^{-u}),$$

which follows from equation (1.8.1.11) of Slater (1966, pp. 35–36).

Using this observation to substitute out the first term in (87), we have

$$I = \frac{1}{B(\lambda_1 - \lambda_2)} \left[\frac{e^{\gamma u/2}}{\gamma/2 + \lambda_1} F(\gamma, \gamma/2 + \lambda_1; 1 + \gamma/2 + \lambda_1; -e^u) + \frac{e^{-\gamma u/2}}{\gamma/2 - \lambda_2} F(\gamma, \gamma/2 - \lambda_2; 1 + \gamma/2 - \lambda_2; -e^{-u}) \right].$$

Substituting this expression into (79) gives the formula

$$P/D_1(u) = \frac{[2 \cosh(u/2)]^\gamma}{B(\lambda_1 - \lambda_2)} \left[\frac{e^{\gamma u/2}}{\gamma/2 + \lambda_1} F(\gamma, \gamma/2 + \lambda_1; 1 + \gamma/2 + \lambda_1; -e^u) + \frac{e^{-\gamma u/2}}{\gamma/2 - \lambda_2} F(\gamma, \gamma/2 - \lambda_2; 1 + \gamma/2 - \lambda_2; -e^{-u}) \right]; \quad (88)$$

thus far, however, the derivation is valid only under the assumption that $u > 0$.

Step 4. Suppose, now, that $u < 0$. Take the complex conjugate of equation (78). (This leaves the left-hand side unaltered because the price-dividend ratio is real.) Doing so is equivalent to reframing the problem with $(u, \lambda_1, \lambda_2)$ replaced by $(-u, -\lambda_2, -\lambda_1)$. Since $-u > 0, -\lambda_2 > 0$ and $-\lambda_1 < 0$, the method of steps 1–4 applies unchanged. Since the formula (88) is invariant under $(-u, -\lambda_2, -\lambda_1) \mapsto (u, \lambda_1, \lambda_2)$, we can conclude that equation (88) is valid for all u . Substituting $u \mapsto \log(1 - s)/s$ delivers (22).

Step 5. It only remains to find the values of B, λ_1 and λ_2 in terms of the fundamental parameters. The CGF is given, in the general Brownian motion case, by

$$\mathbf{c}(\theta_1, \theta_2) = \mu_1 \theta_1 + \mu_2 \theta_2 + \frac{1}{2} \sigma_{11} \theta_1^2 + \sigma_{12} \theta_1 \theta_2 + \frac{1}{2} \sigma_{22} \theta_2^2$$

We can rewrite $\rho - \mathbf{c}(1 - \gamma/2 - iv, -\gamma/2 + iv)$ in the form

$$\rho - \mathbf{c}(1 - \gamma/2 - iv, -\gamma/2 + iv) = \frac{1}{2} X^2 v^2 + iYv + \frac{1}{2} Z^2, \quad (89)$$

where, as in the main text, I have defined

$$\begin{aligned} X^2 &\equiv \sigma_{11} - 2\sigma_{12} + \sigma_{22} \\ Y &\equiv \mu_1 - \mu_2 + \sigma_{11} - \sigma_{12} - \frac{\gamma}{2} (\sigma_{11} - \sigma_{22}) \\ Z^2 &\equiv 2(\rho - \mu_1 - \sigma_{11}/2) + \gamma(\mu_1 + \mu_2 + \sigma_{11} + \sigma_{12}) - \frac{\gamma^2}{4} (\sigma_{11} + 2\sigma_{12} + \sigma_{22}). \end{aligned}$$

I have chosen to write X^2 and Z^2 to emphasize that these two quantities are positive. The positivity of X^2 follows because it is the variance of the difference of two random variables ($y_{21} - y_{11}$). The positivity of Z^2 , on the other hand, follows from the assumption that $\rho - \mathbf{c}(1 - \gamma/2, -\gamma/2) > 0$ by setting $v = 0$ in (89).

Solving the quadratic equation in (89) for v as a function of X , Y and Z , we have, finally, that

$$\rho - \mathbf{c}(1 - \gamma/2 - iv, -\gamma/2 + iv) = B(v - \lambda_1 i)(v - \lambda_2 i)$$

where

$$\begin{aligned} B &\equiv \frac{1}{2}X^2 \\ \lambda_1 &\equiv \frac{\sqrt{Y^2 + X^2 Z^2} - Y}{X^2} \\ \lambda_2 &\equiv -\frac{\sqrt{Y^2 + X^2 Z^2} + Y}{X^2}. \end{aligned}$$

D.1 Simple special cases with symmetric Brownian motions

In some special subcases, it is possible to obtain considerably simpler expressions for the price-dividend ratio. In this section, I consider the special case in which the world is symmetrical and the log dividend processes of each asset follow independent drifting Brownian motions with drift μ and volatility σ . It follows that the CGF is given by

$$\mathbf{c}(\theta_1, \theta_2) = \mu(\theta_1 + \theta_2) + \frac{1}{2}\sigma^2(\theta_1^2 + \theta_2^2) \quad (90)$$

Recall the general pricing formula, in the form of (14):

$$\frac{P_\alpha}{D_\alpha} = [2 \cosh(u/2)]^\gamma \cdot \int_{-\infty}^{\infty} \frac{e^{iuv} \mathcal{F}_\gamma(v)}{\rho - \mathbf{c}(\alpha_1 - \gamma/2 - iv, \alpha_2 - \gamma/2 + iv)} dv$$

I will focus on pricing the claim to asset 1, so $\alpha_1 = 1, \alpha_2 = 0$. Substituting in from (90), a little algebra confirms the fact that

$$\rho - \mathbf{c}(1 - \gamma/2 - iv, -\gamma/2 + iv) = \sigma^2 \left[(v + i/2)^2 + A^2 \right],$$

where $A^2 \equiv (\rho + \mu(\gamma - 1))/\sigma^2 - (\gamma - 1)^2/4$. The finiteness condition requires that

$$\rho - \mathbf{c}(1 - \gamma/2, -\gamma/2) > 0 \quad \text{and} \quad \rho - \mathbf{c}(1 - \gamma, 0) > 0$$

which amounts to the requirement that $A > (\gamma - 1)/2$.

The general pricing formula gives the price-dividend ratio of asset 1, written P/D_1 , as

$$P/D_1 = [2 \cosh(u/2)]^\gamma \cdot \int_{-\infty}^{\infty} \frac{e^{iuv} \mathcal{F}_\gamma(v)}{\sigma^2 \left[(v + i/2)^2 + A^2 \right]} dv. \quad (91)$$

The question, as before, is where the poles of the integrand are. In the upper half plane, $\mathcal{F}_\gamma(v)$ has infinitely many regularly spaced poles on the imaginary axis, at $(\gamma/2)i$, $(\gamma/2 + 1)i$, $(\gamma/2 + 2)i$, \dots . The other pole is at the zero, in the upper half-plane, of the denominator $\sigma^2 \left[(v + i/2)^2 + A^2 \right]$ —that is, at $(A - 1/2)i$. It turns out that the integral takes on a relatively simple form if we ensure that the pole at $(A - 1/2)i$ is an integer distance from the poles $(\gamma/2)i$, $(\gamma/2 + 1)i$, etc. (The simple example presented in Cochrane, Longstaff and Santa-Clara (2007) has $\rho = \sigma^2$, so $A = 1$.) Thus, we want

$$A \in \{(\gamma + 1)/2, (\gamma + 3)/2, (\gamma + 5)/2, \dots\}$$

For example, if $\gamma = 2$ and $A = 3/2$, the price-dividend ratio of asset 1 is

$$P/D_1(s) = \frac{2(1-s)^3 \log(1-s) + 2s - 5s^2 + 3s^3 - s^3 \log s}{3(1-s)^2 s^3 \sigma^2}.$$

E Small asset asymptotics

I start by establishing the claim made in the text that $\rho - \mathbf{c}(1 - \theta, \theta - \gamma)$ is a concave function of θ . This fact follows directly from

Proposition 11 (A convexity property of $\mathbf{c}(\cdot, \cdot)$). *For arbitrary real numbers α and β , the function $\mathbf{c}(\alpha - \theta, \beta + \theta)$ is a convex function of θ .*

Proof. Define the measure $\widehat{\mathbb{P}}$ by

$$\widehat{\mathbb{E}}(A) \equiv e^{-\mathbf{c}(\alpha, \beta)} \mathbb{E} \left(e^{\alpha y_{11} + \beta y_{21}} A \right).$$

It follows that the CGF of $y_{21} - y_{11}$, calculated with respect to $\widehat{\mathbb{P}}$, is

$$\begin{aligned} \widehat{\mathbf{c}}(\theta) &= \log \widehat{\mathbb{E}} \left(e^{\theta y_{21} - \theta y_{11}} \right) \\ &= -\mathbf{c}(\alpha, \beta) + \log \mathbb{E} \left(e^{(\alpha - \theta) y_{11} + (\beta + \theta) y_{21}} \right) \\ &= -\mathbf{c}(\alpha, \beta) + \mathbf{c}(\alpha - \theta, \beta + \theta). \end{aligned}$$

Therefore, $\mathbf{c}(\alpha - \theta, \beta + \theta) = \mathbf{c}(\alpha, \beta) + \widehat{\mathbf{c}}(\theta)$. (Compare also equations (53) and (54) of Appendix B.1.1.)

The convexity of $\mathbf{c}(\alpha - \theta, \beta + \theta)$ follows immediately, because $\widehat{\mathbf{c}}(\theta)$, as a CGF, is convex, as shown in Billingsley (1995, pp. 147–8). \square

The price-dividend ratio in the small asset limit is given by (15), which I reproduce here for the situation in which asset 1 is small:

$$P/D_1 = \lim_{u \rightarrow \infty} \frac{\int_{-\infty}^{\infty} \frac{e^{iuv} \mathcal{F}_\gamma(v)}{\rho - \mathbf{c}(1 - \gamma/2 - iv, -\gamma/2 + iv)} dv}{\int_{-\infty}^{\infty} e^{iuv} \mathcal{F}_\gamma(v) dv}. \quad (92)$$

By the Riemann-Lebesgue lemma, both the numerator and denominator on the right-hand side of (92) tend to zero in the limit as u tends to infinity.²² What happens to their ratio? This section shows how to calculate limiting price-dividend ratio, riskless rate and excess returns in the small-asset case. For clarity, I work through the price-dividend ratio in detail; the techniques used also apply to the riskless rate and to expected returns, and are very similar to those that were used to provide the closed-form solution in the Brownian motion case.

The following definition provides a convenient label for the poles that will be of interest when evaluating the relevant integrals in the asymptotic limit. (When reading the definition, note that by the finiteness condition and Proposition 9 of Appendix C, the functions to which the definition will be applied will never have poles *on* the real axis.)

Definition 3. *Let f be an arbitrary meromorphic function. A pole (resp. zero) of f is minimal if it lies in the upper half-plane and no other pole (resp. zero) in the upper half-plane has smaller imaginary part.*

Step 1. Consider the integral which makes up the numerator of (92),

$$I \equiv \int_{-\infty}^{\infty} \frac{e^{iuv} \mathcal{F}_{\gamma}(v)}{\rho - \mathbf{c}(1 - \gamma/2 - iv, -\gamma/2 + iv)} dv.$$

If log dividends are drifting Brownian motions, Appendix D showed that this integral could be approached by summing all residues in the upper half-plane. The aim here is to show that the *asymptotic* behavior of this integral is determined only by the minimal residue. Roughly speaking, this is because poles with larger imaginary parts are rendered asymptotically irrelevant by the term e^{iuv} .

To establish this fact, it is convenient to integrate around a contour which avoids all poles except for the minimal pole. If the minimal pole occurs at the minimal zero of $\rho - \mathbf{c}(1 - \gamma/2 - iv, -\gamma/2 + iv)$ then, by Proposition 10 of Appendix C, this pole occurs on the imaginary axis. Otherwise, the minimal pole occurs at the minimal pole of $\mathcal{F}_{\gamma}(v)$, so is at $i\gamma/2$ —which is also on the imaginary axis. In short, we can assume that the minimal pole occurs at the point mi , where $m > 0$ is a real number.

Let \square_N denote the rectangle in the complex plane with corners at $-N$, N , $N + (m + \varepsilon)i$ and $-N + (m + \varepsilon)i$, with the understanding that integration will take place in the anticlockwise direction. Since the integrand is meromorphic, all poles are isolated, so $\varepsilon > 0$ can be chosen to be sufficiently small that the rectangle \square_N only contains the pole at mi .

²²See Körner (1988, pp. 573–4) for a proof of the Riemann-Lebesgue lemma.

By the residue theorem, we have

$$\begin{aligned} J &\equiv \int_{\square_N} \frac{e^{iuv} \mathcal{F}_\gamma(v)}{\rho - \mathbf{c}(1 - \gamma/2 - iv, -\gamma/2 + iv)} dv \\ &= 2\pi i \operatorname{Res} \left\{ \frac{e^{iuv} \mathcal{F}_\gamma(v)}{\rho - \mathbf{c}(1 - \gamma/2 - iv, -\gamma/2 + iv)}; mi \right\} \end{aligned}$$

On the other hand, we can also decompose the integral into four pieces:

$$\begin{aligned} J &= \int_{-N}^N \frac{e^{iuv} \mathcal{F}_\gamma(v)}{\rho - \mathbf{c}(1 - \gamma/2 - iv, -\gamma/2 + iv)} dv + \int_0^{m+\varepsilon} \frac{e^{iu(N+iv)} \mathcal{F}_\gamma(N+iv)}{\rho - \mathbf{c}(\dots)} i dv + \\ &\quad + \int_N^{-N} \frac{e^{iu(v+(m+\varepsilon)i)} \mathcal{F}_\gamma(v+(m+\varepsilon)i)}{\rho - \mathbf{c}(\dots)} dv + \int_{m+\varepsilon}^0 \frac{e^{iu(-N+iv)} \mathcal{F}_\gamma(-N+iv)}{\rho - \mathbf{c}(\dots)} i dv \\ &\equiv J_1 + J_2 + J_3 + J_4 \end{aligned}$$

In brief, the desired result follows on first letting N tend to infinity; then J_2 and J_4 go to zero. Subsequently letting u go to infinity, J_3 becomes asymptotically irrelevant compared to J_1 . By the residue theorem, the integral $I = \lim_{N \rightarrow \infty} J_1$ is therefore asymptotically equivalent²³ to $2\pi i$ times the residue at mi :

$$I \sim 2\pi i \cdot \operatorname{Res} \left\{ \frac{e^{iuv} \mathcal{F}_\gamma(v)}{\rho - \mathbf{c}(1 - \gamma/2 - iv, -\gamma/2 + iv)}; mi \right\}.$$

The following calculations justify these statements. Consider J_2 . Since the range of integration is a closed and bounded interval, the function $|\rho - \mathbf{c}(\dots)|$ attains its maximum and minimum on the range. Since also the function has no zeros on the interval, we can write $|\rho - \mathbf{c}(\dots)| \geq \delta_1 > 0$ for all v in the range of integration. We have

$$\begin{aligned} |J_2| &\leq \int_0^{m+\varepsilon} \left| \frac{e^{iu(N+iv)} \mathcal{F}_\gamma(N+iv)}{\rho - \mathbf{c}(\dots)} i \right| dv \\ &= \int_0^{m+\varepsilon} \frac{e^{-uv} |\mathcal{F}_\gamma(N+iv)|}{|\rho - \mathbf{c}(\dots)|} dv \\ &\leq \frac{1}{\delta_1} \int_0^{m+\varepsilon} |\mathcal{F}_\gamma(N+iv)| dv \\ &\rightarrow 0 \end{aligned}$$

as N tends to infinity because $|\mathcal{F}_\gamma(N+iv)|$ converges to zero uniformly over v in the range of integration. An almost identical argument shows that $|J_4|$ tends to zero as N tends to infinity.

²³I write $f(x) \sim g(x)$ —“ $f(x)$ is asymptotically equivalent to $g(x)$ ”—to indicate that $\lim_{x \rightarrow \infty} f(x)/g(x) = 1$. Below, I also use the “big-O” notation $f(x) = O(g(x))$ —“ $f(x)$ is asymptotically of the same order as $g(x)$ ”—to indicate that $\lim_{x \rightarrow \infty} f(x)/g(x)$ is finite.

Now consider J_3 . Set $\delta_2 = |\rho - \mathbf{c}(1 - \gamma/2 + m + \varepsilon, -\gamma/2 - m - \varepsilon)| > 0$; then by Result 3 of Appendix C, $|\rho - \mathbf{c}(\dots)| \geq \delta_2$ for all v in the range of integration. It follows that

$$\begin{aligned} |J_3| &\leq \int_{-N}^N \frac{e^{-(m+\varepsilon)u} |\mathcal{F}_\gamma(v + (m + \varepsilon)i)|}{|\rho - \mathbf{c}(\dots)|} dv \\ &\leq e^{-u(m+\varepsilon)} \cdot \frac{1}{\delta_2} \int_{-N}^N |\mathcal{F}_\gamma(v + (m + \varepsilon)i)| dv \\ &\rightarrow e^{-u(m+\varepsilon)} \cdot X/\delta_2 \end{aligned}$$

where X is the (finite) limit of the integral $\int_{-N}^N |\mathcal{F}_\gamma(v + (m + \varepsilon)i)| dv$ as N tends to infinity. (X is finite because $\mathcal{F}_\gamma(v + (m + \varepsilon)i)$ decays to zero exponentially fast as $v \rightarrow \pm\infty$.)

By the residue theorem,

$$J_1 + J_2 + J_3 + J_4 = 2\pi i \times \text{residue at } mi = O(e^{-mu}).$$

Let N go to infinity; then J_2 and J_4 go to zero, J_1 tends to I and J_3 tends to $e^{-u(m+\varepsilon)}X$, so

$$I + e^{-u(m+\varepsilon)}X = 2\pi i \times \text{residue at } mi = O(e^{-mu}).$$

In the limit as $u \rightarrow \infty$, $e^{-u(m+\varepsilon)}X$ is exponentially smaller than e^{-mu} , so

$$I \sim 2\pi i \operatorname{Res} \left\{ \frac{e^{iuv} \mathcal{F}_\gamma(v)}{\rho - \mathbf{c}(1 - \gamma/2 - iv, -\gamma/2 + iv)}; mi \right\}$$

as $u \rightarrow \infty$. The asymptotic behavior of the integral I is dictated by the residue closest to the real line.

Essentially identical arguments can be made to show that the other relevant integrals are asymptotically equivalent to $2\pi i$ times the minimal residue of the relevant integrand; they are omitted to prevent an already complicated argument becoming totally unreadable.

Step 2. I now apply the logic of step 1 to (i) the price-dividend ratio, (ii) the riskless rate and (iii) expected returns.

(i) In the price-dividend ratio case, we have to evaluate

$$\lim_{u \rightarrow \infty} P/D(u) = \lim_{u \rightarrow \infty} \frac{\int_{-\infty}^{\infty} \frac{e^{iuv} \mathcal{F}_\gamma(v)}{\rho - \mathbf{c}(1 - \gamma/2 - iv, -\gamma/2 + iv)} dv}{\int_{-\infty}^{\infty} e^{iuv} \mathcal{F}_\gamma(v) dv} \equiv \lim_{u \rightarrow \infty} \frac{I_n}{I_d}.$$

We have just seen that I_n and I_d are asymptotically equivalent to $2\pi i$ times the residue at the pole (of the relevant integrand) with smallest imaginary part. Here, I take this fact as given and refer to the pole (or zero) with least positive imaginary part as the *minimal* pole (or zero).

Consider, then, the more complicated integral I_n . The integrand has a pole at $i\gamma/2$ due to a singularity in $\mathcal{F}_\gamma(v)$. The question is whether or not there is a zero of $\rho - \mathbf{c}(1 - \gamma/2 - iv, -\gamma/2 + iv)$ for some v with imaginary part smaller than $\gamma/2$. If there is, then this is the minimal pole. If not, then $i\gamma/2$ is the minimal pole.

In Appendix C, it was shown that the minimal zero of $\rho - \mathbf{c}(1 - \gamma/2 - iv, -\gamma/2 + iv)$ lies on the imaginary axis. Thus the zero in question is of the form zi for some positive real z , and so we are interested in z^* satisfying

$$\rho - \mathbf{c}(1 - \gamma/2 + z^*, -\gamma/2 - z^*) = 0. \quad (93)$$

If $z^* < \gamma/2$, we are in the supercritical case; if $z^* > \gamma/2$, we are in the subcritical case. (At the end of the proof, I will define $\theta^* = \gamma/2 - z^*$, simply for notational convenience.)

- (a) In the subcritical case, the minimal pole for both integrals is at $i\gamma/2$. We therefore have, asymptotically,

$$\begin{aligned} P/D &\longrightarrow \frac{\text{Res} \left\{ \frac{e^{iuv} \mathcal{F}_\gamma(v)}{\rho - \mathbf{c}(1 - \gamma/2 - iv, -\gamma/2 + iv)}; i\gamma/2 \right\}}{\text{Res} \{ e^{iuv} \mathcal{F}_\gamma(v); i\gamma/2 \}} \\ &= \frac{1}{\rho - \mathbf{c}(1, -\gamma)} \cdot \frac{\text{Res} \{ e^{iuv} \mathcal{F}_\gamma(v); i\gamma/2 \}}{\text{Res} \{ e^{iuv} \mathcal{F}_\gamma(v); i\gamma/2 \}} \\ &= \frac{1}{\rho - \mathbf{c}(1, -\gamma)} \end{aligned}$$

- (b) In the supercritical case, the minimal pole is at iz^* for I_n and at $i\gamma/2$ for I_d . We therefore have

$$\begin{aligned} P/D &\longrightarrow \frac{\text{Res} \left\{ \frac{e^{iuv} \mathcal{F}_\gamma(v)}{\rho - \mathbf{c}(1 - \gamma/2 - iv, -\gamma/2 + iv)}; iz^* \right\}}{\text{Res} \{ e^{iuv} \mathcal{F}_\gamma(v); i\gamma/2 \}} \\ &= e^{u(\gamma/2 - z^*)} \cdot \frac{\text{Res} \left\{ \frac{\mathcal{F}_\gamma(v)}{\rho - \mathbf{c}(1 - \gamma/2 - iv, -\gamma/2 + iv)}; iz^* \right\}}{\text{Res} \{ \mathcal{F}_\gamma(v); i\gamma/2 \}} \\ &\longrightarrow \infty \end{aligned}$$

as u tends to infinity because $\gamma/2 - z^* > 0$.

To see that the price-consumption ratio, $P/C = s \cdot P/D$, remains finite in this limit, we must evaluate $\lim_{s \rightarrow 0} s \cdot P/D$. Since $s = 1/(1 + e^u) \sim e^{-u}$, we have, asymptotically, that

$$P/C \longrightarrow e^{u(\gamma/2 - z^* - 1)} \cdot \frac{\text{Res} \left\{ \frac{\mathcal{F}_\gamma(v)}{\rho - \mathbf{c}(1 - \gamma/2 - iv, -\gamma/2 + iv)}; iz^* \right\}}{\text{Res} \{ \mathcal{F}_\gamma(v); i\gamma/2 \}},$$

which tends to zero as $u \rightarrow \infty$ because $\gamma/2 - z^* - 1 < 0$.

(ii) In the riskless rate case, we seek the limit of

$$r = \frac{\int_{-\infty}^{\infty} \mathcal{F}_\gamma(v) e^{iuv} \cdot [\rho - \mathbf{c}(-\gamma/2 - iv, -\gamma/2 + iv)] dv}{\int_{-\infty}^{\infty} \mathcal{F}_\gamma(v) e^{iuv} dv}.$$

This is much simpler, because the minimal pole is $i\gamma/2$ for both numerator and denominator. It follows that

$$r \longrightarrow \rho - \mathbf{c}(-\gamma/2 - i(i\gamma/2), -\gamma/2 + i(i\gamma/2)) = \rho - \mathbf{c}(0, -\gamma).$$

(iii) In the expected return case, we need the limit of the expected capital gain expression which is the first term on the right-hand side of (17). This expression is asymptotically equivalent to

$$\frac{\int_{-\infty}^{\infty} \frac{e^{iuv} \mathcal{F}_\gamma(v) \mathbf{c}(1 - \gamma/2 - iv, \gamma/2 + iv)}{\rho - \mathbf{c}(1 - \gamma/2 - iv, -\gamma/2 + iv)} dv}{\int_{-\infty}^{\infty} \frac{e^{iuv} \mathcal{F}_\gamma(v)}{\rho - \mathbf{c}(1 - \gamma/2 - iv, -\gamma/2 + iv)} dv} \equiv \frac{J_n}{J_d}$$

since the higher-order exponential terms e^{-mu} for $m \geq 1$ which appear in (17) become irrelevant exponentially fast as u tends to infinity. Again, there are two subcases, depending on whether the minimal zero of $\rho - \mathbf{c}(1 - \gamma/2 - iv, -\gamma/2 + iv)$ has imaginary part greater than or less than $\gamma/2$.

(a) In the subcritical case, the minimal pole of each of J_n and J_d occurs at $i\gamma/2$. Therefore we have

$$\begin{aligned} \lim_{u \rightarrow \infty} \mathbb{E}dP/P &= \frac{\text{Res} \left\{ \frac{e^{iuv} \mathcal{F}_\gamma(v) \mathbf{c}(1 - \gamma/2 - iv, \gamma/2 + iv)}{\rho - \mathbf{c}(1 - \gamma/2 - iv, -\gamma/2 + iv)}; i\gamma/2 \right\}}{\text{Res} \left\{ \frac{e^{iuv} \mathcal{F}_\gamma(v)}{\rho - \mathbf{c}(1 - \gamma/2 - iv, -\gamma/2 + iv)}; i\gamma/2 \right\}} \\ &= \mathbf{c}(1, 0). \end{aligned}$$

(b) In the supercritical case, the minimal pole of each of J_n and J_d occurs at iz^* . Therefore, we have

$$\begin{aligned} \lim_{u \rightarrow \infty} \mathbb{E}dP/P &= \frac{\text{Res} \left\{ \frac{e^{iuv} \mathcal{F}_\gamma(v) \mathbf{c}(1 - \gamma/2 - iv, \gamma/2 + iv)}{\rho - \mathbf{c}(1 - \gamma/2 - iv, -\gamma/2 + iv)}; iz^* \right\}}{\text{Res} \left\{ \frac{e^{iuv} \mathcal{F}_\gamma(v)}{\rho - \mathbf{c}(1 - \gamma/2 - iv, -\gamma/2 + iv)}; iz^* \right\}} \\ &= \mathbf{c}(1 - \gamma/2 + z^*, \gamma/2 - z^*). \end{aligned}$$

Since instantaneous expected returns are the sum of expected capital gains and the dividend-price ratio, expected returns in the asymptotic limit are

$$\mathbf{c}(1, 0) + \rho - \mathbf{c}(1, -\gamma)$$

in the subcritical case, and

$$\mathbf{c}(1 - \gamma/2 + z^*, \gamma/2 - z^*)$$

in the supercritical case.

Subtracting the riskless rate, we have, finally, that excess returns are

$$\mathbf{c}(1, 0) + \mathbf{c}(0, -\gamma) - \mathbf{c}(1, -\gamma)$$

in the subcritical case, and

$$\mathbf{c}(1 - \gamma/2 + z^*, \gamma/2 - z^*) - \rho + \mathbf{c}(0, -\gamma)$$

in the supercritical case. Recalling that $\rho = \mathbf{c}(1 - \gamma/2 + z^*, -\gamma/2 - z^*)$ by the definition of z^* , the excess return in the supercritical case can be rewritten as

$$\mathbf{c}(1 - \gamma/2 + z^*, \gamma/2 - z^*) + \mathbf{c}(0, -\gamma) - \mathbf{c}(1 - \gamma/2 + z^*, -\gamma/2 - z^*).$$

This concludes the derivation of the various asymptotics in the general case.

Step 3. If dividends are also independent across assets then we can decompose

$$\mathbf{c}(\theta_1, \theta_2) = \mathbf{c}_1(\theta_1) + \mathbf{c}_2(\theta_2)$$

where $\mathbf{c}_i(\theta) \equiv \log \mathbb{E} \exp \theta y_{i1}$. It follows that in the subcritical case,

$$XS \longrightarrow \mathbf{c}(1, 0) + \mathbf{c}(0, -\gamma) - \mathbf{c}(1, -\gamma) = 0$$

and in the supercritical case,

$$\begin{aligned} XS &\longrightarrow \mathbf{c}(1 - \gamma/2 + z^*, \gamma/2 - z^*) + \mathbf{c}(0, -\gamma) - \mathbf{c}(1 - \gamma/2 + z^*, -\gamma/2 - z^*) \\ &= \mathbf{c}_2(\gamma/2 - z^*) + \mathbf{c}_2(-\gamma) - \mathbf{c}_2(-\gamma/2 - z^*). \end{aligned}$$

Step 4. I now show that this last expression is positive. First, note that because $\mathbf{c}_2(x)$ —as a CGF—is convex, we have that

$$\frac{\mathbf{c}_2(e) - \mathbf{c}_2(d)}{e - d} < \frac{\mathbf{c}_2(g) - \mathbf{c}_2(f)}{g - f} \quad \text{whenever } d < e < f < g.$$

Next, observe that in the supercritical case, we have

$$-\gamma < -\gamma/2 - z^* < 0 < \gamma/2 - z^*.$$

It follows that

$$\frac{\mathbf{c}_2(-\gamma/2 - z^*) - \mathbf{c}_2(-\gamma)}{(-\gamma/2 - z^*) - (-\gamma)} < \frac{\mathbf{c}_2(\gamma/2 - z^*) - \mathbf{c}_2(0)}{(\gamma/2 - z^*) - 0},$$

or equivalently, because $\mathbf{c}_2(0) = 0$,

$$\mathbf{c}_2(-\gamma/2 - z^*) - \mathbf{c}_2(-\gamma) < \mathbf{c}_2(\gamma/2 - z^*);$$

and so

$$\mathbf{c}_2(\gamma/2 - z^*) + \mathbf{c}_2(-\gamma) - \mathbf{c}_2(-\gamma/2 - z^*) > 0$$

as required.

Step 5. The last step showed that $R_1 = R_f$ in the subcritical case and $R_1 > R_f$ in the supercritical case. It only remains to show that the other bounds on expected returns hold: that (i) $R_1 < R_2$, assuming independence, and that (ii) in the supercritical case $R_1 < G_1$, assuming $G_1 \geq G_2$.

Step 5(i). Proof that $R_1 < R_2$, assuming independence:

In the subcritical case, $R_1 = \rho + \mathbf{c}(1, 0) - \mathbf{c}(1, -\gamma)$ and $R_2 = \rho + \mathbf{c}(0, 1) - \mathbf{c}(0, 1 - \gamma)$. Since we are assuming independence, it remains to show that

$$-\mathbf{c}_2(-\gamma) < \mathbf{c}_2(1) - \mathbf{c}_2(1 - \gamma),$$

or equivalently that

$$\mathbf{c}_2(1 - \gamma) < \mathbf{c}_2(1) + \mathbf{c}_2(-\gamma),$$

which follows immediately by convexity of $\mathbf{c}_2(\cdot)$.

In the supercritical case, $R_1 = \mathbf{c}(1 - \gamma/2 + z^*, \gamma/2 - z^*)$ and $R_2 = \mathbf{c}(1 - \gamma/2 + z^*, -\gamma/2 - z^*) + \mathbf{c}(0, 1) - \mathbf{c}(0, 1 - \gamma)$ (substituting in for ρ from the definition of z^*). By independence, it remains to show that

$$\mathbf{c}_2(\gamma/2 - z^*) < \mathbf{c}_2(-\gamma/2 - z^*) + \mathbf{c}_2(1) - \mathbf{c}_2(1 - \gamma),$$

or equivalently that

$$\mathbf{c}_2(1 - \gamma) + \mathbf{c}_2(\gamma/2 - z^*) < \mathbf{c}_2(1) + \mathbf{c}_2(-\gamma/2 - z^*)$$

which also follows directly by convexity of $\mathbf{c}_2(\cdot)$, noting that $\gamma/2 - z^* \in (0, 1)$.

Step 5(ii). Next, I show that in the supercritical case, $R_1 \leq G_1$ if $G_1 \geq G_2$. We do not need the independence assumption here. It will be helpful to write $\theta = \gamma/2 - z^* \in (0, 1)$. With this notation, the limiting $R_1 = \mathbf{c}(1 - \theta, \theta)$. The claim is that $\mathbf{c}(1 - \theta, \theta) \leq \mathbf{c}(1, 0)$. To show this, we make the same change of measure as was used in the proof of Proposition 11. We have $R_1 = \mathbf{c}(1 - \theta, \theta) = \mathbf{c}(1, 0) + \widehat{\mathbf{c}}(-\theta)$. It suffices to show that $\widehat{\mathbf{c}}(-\theta) \leq 0$ for all θ in $(0, 1)$. We have $\mathbf{c}(0, 1) = \mathbf{c}(1, 0) + \widehat{\mathbf{c}}(-1)$, and so by assumption $\widehat{\mathbf{c}}(-1) \leq 0$. Since $\widehat{\mathbf{c}}(0) = 0$, the claim follows by convexity of $\widehat{\mathbf{c}}(\cdot)$.

Finally, it is notationally convenient to set $\theta^* = \gamma/2 - z^*$. It follows from (93) that the defining property of θ^* in the supercritical case is that $\rho - \mathbf{c}(1 - \theta^*, \theta^* - \gamma) = 0$.

F The N -tree case

F.1 The Fourier transform $\mathcal{F}_\gamma^N(\mathbf{v})$

To make a start, we seek the integral

$$I_N \equiv \int_{\mathbb{R}^{N-1}} \frac{e^{-ix_1v_1 - ix_2v_2 - \dots - ix_{N-1}v_{N-1}}}{(e^{x_1/N} + \dots + e^{x_{N-1}/N} + e^{-(x_1+x_2+\dots+x_{N-1})/N})^\gamma} dx_1 \dots dx_{N-1}. \quad (94)$$

For notational convenience, write $x_N \equiv -x_1 - \dots - x_{N-1}$ —so $\sum_1^N x_i = 0$ —and, for $i = 1, \dots, N$, define

$$t_i = \frac{e^{x_i/N}}{e^{x_1/N} + \dots + e^{x_N/N}}. \quad (95)$$

Note that the variables t_i range between 0 and 1 (and, by construction, sum to 1) as the variables $\{x_i\}$ range around. Furthermore, we have

$$\begin{aligned} \prod_{k=1}^N t_k &= \frac{e^{(x_1+\dots+x_N)/N}}{(e^{x_1/N} + \dots + e^{x_N/N})^N} \\ &= \frac{1}{(e^{x_1/N} + \dots + e^{x_N/N})^N} \\ \text{and } t_i^N &= \frac{e^{x_i}}{(e^{x_1/N} + \dots + e^{x_N/N})^N}, \end{aligned}$$

so

$$e^{x_i} = \frac{t_i^N}{\prod_{k=1}^N t_k}. \quad (96)$$

Of course, because of the linear dependence $\sum_{k=1}^N t_k = 1$, there are only $N - 1$ independent variables and $t_N = 1 - t_1 - \dots - t_{N-1}$, so we can rewrite

$$x_i = N \log t_i - \sum_{k=1}^{N-1} \log t_k - \log \left(1 - \sum_{k=1}^{N-1} t_k \right), \quad i = 1, \dots, N - 1. \quad (97)$$

To make the change of variables specified in (95), we have to calculate the Jacobian

$$J \equiv \left| \frac{\partial(x_1, \dots, x_{N-1})}{\partial(t_1, \dots, t_{N-1})} \right|.$$

From (97),

$$\frac{\partial x_i}{\partial t_j} = \frac{1}{t_N} - \frac{1}{t_j} + \frac{N\delta_{ij}}{t_i},$$

where δ_{ij} equals one if $i = j$ and zero otherwise, so we can write

$$\begin{aligned} \frac{\partial(x_1, \dots, x_{N-1})}{\partial(t_1, \dots, t_{N-1})} &= \begin{pmatrix} \frac{N}{t_1} & & & \\ & \frac{N}{t_2} & & \\ & & \ddots & \\ & & & \frac{N}{t_{N-1}} \end{pmatrix} + \begin{pmatrix} \frac{1}{t_N} - \frac{1}{t_1} & \frac{1}{t_N} - \frac{1}{t_2} & \cdots & \frac{1}{t_N} - \frac{1}{t_{N-1}} \\ \frac{1}{t_N} - \frac{1}{t_1} & \frac{1}{t_N} - \frac{1}{t_2} & \cdots & \frac{1}{t_N} - \frac{1}{t_{N-1}} \\ \vdots & \vdots & \ddots & \vdots \\ \frac{1}{t_N} - \frac{1}{t_1} & \frac{1}{t_N} - \frac{1}{t_2} & \cdots & \frac{1}{t_N} - \frac{1}{t_{N-1}} \end{pmatrix} \\ &= \begin{pmatrix} \frac{N}{t_1} & & & \\ & \frac{N}{t_2} & & \\ & & \ddots & \\ & & & \frac{N}{t_{N-1}} \end{pmatrix} + \begin{pmatrix} 1 \\ 1 \\ \vdots \\ 1 \end{pmatrix} \begin{pmatrix} \frac{1}{t_N} - \frac{1}{t_1} \\ \frac{1}{t_N} - \frac{1}{t_2} \\ \vdots \\ \frac{1}{t_N} - \frac{1}{t_{N-1}} \end{pmatrix}' \\ &\equiv \mathbf{A} + \boldsymbol{\alpha}\boldsymbol{\beta}'. \end{aligned}$$

The last line defines the $(N-1) \times (N-1)$ matrix \mathbf{A} and the $(N-1)$ -dimensional column vectors $\boldsymbol{\alpha}$ and $\boldsymbol{\beta}$. \mathbf{A} is a diagonal matrix: blanks indicate zeros. The prime symbol ($'$) denotes a transpose.

In order to calculate $J = \det(\mathbf{A} + \boldsymbol{\alpha}\boldsymbol{\beta}')$ we can use the following

Fact 1 (Matrix determinant lemma). *Suppose that \mathbf{A} is an invertible square matrix and that $\boldsymbol{\alpha}$ and $\boldsymbol{\beta}$ are column vectors, each of length equal to the dimension of \mathbf{A} . Then*

$$\det(\mathbf{A} + \boldsymbol{\alpha}\boldsymbol{\beta}') = (1 + \boldsymbol{\beta}'\mathbf{A}^{-1}\boldsymbol{\alpha}) \det \mathbf{A}.$$

This fact is useful in the present case because \mathbf{A} is diagonal, so its inverse and determinant are easily calculated. To be specific,

$$\begin{aligned} \det \mathbf{A} &= \frac{N^{N-1}}{t_1 \cdots t_{N-1}} \\ \text{and } \mathbf{A}^{-1} &= \begin{pmatrix} \frac{t_1}{N} & & & \\ & \frac{t_2}{N} & & \\ & & \ddots & \\ & & & \frac{t_{N-1}}{N} \end{pmatrix}. \end{aligned}$$

It follows that

$$\begin{aligned} J &= \left[1 + \begin{pmatrix} \frac{1}{t_N} - \frac{1}{t_1} \\ \frac{1}{t_N} - \frac{1}{t_2} \\ \vdots \\ \frac{1}{t_N} - \frac{1}{t_{N-1}} \end{pmatrix}' \begin{pmatrix} \frac{t_1}{N} & & & \\ & \frac{t_2}{N} & & \\ & & \ddots & \\ & & & \frac{t_{N-1}}{N} \end{pmatrix} \begin{pmatrix} 1 \\ 1 \\ \vdots \\ 1 \end{pmatrix} \right] \times \frac{N^{N-1}}{t_1 \cdots t_{N-1}} \\ &= \frac{N^{N-2}}{t_1 \cdots t_N}. \end{aligned}$$

We can now return to the integral I_N . For typographical reasons, I write Π for the product $\prod_{k=1}^N t_k$ and suppress the range of integration, which is $[0, 1]^{N-1}$. Making the substitution suggested in (95),

$$\begin{aligned}
I_N &= \int \frac{\left(\frac{t_1^N}{\Pi}\right)^{-iv_1} \left(\frac{t_2^N}{\Pi}\right)^{-iv_2} \cdots \left(\frac{t_{N-1}^N}{\Pi}\right)^{-iv_{N-1}}}{\left(\frac{t_1+t_2+\cdots+t_N}{\Pi^{1/N}}\right)^\gamma} \cdot J dt_1 \cdots dt_{N-1} \\
&= N^{N-2} \int \Pi^{\gamma/N} \left(\frac{t_1^N}{\Pi}\right)^{-iv_1} \cdots \left(\frac{t_{N-1}^N}{\Pi}\right)^{-iv_{N-1}} \frac{dt_1 \cdots dt_{N-1}}{t_1 \cdots t_{N-1} t_N} \\
&= N^{N-2} \int \left(t_1^{\gamma/N+iv_1+\cdots+iv_{N-1}-Niv_1} t_2^{\gamma/N+iv_1+\cdots+iv_{N-1}-Niv_2} \cdots \right. \\
&\quad \left. \cdots t_{N-1}^{\gamma/N+iv_1+\cdots+iv_{N-1}-Niv_{N-1}} \cdot t_N^{\gamma/N+iv_1+\cdots+iv_{N-1}}\right) \frac{dt_1 \cdots dt_{N-1}}{t_1 \cdots t_{N-1} t_N}.
\end{aligned}$$

As in the two-asset case, this is a Dirichlet surface integral. As shown in Edwards (1922, pp. 166–7) and Andrews, Askey and Roy (1999, p. 34), it can be evaluated in terms of Γ -functions: we have

$$I_N = \frac{N^{N-2}}{\Gamma(\gamma)} \cdot \Gamma(\gamma/N + iv_1 + iv_2 + \cdots + iv_{N-1}) \cdot \prod_{k=1}^{N-1} \Gamma(\gamma/N + iv_1 + \cdots + iv_{N-1} - Niv_k).$$

Defining $\mathcal{G}_\gamma^N(\mathbf{v}) = I_N/(2\pi)^{N-1}$, where $\mathbf{v} = (v_1, \dots, v_{N-1})$, we have

$$\mathcal{G}_\gamma^N(\mathbf{v}) = \frac{N^{N-2}}{(2\pi)^{N-1}} \cdot \frac{\Gamma(\gamma/N + iv_1 + iv_2 + \cdots + iv_{N-1})}{\Gamma(\gamma)} \cdot \prod_{k=1}^{N-1} \Gamma(\gamma/N + iv_1 + \cdots + iv_{N-1} - Niv_k). \quad (98)$$

It follows from this definition of $\mathcal{G}_\gamma^N(\mathbf{v})$, by the Fourier inversion theorem, that

$$\frac{1}{\left(e^{x_1/N} + e^{x_2/N} + \cdots + e^{-(x_1+x_2+\cdots+x_{N-1})/N}\right)^\gamma} = \int_{\mathbb{R}^{N-1}} \mathcal{G}_\gamma^N(\mathbf{v}) e^{i\mathbf{v}'\mathbf{x}} d\mathbf{v}, \quad (99)$$

where $\mathbf{x} = (x_1, \dots, x_{N-1})$.

F.2 The expectation

We seek the expectation

$$E = \mathbb{E} \left[\frac{e^{\boldsymbol{\alpha}'\tilde{\mathbf{y}}_t}}{\left(e^{y_{10}+\tilde{y}_{1t}} + \cdots + e^{y_{N0}+\tilde{y}_{Nt}}\right)^\gamma} \right],$$

where $\boldsymbol{\alpha} \equiv (\alpha_1, \dots, \alpha_N)'$ and $\tilde{\mathbf{y}}_t \equiv (\tilde{y}_{1t}, \dots, \tilde{y}_{Nt})'$.

The calculation is carried out by applying the same three tricks that were useful in the two-tree case: namely, by putting the denominator in a form amenable to a Fourier

transform; then changing measure, to take care of the numerator; and finally applying the Fourier transform.

The calculations below also use the vectors \mathbf{y}_0 and $\boldsymbol{\gamma}$ defined in the main text. In addition, define the $(N-1) \times N$ matrix \mathbf{Q} and vectors \mathbf{q}_i by

$$\mathbf{Q} \equiv \begin{pmatrix} \mathbf{q}'_2 \\ \mathbf{q}'_3 \\ \vdots \\ \mathbf{q}'_N \end{pmatrix} \equiv \begin{pmatrix} -1 & N-1 & -1 & \cdots & -1 \\ -1 & -1 & N-1 & \ddots & \vdots \\ \vdots & \vdots & \ddots & \ddots & -1 \\ -1 & -1 & \cdots & -1 & N-1 \end{pmatrix}, \quad (100)$$

and let $\mathbf{q}_1 \equiv (N-1, \dots, -1, -1)'$ —the “missing” row which does *not* appear as the top row of \mathbf{Q} . (This definition is only introduced to make certain expressions neater, since $\mathbf{q}_1 = -\sum_{k=2}^N \mathbf{q}_k$.)

We will also need to make a change of measure at one stage, as in the two asset case. Define $\tilde{\mathbb{E}}$ by

$$\tilde{\mathbb{E}}[Y] \equiv e^{-tc(\boldsymbol{\alpha}-\boldsymbol{\gamma}/N)} \cdot \mathbb{E} \left[e^{(\boldsymbol{\alpha}-\boldsymbol{\gamma}/N)' \tilde{\mathbf{y}}_t} \cdot Y \right]. \quad (101)$$

It follows that

$$\tilde{c}(\mathbf{v}) \equiv \log \tilde{\mathbb{E}} \left[e^{\tilde{\mathbf{y}}_1' \mathbf{v}} \right] = \mathbf{c}(\boldsymbol{\alpha} - \boldsymbol{\gamma}/N + \mathbf{v}) - \mathbf{c}(\boldsymbol{\alpha} - \boldsymbol{\gamma}/N). \quad (102)$$

Using the new notation,

$$\begin{aligned} E &= \mathbb{E} \left[\frac{e^{\boldsymbol{\alpha}' \tilde{\mathbf{y}}_t}}{\left(e^{y_{10} + \tilde{y}_{1t}} + \dots + e^{y_{N0} + \tilde{y}_{Nt}} \right)^\gamma} \right] \\ &= \mathbb{E} \left[\frac{e^{\boldsymbol{\alpha}' \tilde{\mathbf{y}}_t - \boldsymbol{\gamma}'(\mathbf{y}_0 + \tilde{\mathbf{y}}_t)/N}}{\left(e^{\mathbf{q}'_1(\mathbf{y}_0 + \tilde{\mathbf{y}}_t)/N} + \dots + e^{\mathbf{q}'_N(\mathbf{y}_0 + \tilde{\mathbf{y}}_t)/N} \right)^\gamma} \right] \\ &= e^{-\boldsymbol{\gamma}' \mathbf{y}_0/N} e^{\mathbf{c}(\boldsymbol{\alpha}-\boldsymbol{\gamma}/N)t} \tilde{\mathbb{E}} \left[\frac{1}{\left(e^{\mathbf{q}'_1(\mathbf{y}_0 + \tilde{\mathbf{y}}_t)/N} + \dots + e^{\mathbf{q}'_N(\mathbf{y}_0 + \tilde{\mathbf{y}}_t)/N} \right)^\gamma} \right]. \end{aligned}$$

Now, $\mathbf{Q}(\mathbf{y}_0 + \tilde{\mathbf{y}}_t)$ plays the role of \mathbf{x} in expression (99). It follows that

$$\begin{aligned} E &= e^{-\boldsymbol{\gamma}' \mathbf{y}_0/N} e^{\mathbf{c}(\boldsymbol{\alpha}-\boldsymbol{\gamma}/N)t} \tilde{\mathbb{E}} \left[\int \mathcal{G}_\gamma^N(\mathbf{v}) e^{i\mathbf{v}' \mathbf{Q}(\mathbf{y}_0 + \tilde{\mathbf{y}}_t)} d\mathbf{v} \right] \\ &= e^{-\boldsymbol{\gamma}' \mathbf{y}_0/N} e^{\mathbf{c}(\boldsymbol{\alpha}-\boldsymbol{\gamma}/N)t} \int \mathcal{G}_\gamma^N(\mathbf{v}) e^{i\mathbf{v}' \mathbf{Q} \mathbf{y}_0} e^{\tilde{c}(i\mathbf{Q}' \mathbf{v})t} d\mathbf{v} \\ &= e^{-\boldsymbol{\gamma}' \mathbf{y}_0/N} \int \mathcal{G}_\gamma^N(\mathbf{v}) e^{i\mathbf{v}' \mathbf{Q} \mathbf{y}_0} e^{\mathbf{c}(\boldsymbol{\alpha}-\boldsymbol{\gamma}/N + i\mathbf{Q}' \mathbf{v})t} d\mathbf{v}. \end{aligned} \quad (103)$$

F.3 Prices

Now we proceed along the same lines as in the two-tree case. First, the price of the α -asset is given by

$$\begin{aligned} P &= \mathbb{E} \int_0^\infty e^{-\rho t} \left(\frac{C_t}{C_0} \right)^{-\gamma} D_{1t}^{\alpha_1} \cdots D_{Nt}^{\alpha_N} dt \\ &= C_0^\gamma \int_0^\infty e^{-\rho t} \mathbb{E} \left[\frac{e^{\alpha_1(y_{10} + \tilde{y}_{1t}) + \cdots + \alpha_N(y_{N0} + \tilde{y}_{Nt})}}{(e^{y_{10} + \tilde{y}_{1t}} + \cdots + e^{y_{N0} + \tilde{y}_{Nt}})^\gamma} \right] dt. \end{aligned}$$

The price-dividend ratio is therefore equal to

$$P/D = C_0^\gamma \int_0^\infty e^{-\rho t} \mathbb{E} \left[\frac{e^{\alpha_1 \tilde{y}_{1t} + \cdots + \alpha_N \tilde{y}_{Nt}}}{(e^{y_{10} + \tilde{y}_{1t}} + \cdots + e^{y_{N0} + \tilde{y}_{Nt}})^\gamma} \right] dt,$$

and the expectation was calculated, as E , in the previous section. Substituting in from (103),

$$\begin{aligned} P/D &= C_0^\gamma \int_{t=0}^\infty e^{-\rho t} \left(e^{-\gamma' \mathbf{y}_0/N} \int \mathcal{G}_\gamma^N(\mathbf{v}) e^{i\mathbf{v}' \mathbf{Q} \mathbf{y}_0} e^{c(\alpha - \gamma/N + i\mathbf{Q}' \mathbf{v})t} d\mathbf{v} \right) dt \\ &= C_0^\gamma e^{-\gamma' \mathbf{y}_0/N} \int \mathcal{G}_\gamma^N(\mathbf{v}) e^{i\mathbf{v}' \mathbf{Q} \mathbf{y}_0} \left(\int_{t=0}^\infty e^{-[\rho - c(\alpha - \gamma/N + i\mathbf{Q}' \mathbf{v})]t} dt \right) d\mathbf{v} \\ &= C_0^\gamma e^{-\gamma' \mathbf{y}_0/N} \int \frac{\mathcal{G}_\gamma^N(\mathbf{v}) e^{i\mathbf{v}' \mathbf{Q} \mathbf{y}_0}}{\rho - c(\alpha - \gamma/N + i\mathbf{Q}' \mathbf{v})} d\mathbf{v} \end{aligned} \quad (104)$$

$$= \left(e^{\mathbf{q}'_1 \mathbf{y}_0/N} + \cdots + e^{\mathbf{q}'_N \mathbf{y}_0/N} \right)^\gamma \int \frac{\mathcal{G}_\gamma^N(\mathbf{v}) e^{i\mathbf{v}' \mathbf{Q} \mathbf{y}_0}}{\rho - c(\alpha - \gamma/N + i\mathbf{Q}' \mathbf{v})} d\mathbf{v}. \quad (105)$$

F.4 Returns

From (104), the price of the α -asset is

$$P = (e^{y_{10}} + \cdots + e^{y_{N0}})^\gamma e^{(\alpha - \gamma/N)' \mathbf{y}_0} \int \frac{\mathcal{G}_\gamma^N(\mathbf{v}) e^{i\mathbf{v}' \mathbf{Q} \mathbf{y}_0}}{\rho - c(\alpha - \gamma/N + i\mathbf{Q}' \mathbf{v})} d\mathbf{v}.$$

Introducing the *multinomial coefficient*,

$$\binom{\gamma}{\mathbf{m}} \equiv \frac{\gamma!}{m_1! m_2! \cdots m_N!},$$

we can express the price as

$$P = \sum_{\mathbf{m}} \binom{\gamma}{\mathbf{m}} \int \frac{\mathcal{G}_\gamma^N(\mathbf{v}) e^{(\alpha - \gamma/N + \mathbf{m} + i\mathbf{Q}' \mathbf{v})' \mathbf{y}_0}}{\rho - c(\alpha - \gamma/N + i\mathbf{Q}' \mathbf{v})} d\mathbf{v}.$$

The sum is taken over all N -dimensional vectors \mathbf{m} whose entries are nonnegative integers which add up to γ .

Using the result of Appendix B.1.3, it follows that

$$\mathbb{E}dP = \sum_{\mathbf{m}} \binom{\gamma}{\mathbf{m}} \int \frac{\mathcal{G}_{\gamma}^N(\mathbf{v}) e^{(\boldsymbol{\alpha} - \gamma/N + \mathbf{m} + i\mathbf{Q}'\mathbf{v})' \mathbf{y}_0} \mathbf{c}(\boldsymbol{\alpha} - \gamma/N + \mathbf{m} + i\mathbf{Q}'\mathbf{v})}{\rho - \mathbf{c}(\boldsymbol{\alpha} - \gamma/N + i\mathbf{Q}'\mathbf{v})} d\mathbf{v} dt,$$

and hence

$$\begin{aligned} \mathbb{E}dP/D &= \sum_{\mathbf{m}} \binom{\gamma}{\mathbf{m}} \int \frac{\mathcal{G}_{\gamma}^N(\mathbf{v}) e^{(-\gamma/N + \mathbf{m} + i\mathbf{Q}'\mathbf{v})' \mathbf{y}_0} \mathbf{c}(\boldsymbol{\alpha} - \gamma/N + \mathbf{m} + i\mathbf{Q}'\mathbf{v})}{\rho - \mathbf{c}(\boldsymbol{\alpha} - \gamma/N + i\mathbf{Q}'\mathbf{v})} d\mathbf{v} dt \\ &= \sum_{\mathbf{m}} \binom{\gamma}{\mathbf{m}} e^{m_1 \mathbf{q}'_1 \mathbf{y}_0/N + \dots + m_N \mathbf{q}'_N \mathbf{y}_0/N} \int \frac{\mathcal{G}_{\gamma}^N(\mathbf{v}) e^{i\mathbf{v}' \mathbf{Q} \mathbf{y}_0} \mathbf{c}(\boldsymbol{\alpha} - \gamma/N + \mathbf{m} + i\mathbf{Q}'\mathbf{v})}{\rho - \mathbf{c}(\boldsymbol{\alpha} - \gamma/N + i\mathbf{Q}'\mathbf{v})} d\mathbf{v} dt. \end{aligned}$$

We then get expected capital gains by dividing through by the price-dividend ratio, calculated above. The other component of expected return is the dividend yield, which is the reciprocal of the price-dividend ratio.

F.5 Interest rates

The price of a time- T zero-coupon bond is

$$B_T = \mathbb{E} e^{-\rho T} \left(\frac{C_T}{C_0} \right)^{-\gamma}.$$

Using the expectation calculated in section F.2, we have

$$\begin{aligned} B_T &= e^{-\rho T} C_0^{\gamma} \mathbb{E} \frac{1}{(e^{y_{10} + \tilde{y}_{1T}} + \dots + e^{y_{N0} + \tilde{y}_{NT}})^{\gamma}} \\ &= e^{-\rho T} C_0^{\gamma} e^{-\gamma' \mathbf{y}_0/N} \int \mathcal{G}_{\gamma}^N(\mathbf{v}) e^{i\mathbf{v}' \mathbf{Q} \mathbf{y}_0} e^{\mathbf{c}(-\gamma/N + i\mathbf{Q}'\mathbf{v})T} d\mathbf{v} \\ &= e^{-\rho T} \left(e^{\mathbf{q}'_1 \mathbf{y}_0/N} + \dots + e^{\mathbf{q}'_N \mathbf{y}_0/N} \right)^{\gamma} \int \mathcal{G}_{\gamma}^N(\mathbf{v}) e^{i\mathbf{v}' \mathbf{Q} \mathbf{y}_0} e^{\mathbf{c}(-\gamma/N + i\mathbf{Q}'\mathbf{v})T} d\mathbf{v}. \end{aligned}$$

The yield $\mathcal{Y}(T) = -(\log B_T)/T$. Using the above expression,

$$\mathcal{Y}(T) = \rho - \frac{1}{T} \log \left\{ \left(e^{\mathbf{q}'_1 \mathbf{y}_0/N} + \dots + e^{\mathbf{q}'_N \mathbf{y}_0/N} \right)^{\gamma} \int \mathcal{G}_{\gamma}^N(\mathbf{v}) e^{i\mathbf{v}' \mathbf{Q} \mathbf{y}_0} e^{\mathbf{c}(-\gamma/N + i\mathbf{Q}'\mathbf{v})T} d\mathbf{v} \right\}.$$

To calculate the riskless rate, rearrange this expression slightly, using (99)—

$$\mathcal{Y}(T) = \rho - \frac{1}{T} \log \left\{ 1 + \left(e^{\mathbf{q}'_1 \mathbf{y}_0/N} + \dots + e^{\mathbf{q}'_N \mathbf{y}_0/N} \right)^{\gamma} \int \mathcal{G}_{\gamma}^N(\mathbf{v}) e^{i\mathbf{v}' \mathbf{Q} \mathbf{y}_0} \left(e^{\mathbf{c}(-\gamma/N + i\mathbf{Q}'\mathbf{v})T} - 1 \right) d\mathbf{v} \right\}.$$

Using L'Hôpital's rule, as in the two-tree case, we have

$$\begin{aligned} r &= \lim_{T \downarrow 0} \mathcal{Y}(T) \\ &= \rho - \left(e^{\mathbf{q}'_1 \mathbf{y}_0/N} + \dots + e^{\mathbf{q}'_N \mathbf{y}_0/N} \right)^{\gamma} \int \mathcal{G}_{\gamma}^N(\mathbf{v}) e^{i\mathbf{v}' \mathbf{Q} \mathbf{y}_0} \mathbf{c}(-\gamma/N + i\mathbf{Q}'\mathbf{v}) d\mathbf{v} \\ &= \left(e^{\mathbf{q}'_1 \mathbf{y}_0/N} + \dots + e^{\mathbf{q}'_N \mathbf{y}_0/N} \right)^{\gamma} \int \mathcal{G}_{\gamma}^N(\mathbf{v}) e^{i\mathbf{v}' \mathbf{Q} \mathbf{y}_0} [\rho - \mathbf{c}(-\gamma/N + i\mathbf{Q}'\mathbf{v})] d\mathbf{v}. \end{aligned}$$

F.6 Simplification of preceding results

The results so far establish the following proposition.

Proposition 12 (Integral formulas in the N -tree case, preliminary version). *The price-dividend ratio on asset j is*

$$P/D = \left(e^{\mathbf{q}'_1 \mathbf{y}_0/N} + \dots + e^{\mathbf{q}'_N \mathbf{y}_0/N} \right)^\gamma \int \frac{\mathcal{G}_\gamma^N(\mathbf{v}) e^{i\mathbf{v}' \mathbf{Q} \mathbf{y}_0}}{\rho - \mathbf{c}(\mathbf{e}_j - \gamma/N + i\mathbf{Q}' \mathbf{v})} d\mathbf{v}.$$

Defining the expected return by $ER dt \equiv \mathbb{E}(dP + D dt)/P$, we have

$$ER = \frac{\Phi}{P/D} + D/P,$$

where

$$\Phi = \sum_{\mathbf{m}} \binom{\gamma}{\mathbf{m}} e^{m_1 \mathbf{q}'_1 \mathbf{y}_0/N + \dots + m_N \mathbf{q}'_N \mathbf{y}_0/N} \int \frac{\mathcal{G}_\gamma^N(\mathbf{v}) e^{i\mathbf{v}' \mathbf{Q} \mathbf{y}_0} \mathbf{c}(\mathbf{e}_j - \gamma/N + \mathbf{m} + i\mathbf{Q}' \mathbf{v})}{\rho - \mathbf{c}(\mathbf{e}_j - \gamma/N + i\mathbf{Q}' \mathbf{v})} d\mathbf{v}.$$

The summation is taken over all vectors $\mathbf{m} = (m_1, \dots, m_N)'$ whose entries are non-negative and add up to γ .

The zero-coupon yield to time T is

$$\mathcal{Y}(T) = \rho - \frac{1}{T} \log \left\{ \left(e^{\mathbf{q}'_1 \mathbf{y}_0/N} + \dots + e^{\mathbf{q}'_N \mathbf{y}_0/N} \right)^\gamma \int \mathcal{G}_\gamma^N(\mathbf{v}) e^{i\mathbf{v}' \mathbf{Q} \mathbf{y}_0} e^{\mathbf{c}(-\gamma/N + i\mathbf{Q}' \mathbf{v})T} d\mathbf{v} \right\}.$$

The riskless rate is

$$r = \left(e^{\mathbf{q}'_1 \mathbf{y}_0/N} + \dots + e^{\mathbf{q}'_N \mathbf{y}_0/N} \right)^\gamma \int \mathcal{G}_\gamma^N(\mathbf{v}) e^{i\mathbf{v}' \mathbf{Q} \mathbf{y}_0} [\rho - \mathbf{c}(-\gamma/N + i\mathbf{Q}' \mathbf{v})] d\mathbf{v}.$$

Proposition 8 is a slight simplification of Proposition 12; it requires a final change of variables. Define $\hat{\mathbf{v}} \equiv \mathbf{B} \mathbf{v}$, where \mathbf{B} is the $(N-1) \times (N-1)$ square matrix

$$\mathbf{B} \equiv \begin{pmatrix} N-1 & -1 & \dots & -1 \\ -1 & N-1 & \ddots & \vdots \\ \vdots & \ddots & \ddots & -1 \\ -1 & \dots & -1 & N-1 \end{pmatrix}.$$

With this definition, we have $\hat{v}_k = Nv_k - v_1 - \dots - v_{N-1}$ and $\hat{v}_1 + \dots + \hat{v}_{N-1} = v_1 + \dots + v_{N-1}$. It is simple to verify that

$$\mathbf{B}^{-1} = \frac{1}{N} \begin{pmatrix} 2 & 1 & \dots & 1 \\ 1 & 2 & \ddots & \vdots \\ \vdots & \ddots & \ddots & 1 \\ 1 & \dots & 1 & 2 \end{pmatrix}.$$

Using the matrix determinant lemma (Fact 1 above) it is easy to calculate the Jacobian: $\det \mathbf{B}^{-1} = 1/N^{N-2}$, so—since $\mathbf{v} = \mathbf{B}^{-1}\hat{\mathbf{v}} - d\mathbf{v}$ is replaced by $d\hat{\mathbf{v}}/N^{N-2}$. Next, $\hat{\mathbf{v}}$ was defined in such a way that $\mathcal{G}_\gamma^N(\mathbf{v})$, defined in equation (98), is equal to $N^{N-2}\mathcal{F}_\gamma^N(\hat{\mathbf{v}})$, defined in equation (42). Finally, noting that $\mathbf{B}^{-1}\mathbf{Q} = \mathbf{U}$ and $\mathbf{u} \equiv \mathbf{U}\mathbf{y}_0$, as defined in (43), we have

$$\begin{aligned} \mathbf{Q}'\mathbf{v} &= \mathbf{Q}'\mathbf{B}^{-1}\hat{\mathbf{v}} \\ &= \mathbf{U}'\hat{\mathbf{v}}, \end{aligned}$$

and

$$\begin{aligned} \mathbf{v}'\mathbf{Q}\mathbf{y}_0 &= \hat{\mathbf{v}}'\mathbf{U}\mathbf{y}_0 \\ &= \hat{\mathbf{v}}'\mathbf{u} \\ &= \mathbf{u}'\hat{\mathbf{v}}. \end{aligned}$$

Proposition 8 follows after making these substitutions throughout the various integrals and dropping hats on the integration variables $\hat{\mathbf{v}}$.

G Supplementary figures

G.1 Supplementary figures for calibration 1

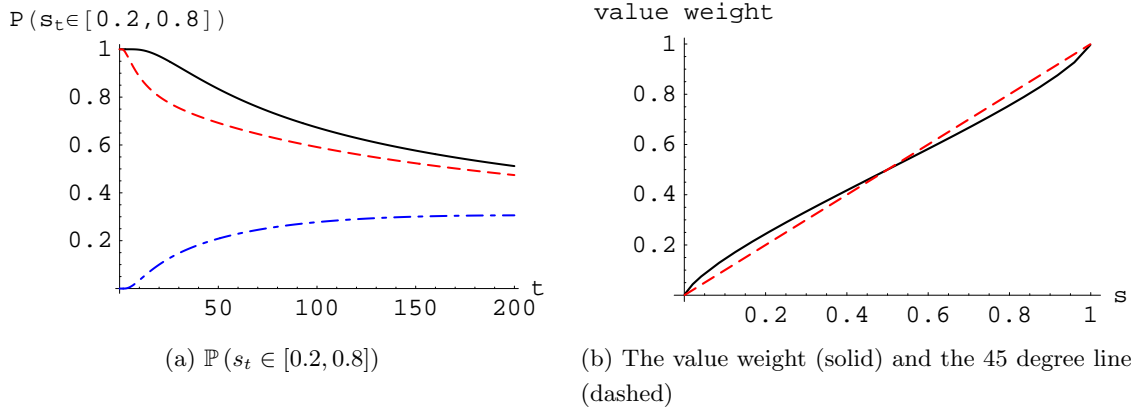


Figure 17: Left: The probability that s_t lies between 0.2 and 0.8, plotted against time t , measured in years, assuming starting shares $s_0 = 0.5$ (solid), $s_0 = 0.3$ (dashed), and $s_0 = 0.1$ (dot-dashed). Right: The value weight of asset 1 (solid), and the 45 degree line (dashed), against s .

G.2 Supplementary figures for calibration 2

Figure 18 plots some supplementary figures using the second calibration.

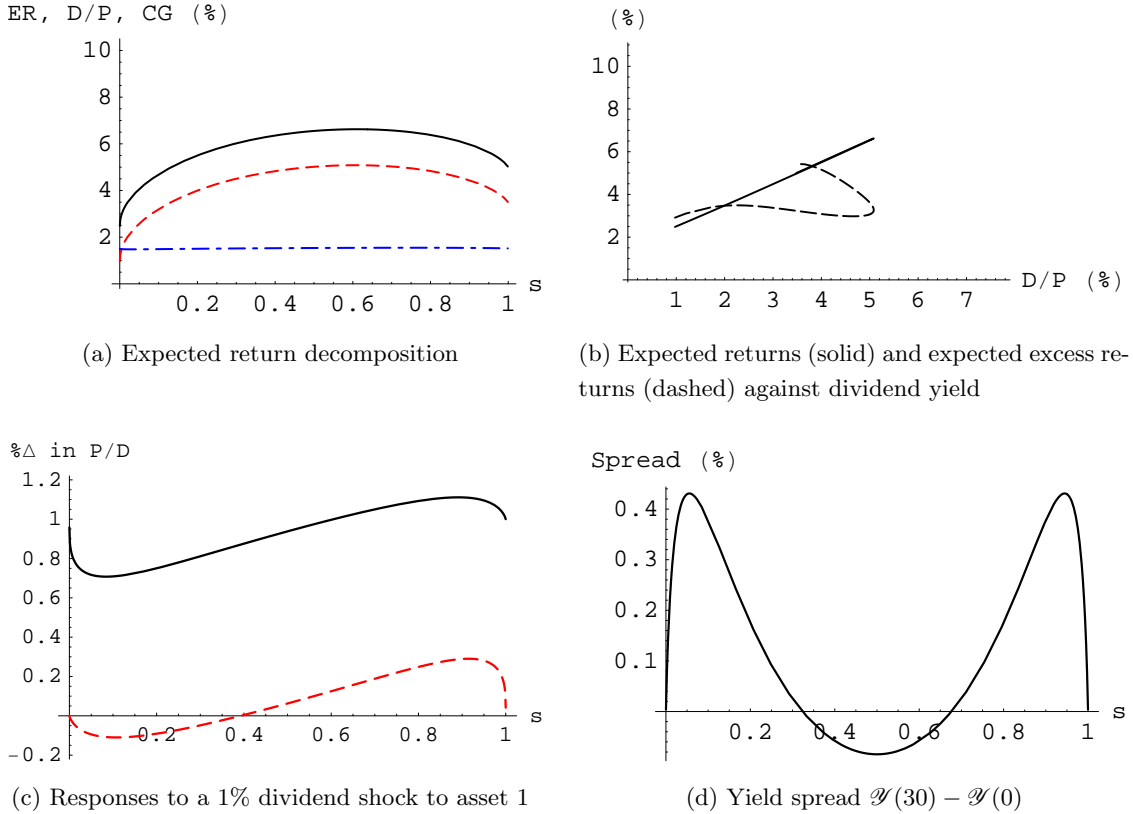


Figure 18: Supplementary figures for the second calibration with disasters and $\gamma = 4$. Figure 18a decomposes expected returns (solid) into dividend yield (dashed) and expected capital gains (dot-dashed). Figure 18b plots expected returns (solid) and expected excess returns (dashed) on asset 1 against asset 1's dividend yield. Figure 18c has the response of asset 1 (solid) and asset 2 (dashed) to a 1% dividend shock to asset 1.

Figures 19–24 explore the consequences of using log utility or removing jumps from the second calibration. They show that both high risk aversion ($\gamma = 4$) and occasional disasters are needed to generate interesting predictions using parameter values normally considered reasonable in the consumption-based asset pricing literature.

I repeat the calculations of section 5.2 in three alternative scenarios. In the first, γ is set equal to 1 and jumps are retained. In the second, γ is left equal to 4 but the jumps are dropped from the model. In the third, $\gamma = 1$ and jumps are dropped. Note the scales on the axes. Figures 19–20 show that the interesting dynamics displayed by the model are quantitatively irrelevant with log utility. Figures 21–22 show that the interesting dynamics displayed by the model are quantitatively irrelevant without jumps. With log utility and no jumps, Figures 23–24 show that we are orders of magnitude away from quantitative significance.

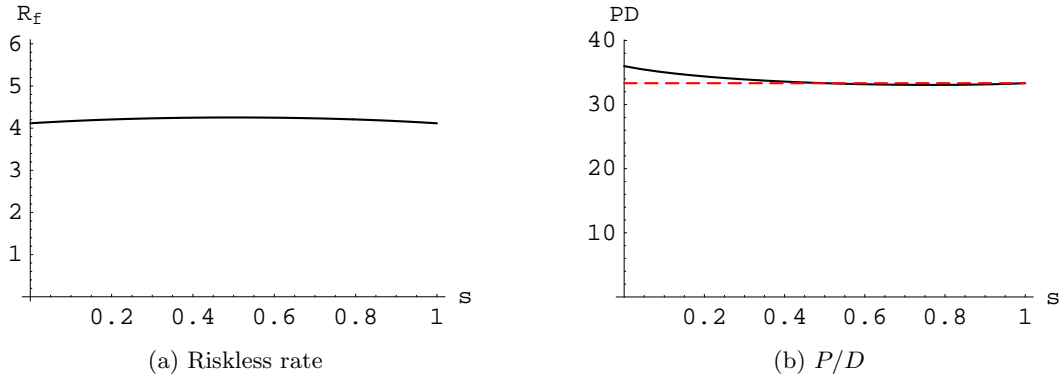


Figure 19: Left: The riskless rate against s . Right: The price-dividend ratio of asset 1 (solid) and of the market (dashed), against s . Log utility with jumps.

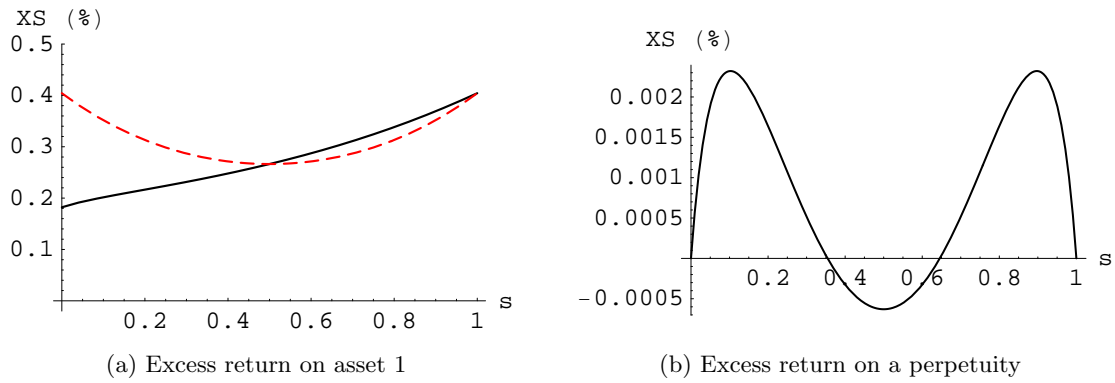


Figure 20: Left: The excess return on asset 1 (solid) and on the market (dashed) against s . Right: The excess return on a perpetuity against s . Log utility with jumps.

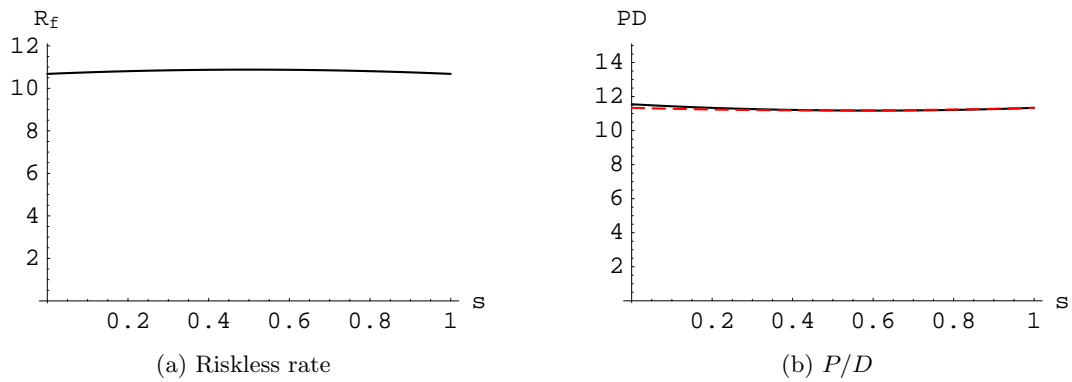


Figure 21: Left: The riskless rate against s . Right: The price-dividend ratio on asset 1 (solid) and on the market (dashed), against s . $\gamma = 4$, no jumps.

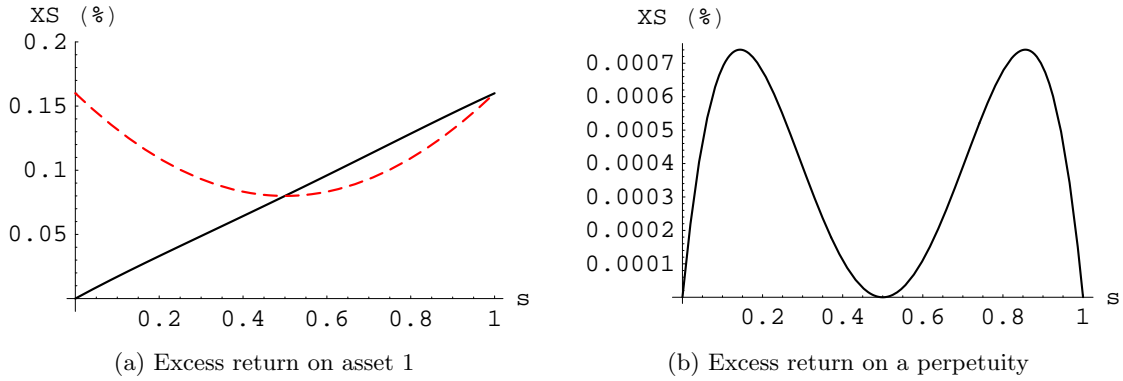


Figure 22: Left: The excess return on asset 1 (solid) and on the market (dashed), against s . Right: The excess return on a perpetuity against s . $\gamma = 4$, no jumps.

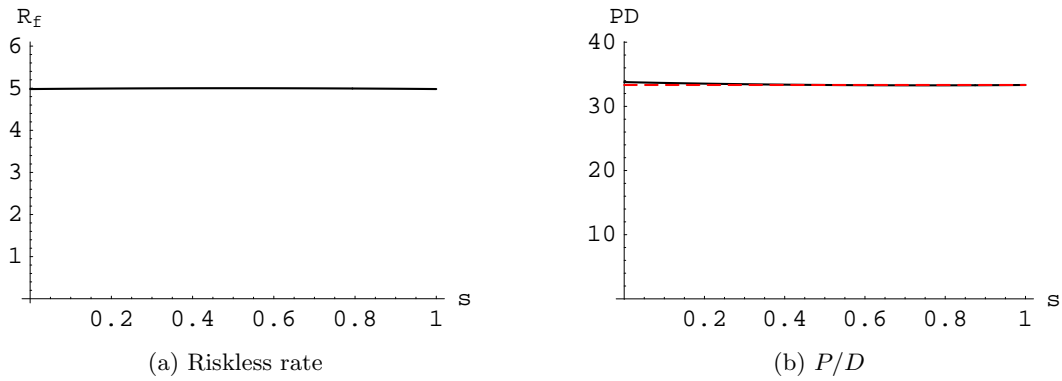


Figure 23: Left: The riskless rate against s . Right: The price-dividend ratio of asset 1 (solid) and of the market (dashed), against s . Log utility, no jumps.

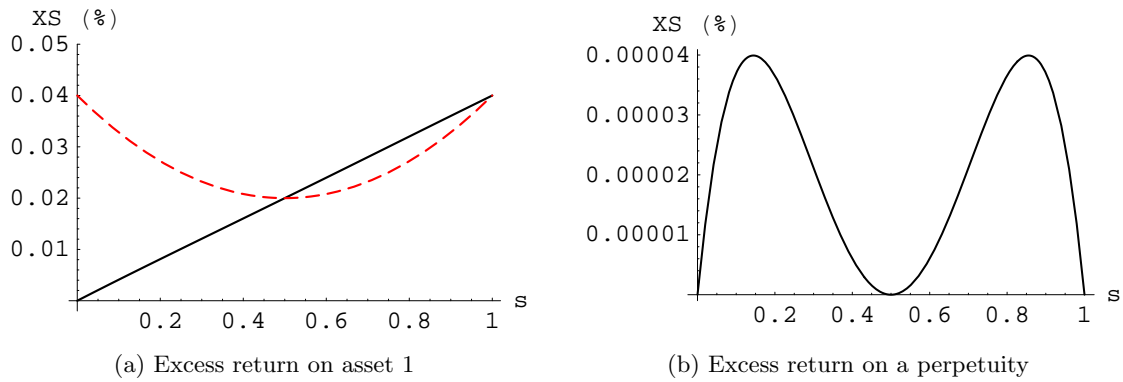


Figure 24: Left: The excess return on asset 1 (solid) and on the market (dashed) against s . Right: The excess return on a perpetuity against s . Log utility, no jumps.